Università del Piemonte Orientale Amedeo Avogadro
Dipartimento di Scienze Mediche di Novara

Dottorato di ricerca in Medicina Molecolare

XIX Ciclo

ROLE OF RIBOSOMAL PROTEIN S19 IN THE PATHOGENESIS OF DIAMOND BLACKFAN ANEMIA

Tesi di dottorato di

Anna Aspesi

Coordinatore: Prof. Umberto Dianzani

Responsabile Scientifico: Prof. Irma Dianzani

RIASSUNTO

L'anemia di Diamond Blackfan (DBA) è una rara patologia congenita causata da un difetto di maturazione dei progenitori eritroidi. La maggiore caratteristica clinica è una grave anemia, associata nel 30% dei pazienti a malformazioni dell'apparato scheletrico, cardiaco e genitourinario. La terapia a base di steroidi è utile solo in metà dei casi, negli altri si deve ricorrere a trasfusioni croniche di sangue.

Un quarto dei pazienti DBA presenta mutazioni in eterozigosi nel gene che codifica per la proteina ribosomiale (RP) S19, mentre mutazioni in *RPS24* e *RPS17* sono presenti nell'1-2% dei casi.

La DBA è ad oggi l'unica patologia nota causata da un difetto delle proteine costituenti il ribosoma. I meccanismi molecolari per cui l'aploinsufficienza di *RPS19* provoca il difetto dell'eritropoiesi non sono stati chiariti. Le ipotesi patogenetiche avanzate implicano una diminuzione della sintesi proteica nei progenitori eritroidi o in alternativa la perdita di una seconda, ancora sconosciuta funzione di RPS19 essenziale per l'eritropoiesi.

Questa tesi di dottorato presenta uno studio del ruolo funzionale di RPS19 in condizioni fisiologiche e nella DBA.

A questo scopo sono stati ricercati gli interattori proteici di RPS19. Dapprima è stato utilizzato il saggio del doppio ibrido in lievito che ha portato all'identificazione dell'oncoproteina PIM-1. PIM-1 è una serina/treonina chinasi coinvolta nel pathway di segnalazione dell'eritropoietina (EPO), uno dei principali fattori per il differenziamento eritroide. PIM-1 interagisce con RPS19 *in vitro* ed *in vivo* ed è in grado di fosforilarla in un

saggio *in vitro*. E' interessante notare che questa chinasi localizza sui ribosomi traduzionalmente attivi, il che suggerisce un possibile ruolo nel controllo traduzionale. Inoltre alcune mutazioni missense di *RPS19* trovate nei pazienti DBA alterano l'affinità di legame con PIM-1.

Altri interattori di RPS19 sono stati trovati con un approccio proteomico: una proteina di fusione GST-RPS19 è stata utilizzata come esca in un esperimento di pull-down e le proteine interattrici sono state purificate e analizzate tramite spettrometria di massa. Alcune delle interazioni sono state poi confermate *in vivo*. Tra le 159 proteine individuate ci sono numerose idrolasi e elicasi, fattori di trascrizione, proteine che legano DNA e RNA e proteine ribosomiali. La maggior parte degli interattori hanno localizzazione nucleolare e molti sono importanti per la biogenesi dei ribosomi.

Il coinvolgimento di RPS19 in questi processi cellulari è stato studiato tramite l'utilizzo di una linea di eritroleucemia umana (TF-1) in cui l'espressione di RPS19 è stata silenziata. La deplezione di RPS19 impedisce il corretto processamento dell'RNA ribosomiale (rRNA) e provoca la diminuzione dell'rRNA 18S maturo e l'accumulo del suo precursore, l'rRNA 21S. Abbiamo trovato lo stesso difetto nelle cellule di midollo osseo dei pazienti DBA con RPS19 mutata, ma non in pazienti con RPS19 wild type. Inoltre, cellule TF-1 che esprimono siRNA per RPS19 hanno una diminuzione delle subunità ribosomiali 40S.

I nostri studi propendono per un effetto di RPS19 sulla biogenesi del ribosoma e sulle sue funzioni e contribuiscono a comprendere meglio il ruolo patogenetico di RPS19 nell'anemia di Diamond Blackfan.

SUMMARY

Diamond Blackfan anemia (DBA) is a rare congenital disease caused by a defect in the maturation of erythroid progenitors. Main clinical features are severe anemia and in 30% of cases craniofacial, limb or urogenital malformations. Steroid therapy is effective only in half of the cases; chronic blood transfusions are otherwise required.

One fourth of DBA patients show mutations on one allele of the gene encoding for ribosomal protein (RP) S19, whereas *RPS24* and *RPS17* are mutated in 1-2% of cases.

DBA is to date the only known disease due to mutations in structural ribosomal proteins. Molecular mechanisms underlying the causal effect between *RPS19* haploinsufficiency and defective erythropoiesis have not been elucidated. Pathogenetic hypotheses imply either a decreased protein synthesis rate in erythroid progenitors or the loss of a second, so far unknown function of RPS19 that is essential for erythropoiesis.

This dissertation presents a study of the functional role of RPS19 both under physiological conditions and in DBA.

To this purpose proteins interacting with RPS19 have been searched for. At first a yeast two-hybrid assay was used and led to the identification of the oncoprotein PIM-1. PIM-1 is a serine/threonine kinase involved in the signaling pathway of erythropoietin (EPO), one of the most important erythroid differentiation factors. PIM-1 interacts with RPS19 *in vitro* and *in vivo* and is able to phosphorilate it *in vitro*. Interestingly this kinase localizes on translationally active ribosomes, and this suggests a possible role in translational control.

Moreover some *RPS19* missense mutations found in DBA patients impair binding affinity with PIM-1.

Other RPS19 interactors have been detected with a proteomic approach: a GST-RPS19 fusion protein has been used as a bait in a pull-down assay and interacting proteins have been purified and analyzed by mass spectrometry. Some of the interactions have also been validated *in vivo*. Among the 159 identified proteins there are several hydrolases, helicases, transcription factors, DNA and RNA binding proteins and ribosomal proteins. Most of the interactors localize to the nucleolus and many are important for ribosomal biogenesis.

The involvement of RPS19 in these cellular processes has been studied by using human erythroleukemia cell line TF-1 in which the expression of RPS19 can be silenced.

Depletion of RPS19 inhibits the proper processing of ribosomal RNA (rRNA), resulting in the decrease of 18S mature rRNA and in the accumulation of its precursor, the 21S rRNA. We found the same defect in bone marrow cells from DBA patients with mutated RPS19, but not in patients with wild type RPS19. Moreover, TF-1 cells expressing siRNA against RPS19 have a deficiency of the 40S ribosomal subunit.

Our studies support the involvement of RPS19 in ribosome biogenesis and functions and contribute to a better understanding of the pathogenetic role of this protein in Diamond Blackfan anemia.

ACKNOWLEDGMENTS

I would like to express my gratitude to my supervisor Prof. Irma Dianzani for the opportunity to work in her group, for the support and for the freedom she gives me to explore my own ideas.

I thank Prof. Claudio Santoro for constructive criticisms and helpful scientific discussions.

I am very grateful to Dr Steve Ellis for being a terrific mentor during my stay in Louisville.

Thanks to my family for always supporting me, in their own special way.

I wish to thank my coworkers for making the long hours of work as fun as possible.

A special thanks to my little sister and to all my friends.

TABLE OF CONTENTS

Chapter 1

Introduction

Clinical features of Diamond Blackfan anemia

Diamond Blackfan anemia (DBA, OMIM 105650) is a rare congenital disease of childhood characterized by a decreased or absent number of erythroid progenitors in the bone marrow (Campagnoli *et al.*, 2004). It was first reported by Josephs in 1936 and further described by Diamond and Blackfan in 1938. Patients are affected by severe normochromic macrocytic anemia and reticulocytopenia, usually since the first year of life. The other bone marrow cell lineages show normal counts.

Erythrocytes can express fetal hemoglobin (HbF) and the activity of erythrocyte adenosine deaminase (eADA), a crucial enzyme of the purine salvage pathway, is elevated in 85% of cases (Glader and Backer, 1988). DBA is associated with an increased risk of malignancies, expecially hematopoietic neoplasms and osteogenic sarcomas. In 30% to 47% of cases patients show physical malformations involving head, thumb, heart and urogenital system (Lipton, 2006). A typical facial appearance has been described as the Cathie facies, characterized by snub nose and wide-spaced eyes (Cathie, 1950). Prenatal or postnatal growth retardation independent of steroid therapy is also often present.

The incidence of DBA is around 6 per 1 million of live births. Most cases are sporadic, but the disease can be inherited with an autosomal dominant pattern. Penetrance is incomplete and expressivity widely variable, even in patients from the same family (Campagnoli *et al.*, 2004).

First-line therapy in DBA patients is steroid treatment, typically with prednisone, that is effective in at least half the cases. Notwithstanding, some patients may experience temporary or definitive steroid-resistance (Dianzani *et al.*, 2000). The therapeutic properties of steroids in DBA have not been explained but they are likely to be due to their transcription regulation activity. Patients non responsive to steroids undergo chronic blood

transfusions associated to iron chelation to avoid iron accumulation that can cause secondary hemochromatosis with damage to heart, liver and other organs. 20% of patients inexplicably achieve spontaneous remission (Lipton, 2006). Remission can also be obtained by allogeneic bone marrow or stem cell transplantation, but the mortality from infections, graft-versus-host disease and graft failure is significant (Roy *et al.*, 2005).

Etiology of DBA

DBA is considered an intrinsic defect of erythroid progenitors and not, for instance, of the bone marrow stromal cells; this is also corroborated by the efficacy of bone marrow transplantation. In several *in vitro* studies bone marrow cells from DBA patients were stimulated with different cytokines, but they showed a low response compared to control cells (Nathan *et al.*, 1978; Bagnara *et al.*, 1991). The only treatment that significantly increased the proliferation rate of patients erythroid progenitors was a cocktail composed by EPO, IL-3 and SCF (Bagnara *et al.*, 1991). This effect was enhanced by IL-9 (Dianzani *et al.*, 1997). Thus, the first candidate genes considered were SCF, EPO, EPOR, IL-3, IL-9 and some genes mapping to chromosome 5q important for hemopoiesis, but their involvement in the disease was ruled out (Bagnara *et al.*, 1991; Dianzani *et al.*, 1996; Dianzani *et al.*, 1997).

In 1997 a balanced translocation (X;19)(p21;q13) was discovered in an affected female (Gustavsson *et al.*, 1997). Since DBA is not X-linked, studies focused on the breakpoint on chromosome 19 and led two years later to the identification of the first DBA gene, which encodes for the ribosomal protein (RP) S19, a component of the small subunit of ribosome. This gene is 11 kbp long and it includes 6 exons; translation begins at the first codon of the

second exon. The human genome also contains 2 processed pseudogenes for *RPS19* that are not expressed (Cmejla *et al.*, 2000). Mutations in *RPS19* have been identified in 25% of patients, always on one allele (Willig *et al.*, 1999).

A large variety of mutations, such as deletions, insertions, frameshift and missense mutations, cover the whole gene. A hot spot has been detected between residues 52 and 62. Since most *RPS19* mutations are predicted to result in a nonfunctional protein, haploinsufficiency is probably the pathogenetic mechanism underlying DBA (Gazda *et al.*, 2004). There is no correlation between transmission, phenotype or response to therapy and the type of *RPS19* mutations.

Linkage analysis on 38 families suggests the existence of another DBA locus on chromosome 8 (8p23.3-p22) (Gazda *et al.*, 2001).

Mutations in other two ribosomal proteins of the 40S subunit, RPS24 and RPS17, have been recently reported to account for 1-2% of DBA cases (Gazda *et al.*, 2006; Cmejla *et al.*, 2007). Up-to-date studies also reveal the involvement of some proteins of the large ribosomal subunit, namely RPL35a, RPL5, RPL11 (Farrar *et al.*, 2007; Gazda *et al.*, 2007). Therefore, the molecular basis of DNA is probably to be searched in the alteration of a cellular function that all these proteins share.

DBA is to date the only human disease due to mutations in structural ribosomal proteins.

The eukaryotic ribosome

In eukaryotes, the ribosome is constituted by four different ribosomal RNA (rRNA) and 79 ribosomal proteins. While 5S rRNA is transcribed by RNA polymerase III, 28S, 5.8S and 18S rRNAs are processed from a 45S precursor transcribed by RNA polymerase I. The

maturation of rRNAs occurs in the nucleolus through a complex pathway involving both endo- and exonucleases that remove external and internal transcribed spacers (ETS and ITS) (Fig. 1). During these steps the 45S pre-RNA associates with a number of ribonucleases, ribosomal proteins, RNA helicases, small nucleolar RNPs (snoRNPs) and other accessory factors, thus forming the 90S pre-ribosomes.

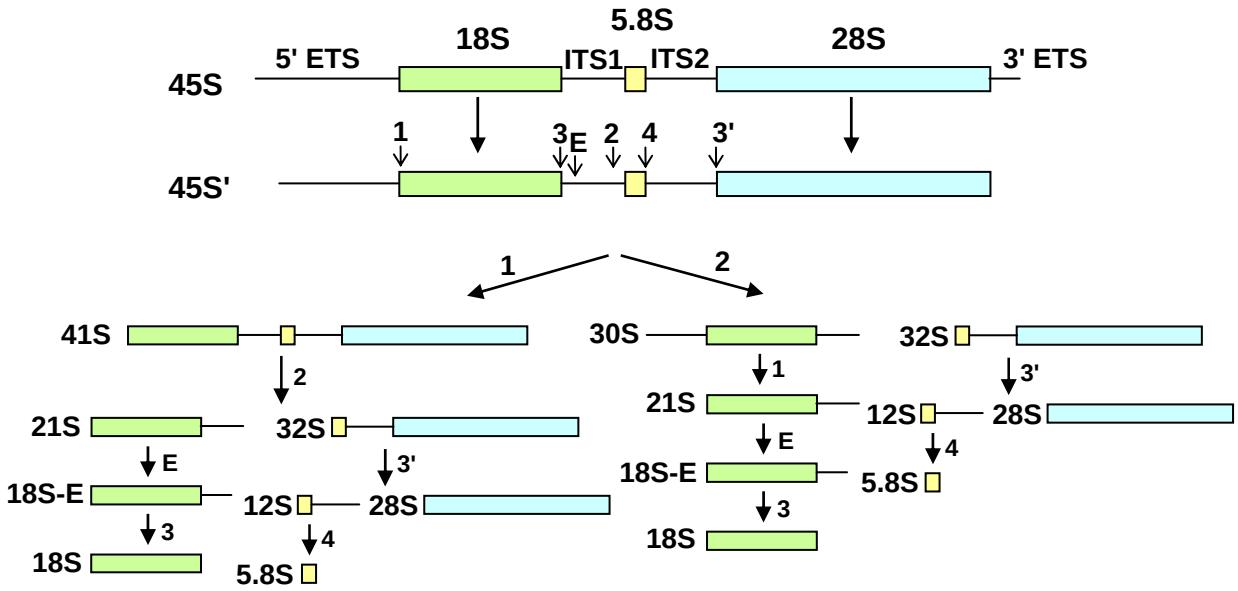

Fig. 1. Pre-rRNA processing pathway in human cells (from Rouquette *et al.*, 2005).

At the end of the maturation process, the pre-ribosome is separated into pre-60S and pre-40S subunits that are exported to the cytoplasm (Tschochner and Hurt, 2003). 60S subunits contain 28S, 5.8S and 5S rRNA and 46 ribosomal proteins; 40S subunits includes one rRNA, the 18S form, and 33 ribosomal proteins. In eukaryotes there are several loci for the rRNAs, but only one gene for each ribosomal protein. Since a large proportion of a cell's

energy is expended in ribosome biogenesis (Warner, 1999) the production of rRNA and ribosomal proteins is expected to be tightly coordinated in order to obtain equimolar amounts of these molecules. In human cells the genes encoding ribosomal proteins have distinctive promoters and they apparently share no common regulation motif (Perry, 2005). Nevertheless, studies aimed to quantify the abundance of RP mRNAs showed that the RP genes are coordinately expressed (Li *et al.*, 2005), even if some tissue specific differences have been demonstrated (Angelastro *et al.*, 2002; Bortoluzzi *et al.*, 2001).

Structure and functions of RPS19

RPS19 is a highly conserved protein (e.g. *Rattus norvegicus* 99%, *Mus musculus* 98%). Since there is no ortholog for RPS19 in eubacteria, whose ribosomes have been thoroughly studied, the precise localization of RPS19 on the 40S subunit is unknown. Immunoelectron microscope studies locate RPS19 to the external surface of the 40S subunit, close to the region that interacts with eIF-2 during ribosomal scanning and translation initiation (Lutsch *et al.*, 1990; Bommer *et al.*, 1988). Recently the structure of RPS19 from *Pyrococcus abyssi*, that shares 36% identity and 57% similarity with human RPS19, has been resolved by crystallography (Gregory et al., 2007). It is formed by 5 α-helices organized around a central amphipathic α-helix that contains the DBA mutational hot spot. It has been demonstrated that some missense mutations found in DBA patients affect residues located in this hydrophobic core that are necessary either for the proper folding or for the stability of the protein (Fig. 2). Other missense mutations, on the contrary, affect surface residues

placed on two highly conserved basic patches that are essential for the incorporation of RPS19 into pre-40S ribosomal particles.

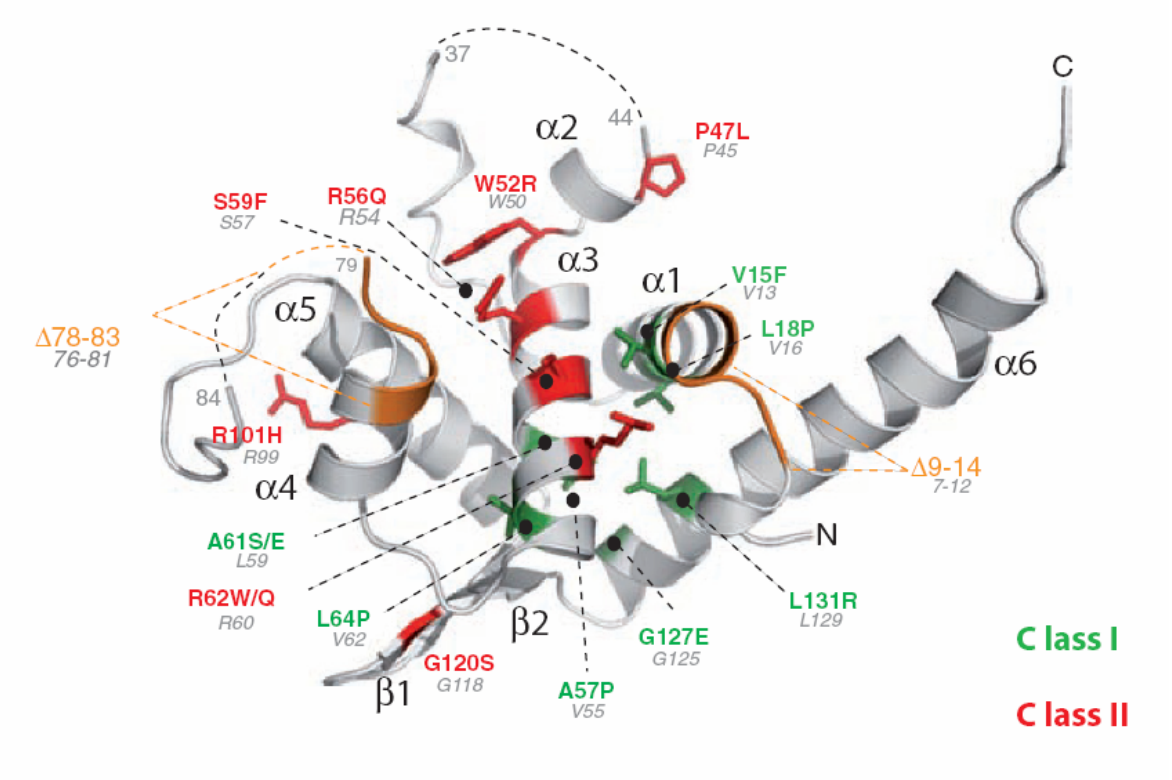

Fig. 2. RPS19 structure model and point mutations found in DBA patients. Class I mutations, in green, affect core residues essential for the proper folding of the protein; class II mutations, in red, affect surface residues likely involved in molecular interactions (from Gregory *et al.*, 2007).

In yeast RPS19 is required for the maturation of 18S rRNA and its deficiency results in a defect in the biogenesis of 40S ribosomal subunit (Léger-Silvestre *et al.*, 2005).

Although the link between RPS19 and erythropoietic failure in DBA is an enigma, a role of this protein in erythroid differentiation has been clearly demonstrated. Most data have been

obtained from experiments performed on DBA patients cells or using cellular models where RPS19 is knocked-down by siRNA. A murine model for DBA is not available yet, as the *Rps19*$^{+/-}$ mouse is healthy and does not show any hematological phenotype, and the *Rps19*$^{-/-}$ mice do not form blastocysts (Mattson *et al.*, 2004).

CD34^{+} cells are the progenitors of all hemopoietic lineages and thus represent the ultimate model to study DBA. CD34^{+} cells isolated from the bone marrow of DBA patients contain fewer erythroid burst-forming units (BFU-E) and erythroid colony-forming units (CFU-E) than controls (Hamaguchi *et al.*, 2003). The erythroid failure in DBA occurs during the terminal EPO-dependent maturation stage, when DBA cells fail to proliferate in response to EPO, suggesting that the defect lies downstream of the EPO receptor (Ohene-Abuakwa *et al.*, 2005). A recent study shows that EPO receptor expression and EPO signal transduction are normal in a RPS19 deficient model cell line (Miyake *et al.*, 2007) and reveals accumulation of p21 and p27 and arrest in G0/G1 phase. The proportion of apoptotic cells is increased in a RPS19 deficient cell model and in CD34^{+} cells from DBA patients with mutations in *RPS19* (Miyake *et al.*, 2007). This is in agreement with previous data showing that erythroid progenitors from DBA patients succumb to apoptosis after EPO deprivation more quickly than control cells (Perdahl *et al.*, 1994).

RPS19 expression level has been measured in bone marrow cells and it appears to decrease during erythroid differentiation (Hamaguchi *et al.*, 2003). Importantly, transfection of wild type RPS19 cDNA in CD34^{+} cells with silenced RPS19 or CD34^{+} cells from DBA patients with mutations in *RPS19* rescues their phenotype (Flygare *et al.*, 2005; Hamaguchi *et al.*, 2002; Hamaguchi *et al.*, 2003).

Bone marrow failure syndromes and ribosomes

DBA is not the only human disease linked to ribosome dysfunction. Dyskeratosis congenita (DC), Shwachman-Diamond syndrome (SDS) and cartilage-hair hypoplasia (CHH) are all believed to be caused by defects in the synthesis or function of ribosomes.

Patients affected by dyskeratosis congenita show pancytopenia associated to abnormal skin pigmentation and other somatic abnormalities (Kirwan and Dokal, 2008). DC X-linked form is due to mutations in the gene *DKC1*, that encodes for dyskerin. Dyskerin is a nucleolar protein involved both in telomere maintenance and rRNA pseudouridylation. The other DC genes, *TERC* and *TERT*, that are also components of the telomere complex, are responsible for a milder form of the disease, suggesting that in addition to telomere instability, impaired ribosome maturation may contribute to the phenotype. In fact, it has been reported that in hypomorphic DKC1 mice and in cells from DC patients IRES-mediated translation is defective (Yoon *et al.*, 2006).

Shwachman-Diamond syndrome, characterized by neutropenia, exocrine pancreatic insufficiency and predisposition to leukemia, is caused by heterozygous mutations in the *SBDS* gene. SBDS coprecipitates with the 60S ribosomal subunits but not with mature ribosomes (Ganapathi *et al.*, 2007). Its yeast orthologue, Sdo1, is required to allow the joining of the large and the small ribosomal subunits and the translational activation of ribosomes (Menne *et al.*, 2007).

CHH is characterized by skeletal and cartilage abnormalities, short stature, hypoplastic hair, anemia and predisposition to cancer. The affected gene encodes for the RNA component of the mitochondrial RNA processing (MRP) complex, a RNase involved in the endonucleolytic cleavage of the precursor of 5.8S rRNA in *Saccharomyces cerevisiae*.

DC, SDS, CHH and DBA are a heterogeneous group of disorders but they share some clinical features: bone marrow failure, congenital anomalies and cancer predisposition. The proteins encoded by the genes mutated in these diseases are all involved in different aspects of ribosome synthesis, but the link between impaired hematopoiesis and ribosome dysfunction remains obscure.

Hypotheses on DBA pathogenesis

Several hypotheses have been proposed to explain the pathogenesis of DBA. The suggested mechanisms are not mutually exclusive and might cooperate to cause the complex DBA phenotype.

Since RPS19 is a ribosomal protein, the most obvious explanation is that RPS19 deficiency can impair the stoichiometry of ribosomal proteins, resulting in a decreased translational capacity. According to this theory, if ribosomal proteins are expressed in amounts that differ in a tissue-specific manner, haploinsufficiency for a particular protein may make that protein limiting for ribosome assembly in some tissues and not others (Ellis and Massey, 2005). RPS19 expression level in bone marrow cells decreases during erythroid differentiation (Da Costa *et al.*, 2003; Hamaguchi *et al.*, 2003) while the demand for ribosome synthesis raises, as the cell needs to produce huge amounts of globin. A study analyzing RPS19 mRNA and protein levels in DBA patients with RPS19 mutations showed that whereas RPS19 mRNA is decreased both in $CD34^+$ cells and in peripheral blood mononuclear cells, RPS19 protein is decreased only in $CD34^+$ cells (Gazda *et al.*, 2004). Therefore, erythroid progenitors could be more sensitive than other tissues to haploinsufficiency for RPS19 (Ellis and Massey, 2005). It has been demonstrated that

translational efficiency is reduced in DBA patients with or without a mutation in *RPS19* (Cmejla *et al.*, 2007) suggesting that in erythroid progenitors the level of translation of specific transcripts is too low to reach the threshold that triggers differentiation.

A different hypothesis suggests the existence of an extraribosomal function for RPS19 (Flygare and Karlsson, 2007). It is believed that the primordial ribosome was composed of RNA only and that during evolution proteins able to bind nucleic acids associated with it, still retaining their original functions. In eukaryotes several RPs have been demonstrated to be involved in different cellular processes such as transcription, cell cycle regulation, RNA processing and DNA repair (Wool, 1996). Also some human RPs can have extraribosomal functions: for instance RPL5 and RPL11 are p53 activators (Dai and Lu, 2004; Lohrum *et al.*, 2003), RPS6 has a role in proliferation regulation (Volarevic and Thomas, 2001) and RPL13a and RPL26 control the translation of specific mRNAs (Mazumder *et al.*, 2003; Takagi *et al.*, 2005). RPS19 itself can form a homodimer that acts as a chemotactic factor for the recruitment of monocytes to apoptotic cells (Shrestha *et al.*, 1999). In addition, free intracellular RPS19 can interact with FGF-2 in NIH 3T3 cells (Soulet *et al.*, 2001). FGF-2 is involved in the differentiation process of different cell types, and the interaction between FGF-2 and RPS19 may suggest a link for RPS19 in embryogenesis.

Chapter 2

RPS19 interacts with the PIM-1 oncoprotein

The characterization of the molecular partners interacting with RPS19 is a strategy to dissect RPS19 functions and to shed light on the role of other genes involved in the pathogenesis of non RPS19-dependent DBA.

We performed a yeast two-hybrid screening using a human fetal liver cDNA library.

We found that RPS19 binds PIM-1, a serine-threonine kinase whose expression is strongly increased upon stimulation with erythropoietin and other cytokines having hemopoietin-type receptors. PIM-1 has been reported to protect hematopoietic cells from apoptosis induced by genotoxic stress or growth factor withdrawal (Pircher *et al.*, 2000) and it has been associated with lymphomagenesis (van der Houven *et al.*, 1998). Pim-$1^{-/-}$ mice display impaired proliferative response to cytokines, in particular to interleukin-3 (Domen *et al.*, 1993), and they also show microcytosis (Laird *et al.*, 1993), whereas hyperexpression of Pim-1 in mice causes macrocytosis (van der Houven *et al.*, 1998).

The interaction between RPS19 and PIM-1 was confirmed *in vitro* by a pull-down assay and *in vivo* by coimmunoprecipitation. PIM-1 is able to phosphorylate RPS19, at least *in vitro*, and to associate with ribosomes and polysomes. We hypothesize that PIM-1 can be recruited by RPS19 on ribosomes and have a role in general or specific translational control, as already demonstrated for RPL13a (Mazumder *et al.*, 2003). *PIM-1* is not a major DBA gene, as determined by mutational screening in 116 DBA patients. Nevertheless, we reported two missense mutations of *PIM-1* that are not common polymorphisms. We also studied whether PIM-1/RPS19 interaction is impaired by some *RPS19* mutations found in DBA patients. Binding affinity was altered indeed for three missense mutants. This could unbalance the proportion of PIM-1 bound to RPS19 and make it less or more available for other interactions and functions.

Interactions between *RPS19*, mutated in Diamond-Blackfan anemia, and the PIM-1 oncoprotein

Annalisa Chiocchetti
Luisa Gibello
Adriana Carando
Anna Aspesi
Paola Secco
Emanuela Garelli
Fabrizio Loreni
Mara Angelini
Alessandra Biava
Niklas Dahl
Umberto Dianzani
Ugo Ramenghi
Claudio Santoro[1]
Irma Dianzani[1]

[1]These authors contributed equally to this work.

From the IRCAD and Dipartimento di Scienze Mediche, Università del Piemonte Orientale, Novara, Italy (LG, AA, PS, AB, UD, CS, ID); Dipartimento di Scienze Pediatriche, Università di Torino, Turin, Italy (EG, UR); Dipartmento di Biologia, Università "Tor Vergata", Rome, Italy (MA, FL); Dept. of Genetics and Pathology, Section of Clinical Genetics, The Rudbeck Laboratory, Uppsala University Children's Hospital, Uppsala, Sweden (ND).

Correspondence:
Prof. Irma Dianzani, Dipartimento di Scienze Mediche, Università del Piemonte Orientale, via Solaroli 17, 28100 Novara. E-mail: irma.dianzani@med.unipmn.it

Background and Objectives. Diamond Blackfan anemia (DBA) is a congenital disease characterized by defective erythroid progenitor maturation. Patients' bone marrow progenitor cells do not respond to erythropoietic growth factors, such as erythropoietin. Mutations in the gene encoding for ribosomal protein (RP) S19 account for 25% of cases of DBA. The link between defective erythropoiesis and *RPS19* is still unclear. Two not mutually exclusive hypotheses have been proposed: altered protein synthesis and loss of unknown extraribosomal functions.

Design and Methods. We used yeast two-hybrid screening and a human liver cDNA library obtained at 19-24 weeks of gestation, when hepatic erythropoiesis is efficient, to search for proteins interacting with RPS19.

Results. We found that RPS19 binds PIM-1, an ubiquitous serine-threonine kinase whose expression can be induced in erythropoietic cells by several growth factors, such as erythropoietin. The PIM-1/RPS19 interaction was demonstrated both *in vitro* and in living cells and led to phosphorylation of RPS19 in an *in vitro* kinase assay. We also showed that in human 293T cells PIM-1 interacts with ribosomes and may be involved in translational control. Three DBA-associated *RPS19* mutations alter the binding between RPS19 and PIM-1.

Interpretation and Conclusions. A link between erythropoietic growth factor signaling and RPS19 has been identified for the first time.

Key words: Diamond-Blackfan anemia, ribosomal protein S19, PIM-1, erythropoiesis

Haematologica 2005; 90:1453-1462

Diamond Blackfan anemia (DBA) (MIM 205900) is a congenital disease characterized by defective erythroid progenitor maturation.[1-4] Most cases are sporadic, though a dominant or, more rarely, a recessive inheritance is observed in 10% of patients. The main clinical sign is profound isolated normochromic or macrocytic anemia, with normal numbers and function of the other hematopoietic cells. Defective erythropoiesis is revealed in the bone marrow by a very low number of erythropoietic precursors, and functionally by a reduction of burst-forming unit-erythroid (BFU-E) progenitor cells.[5] DBA patients have high levels of erythropoietin, irrespective of the degree of their anemia. The failure of their hematopoietic progenitors to respond to erythropoietin, both *in vitro* and *in vivo*, suggests erythropoietin insensitivity, and a defect in the erythropoietin-receptor (EPOR) pathway has thus been widely accepted as an explanation of defective erythropoiesis.[6] This has also been suggested by the fact that phenotype reversal can be induced *in vitro* by the addition of stem cell factor (which uses a different transduction pathway from erythropoietin) to interleukin-3 and erythropoietin to CD34$^+$ bone marrow cells from DBA patients.[5,7,8] However, *EPOR* and other genes encoding for erythropoietic growth factors have been ruled out as potential candidates.[9,10,11]

More than 50% of patients respond to steroid therapy, though the mechanisms involved are unknown.[4] Options in steroid-resistant patients are chronic red cell transfusions or allogeneic stem cell transplantation.[12] A number of patients experience spontaneous remission, irrespective of the type of treatment.[4] Patients with DBA also show an increased risk of malignancies.[1] One-third of patients have malformations, usually involving the upper limbs, head, the urogenital or cardiovascular system, and short stature.

One gene on chromosome 19q13.2, encoding ribosomal protein (RP) S19,

accounts for 25% of patients with either the dominant or the sporadic form of DBA.[13,14,4] A second DBA locus has been identified on human chromosome 8p22-p23 by linkage analysis;[15] however, the lack of linkage of DBA to either the 8p or the 19q critical regions in some families suggests that other genes are involved. DBA is the first human disease known to be caused by mutations in a ribosomal structural protein. The malformations and short stature occurring in DBA could be the consequence of defective protein synthesis during embryogenesis. Interestingly, *Drosophila minute* phenotypes, characterized by delayed larval development, diminished viability, reduced body size, diminished fertility and thin bristles, are due to *RP* mutations.[16,17]

The link between defective erythropoiesis and *RPS19* is still unclear. The finding that most *RPS19* mutations completely suppress the expression of the allele has suggested that haploinsufficiency is the main cause of abnormal erythropoiesis in DBA patients.[18,19] However, some patients carry missense mutations in the *RPS19* gene. Deficient nucleolar localization, which may lead to abnormal ribosome incorporation, has been found for three missense mutants,[20,21] and hence this may not be a univocal disease mechanism.

RPS19 expression is greater in the early stages of erythropoiesis, which are characterized by intense proliferation, than in the late stages, characterized by maturation of erythroid precursors.[22] The role of *RPS19* is also shown by the increase of BFU-E formation after overexpression of transfected oncoretroviral vectors containing the wild-type cDNA in $CD34^+$ bone marrow cells from DBA patients[23] and by the decrease of *in vitro* erythropoiesis when *RPS19* expression is impaired by RNA interference.[24] Like other structural ribosomal proteins in humans and other organisms,[25] RPS19 may have extraribosomal functions. Free RPS19 interacts with fibroblast growth factor 2 *in vitro* and the RPS19 dimer released by apoptotic cells induces monocyte chemotaxis.[26,27]

We used yeast two-hybrid screening[28] and a human liver cDNA library obtained at 19-24 weeks of gestation, when hepatic erythropoiesis is efficient, to search for proteins that interact with RPS19.

Design and Methods

Yeast two-hybrid screen

The human *RPS19* cDNA was amplified by reverse transcription polymerase chain reaction (RT-PCR) from peripheral blood leukocytes using the primers 5'-GTGAATTCATGCCTGGAGTTACTGTAAAAG-3' and 5'- GTCTCGAGCCAGCATGGTTTGTTC-TAATG-3' (GenBank database accession nNM_001022). The products were digested with EcoRI and XhoI and inserted into the pLexA vector (CLONTECH Laboratories, Inc.). The expression library was the Human Fetal Liver MATCHMAKER LexA cDNA Library (Clontech) obtained from normal, whole livers pooled from 32 male or female Caucasian fetuses spontaneously aborted at 19-24 weeks of gestation. Plasmids were introduced into the yeast strain EGY48[p8op-lacZ] and interacting proteins were double-selected for growth on His/Leu/Trp/Ura-deficient plates and β-galactosidase production. Interactions were confirmed by transforming yeast cells with DNA from isolated clones. DNA sequencing was carried out on an automated Applied Biosystem apparatus (Applied Biosystems, Foster City, CA, USA).

Analysis of interactions between wild-type and mutant RPS19 and PIM-1 in yeast

Competent cells of EGY48 [p8op-lacZ] were prepared using the lithium acetate method.[29] Transformations were performed using heat shock treatment described in the Matchmaker Library Protocol (Clontech). The EGY48 [p8op-lacZ] yeast strain was transformed with 2 µg of pB42 *PIM-1* to obtain EGY48 PIM-1, and yeast transformants were plated on SD/-Ura/-Trp and incubated for 2 days at 30°C. cDNA corresponding to natural mutants found in DBA (R56Q, R62W, R101H, and the in-frame insertion 53_54insAGA) were inserted into the pLexA vector.

A single colony of EGY48*PIM-1* was inoculated in SD/-Ura/-Trp and grown overnight at 30°C with agitation. For each transformation 1 mL of EGY48*PIM-1*competent cells was mixed with 2 µg of DNA corresponding to wild-type RPS19 and its natural mutants. Yeast transformants were plated on SD/-Ura/-His/-Trp and incubated for 3 days at 30°C. Interactions between wild-type and mutant RPS19 with PIM-1 were qualitatively analyzed by streaking single colonies on SD/-Ura/-Trp/-His/Gal/Raf/X-Gal for 4 days to check for the activation of the lacZ and Leu reporter genes (*data not shown*).

The interactions were quantified by measuring the β-galactosidase activity in solution with yeast β-galactosidase assay kit (75768; Pierce Chemical) at room temperature, with O-nitrophenyl β-D-galactopyranoside as the substrate. Briefly, single colonies of yeast co-transformed with *PIM-1* and natural *RPS19* mutants were used to inoculate 5 mL of –Ura/-Trp/-His/Gal/Raf liquid media and were allowed to grow to mid-log phase overnight at 30°C. The OD_{600} was measured and 350 µL of each cell culture were mixed with 150 µL of yeast protein extraction reagent and with 150 µL of 2X β-galactosidase assay buffer. The reactions were incubated at room temperature until a color change was observed and stopped by adding 300 µL of 2X β-galactosidase assay stop solution. The total reaction time was recorded. The cell debris was pelleted and the

OD_{420} of the supernatants was measured. The β-galactosidase units were calculated using the formula $U=(1000\times OD_{420})/(t \times v \times OD_{600})$, where v = volume of culture used in the assay in milliliters, and t = time of assay in minutes. All assays were performed in parallel with three colonies from each transformation. Each experiment was performed in triplicate. The results were then averaged. Each interaction was also evaluated by pooling six colonies from each transformation. The statistical analysis was performed using Wilcoxon's signed rank test for paired data.

Plasmids and expression vectors

RPS19 expression plasmids were constructed by inserting RT-PCR products into pcDNA3 (Invitrogen, Milan, Italy) downstream from the sequence coding for the FLAG-tag (pFLAG-RPS) or into pGEX4.T1 (Amersham Pharmacia, pGST-RPS). The natural *RPS19* mutants R56Q, R62W, R101H, and an in-frame insertion (53_54insAGA, which is expected to insert an arginine after residue 18) were prepared by RT-PCR from peripheral blood lymphocytes of DBA patients after informed consent or by PCR-dependent mutagenesis. The mutation nomenclature used is that described by den Dunnen and Antonarakis.[30] The full-length *PIM-1* cDNA was obtained by RT-PCR from HeLa cells using the following primers: 5'-CCGGAATTCCCTCTTGTCCAAAATCAACTCGCT-3' and 5'-CCGCTCGAGCTATTTGCTGGGCCCCGGCG-3' (GenBank database accession nNM_002648). The PCR fragment was digested with EcoRI and XhoI and inserted into pGEX-4T.1 (pGST-PIM). All constructs were sequenced.

Cell lines and transfections

Human embryonic kidney 293T cells (ATCC #CRL-11268) were cultured in Dulbecco's modified essential medium supplemented with 10% fetal bovine serum at 37°C with 5% CO_2. For DNA transfections, 3×10^6 cells were plated in 90-mm diameter dishes and transfected with the Lipofectamine 2000 kit (Invitrogen, Milan, Italy) according to the manufacturer's intructions. After 48 hr, the cells were harvested in ice-cold AKT buffer (20 mM Tris, pH 7.5, 5 mM EDTA, 150 mM NaCl,1% Triton X-100,10% glycerol, 0.5 mM DTT, 1 mM PMSF, 1 µg/mL leupeptin, 1 µg/mL aprotinin, 1 µg/mL pepstatin) for 20 min on ice and sonicated three times. Cell debris was removed by centrifugation and cleared lysates were analyzed further. Human erythroleukemia K562 cells (ATCC#CCL-243) were cultured in RPMI-1640 medium supplemented with 10% fetal bovine serum at 37°C with 5%CO_2.

Antibodies and co-immunoprecipitations

Anti-RPS19 sera were prepared (Sigma Genosys, Cambridge, UK) against the RPS19-derived peptide, LDRIAGQVAAANKKH, by injections in a rabbit. After four immunizations, antibody was purified on peptide affinity columns. Antibody activity was tested by immunoblotting with recombinant RPS19.

Antibodies specific for PIM-1 (Santa Cruz Biotechnology, Santa Cruz, CA, USA) and the hemagglutinin (HA) or the FLAG tags (Sigma, St. Louis, MO, USA) were used as directed by the manufacturers. Immunoblots were detected using horseradish peroxidase-conjugated secondary antibodies and enhanced chemiluminescence according to the supplier's instructions (Amersham, Arlington Heights, IL, USA).

Cleared lysates from co-transfected cells (5 mg total proteins) were pre-absorbed to protein-G beads (Amersham, Arlington, Heights, IL, USA) for 1 hour at 4°C. Supernatants were first incubated with anti-FLAG antibody (5 µg) for 16 hours at 4°C on a rocker, and then with new protein-G beads for 1 hour at 4°C. Immunocomplexes were recovered by centrifugation at 3000 rpm for 1 min, washed four times with 1 mL of AKT buffer, loaded onto a 12% polyacrylamide SDS-gel and analyzed by immunoblotting.

GST-fusion proteins and in vitro binding assay (GST pull-down assay)

Recombinant GST-PIM-1 fusion protein was produced in *E. coli* cells (strain JM109) and bound to glutathione-Sepharose 4B resin (Sigma St. Louis, MO, USA) as previously described.[31] For pull-down assays, lysates (5 mg of total protein) from 293T cells transfected with the indicated *RPS19* contructs, were incubated with 50 µL of GST-PIM-1 affinity resin (~100 µg of recombinant protein) in AKT buffer for 16 hr at 4°C on a rocker. The GST-RPS19 wild-type or mutant fusion proteins were similarly produced in *E. coli* cells (strain BL-21) and used to prepare affinity resins. For pull-down assays, K562 cell lysates (5mg of total protein) were incubated with GST-RPS19 affinity resins as described above. Bound proteins were washed with TM 0.1 buffer (50 mM Tris-HCl, pH 7.9, 100 mM KCl, 12.5 mM $MgCl_2$, 1 mM EDTA, 1 mM DTT, 1 mM PMSF), eluted with TM 0.5 buffer (50 mM Tris-HCl, pH 7.9, 500 mM KCl, 12.5 mM $MgCl_2$, 1 mM EDTA, 1 mM DTT, 1 mM PMSF), and precipitated with 10% trichloracetic acid. The pellet was washed twice with acetone, resuspended in SDS-PAGE loading buffer (63 mM Tris-HCl pH 6.8, 5% glycerol, 1% SDS, 2.5% bromophenol-blue), resolved by SDS-PAGE and subjected to immunoblotting with a monoclonal anti-PIM-1 antibody (Santa Cruz Biotechnology).

Kinase assay

To determine whether PIM-1 was able to phosphorylate RPS19, GST fusion proteins were individually affinity purified and eluted from the resins; next, 2.5 µg

of GST-PIM-1 (20 µL of bead slurry) were washed twice in kinase buffer (20 mM PIPES, pH 7.0, 5 mM $MnCl_2$, 7 mM β-mercaptoethanol) and then resuspended in kinase buffer and mixed with 10 µg of GST-RPS19. The reaction was started by adding 10 mM ATP and 10 µCi of γ-^{32}P-ATP. Histone H1, an effective substrate for a number of serine/threonine kinases (Upstate #14155), was used as a positive control, whereas GST alone was used as a negative control. Reactions were incubated at 30°C for 30 min, boiled in SDS-PAGE loading buffer, resolved on an SDS gel, and subsequently analyzed by autoradiography.

Sucrose gradient fractionation

Human embryonic kidney 293T cells were lysed in lysis buffer [10 mM NaCl, 10 mM $MgCl_2$, 10 mM Tris-HCl (pH 7.5), 1% Triton X-100, 1% sodium deoxycholate, aprotinin 1 µg/mL, leupeptin 1 µg/mL, pepstatin A 1 µg/mL, PMSF 100 µg/mL]. After incubation on ice for 1 min, the extract was centrifuged for 1 min in a cold centrifuge and the supernatant was frozen in liquid nitrogen or loaded directly onto a 5%-65% linear sucrose gradient containing 30 mM Tris-HCl (pH 7.5), 100 mM NaCl, and 10 mM $MgCl_2$ and centrifuged in a Beckman SW 41 rotor for 3 hr at 37,000 rpm. Twelve fractions were collected while monitoring the absorbance at 260 nm. Proteins from each fraction were precipitated with 10% trichloracetic acid. The pellet was washed with acetone, dried, and resuspended in SDS-PAGE loading buffer (63 mM Tris-HCl pH 6.8, 5% glycerol, 1% SDS, 2.5% bromophenol-blue) . The first five fractions (polysomes) were pooled and loaded entirely on a single lane, whereas only 1/10 of fraction 11 and 12 was loaded on the gel.

The proteins were separated on 12% SDS polyacrylamide gel, transferred onto a polyvinilydene fluoride membrane and incubated with either rabbit anti-RPS19, or a monoclonal anti-PIM-1 antibody (Santa Cruz Biotechnology) or rabbit anti-S6K1 (Santa Cruz Biotechnology, Sc-230). Immunoblots were detected with SuperSignal reagent (Pierce).

Screening for mutations of PIM-1 in DBA patients

PIM-1 gene mutations were sought in 116 DBA patients: 17 patients carried mutations in *RPS19* and 99 did not. Patients with these mutations were studied to ascertain whether *PIM-1* is a modifier gene. Gene analysis was performed on genomic DNA isolated from peripheral blood leukocytes with standard techniques. Coding sequences and intron-exon boundaries were amplified by PCR and sequenced using the ABI PRISM 310 Genetic Analyzer (Applied Biosystem, Foster City, CA, USA). Restriction digestion of the specific PCR product was used to trace segregation of the identified DNA change in a mutated family and test 50 unrelated normal individuals. Genetic analyses were performed on patients and controls after informed consent had been given.

Results

RPS19 interacts with PIM-1

RPS19 gene mutations account for 25% of DBA cases. Even so, the correlation between *RPS19* functions and normal erythropoiesis is still unknown. We employed yeast two-hybrid screening to identify cellular proteins that interact with RPS19 and were thus likely to link it to pathways involved in the regulation of erythropoiesis. We used a full-length cDNA for *RPS19* to screen a cDNA library of human embryonic liver cells obtained at 19-24 weeks of gestation, when hepatic erythropoiesis is active. Approximately 10^7 yeast transformants, co-expressing the pLexA-*RPS19* bait and the cDNA clones, were tested in the two-hybrid assay and 38 clones that activated two separate reporter genes (β-galactosidase and leucine) in an *RPS19*-dependent fashion were recovered. Four independent clones (a-d) harbored in-frame fragments coding for PIM-1 proteins lacking different N-terminal portions. The most extended clone, designated *PIM-a*, encoded a PIM-1 protein lacking the first 47 codons. To rule out the possibility that the PIM-1/RPS19 interaction was an artifact due to the absence of this N-terminal sequence, we constructed a *PIM-1* full-length cDNA and confirmed the interaction in yeast cells (*data not shown*).

PIM-1 interacts with RPS19 in vitro and in human cells and phosphorylates it

To rule out the possibility that the PIM-1/RPS19 interaction could be mediated by yeast proteins, we performed an *in vitro* pull-down assay. GST-PIM-1 affinity resin was incubated with lysates from human embryonic kidney 293T cells transfected with pFLAG-RPS19 plasmid DNA. Bound proteins were separated by SDS-PAGE and analyzed by western blot using an anti-FLAG antibody. As shown in Figure 1A, tagged RPS19 protein was specifically retained by the GST-PIM resin. A co-immunoprecipitation assay was used to confirm the PIM-1/RPS19 interaction in living human cells. 293T cells were co-transfected with pFLAG-RPS19 and pHA-PIM DNA, and cell lysates were immunoprecipitated with an anti-FLAG antibody. Immunocomplexes were resolved by SDS-PAGE and analyzed by western blot using an anti-HA antibody. As shown in Figure 1B, a band corresponding to the expected HA-PIM-1 protein was exclusively revealed in lysates from cells co-transfected with pFLAG-RPS19 (Figure 1B, right panel).These data demonstrate that HA-tagged PIM-1 interacts with FLAG-RPS19.

Many data show that K562 cells are erythroid-

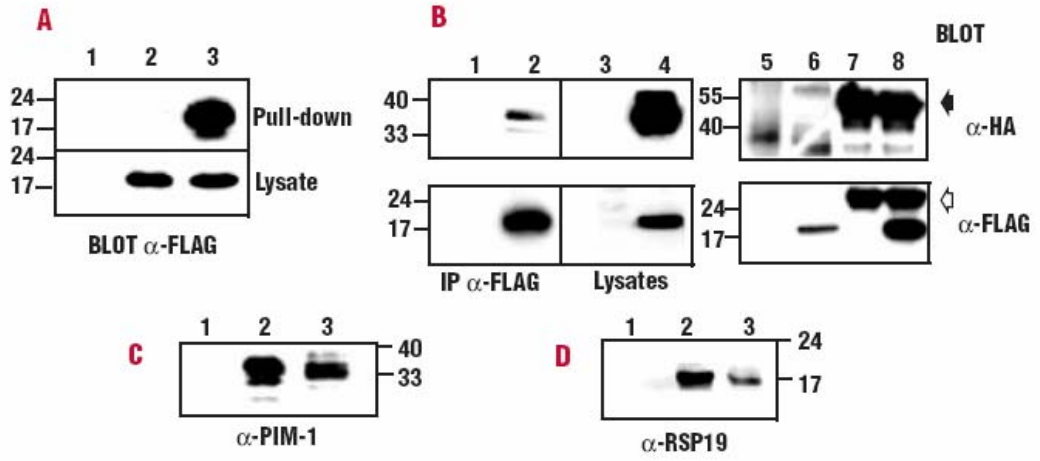

Figure 1. PIM-1 binds RPS19. A. 293T cells were transiently transfected with pcDNA3.1 empty vector (lane 1) or pFLAG-RPS19 construct (lanes 2 and 3) and cell lysates were incubated with either GST (lane 2) or GST-PIM-1 affinity resin (lanes 1 and 3). The bound proteins (upper panel) and total cell lysates (lower panel) were immunoblotted using an anti-FLAG antibody. B. 293T cells were transiently transfected with pcDNA3.1 empty vector (lanes 1, 3) or pFLAG-RPS19 plus pHA-PIM-1 (lanes 2, 4). Cell lysates were immunoprecipitated (left panel) with the anti-FLAG antibody and the immunocomplexes were immunoblotted with the anti-HA or anti-FLAG antibodies. Total lysates are shown in the middle panel. In the right panel 293T cells were transfected with empty vector (lanes 5, 7) or with pFLAG-RPS19 (lanes 6, 8); lysates were immunoprecipitated with anti-FLAG antibody (lanes 7, 8) and all samples were immunoblotted with anti-HA antibody (upper panel) or anti-FLAG antibody (lower panel). C and D. Lysates from human erythroleukemia K562 cells were incubated with either GST alone (C and D: lane 1) or GST-RPS19 (C: lane 2) or GST-PIM-1 affinity resins (D: lane 2). Total cell lysates (C and D: lane 3) were immunoblotted using the anti-PIM-1 antibody (C) or the anti-RPS19 antibody (D). Bold and empty head arrows indicate immunoglobulin heavy and light chains, respectively. Molecular weights are shown.

derived cells capable of hemoglobinization when exposed to erythropoietin.[32] Therefore, we also verified the RPS19/PIM-1 interaction in these cells, which represented a more pertinent model than embryonic kidney 293T cells. A pull-down assay was performed on K562 whole cell extracts with a GST-RPS19 affinity resin, and the bound proteins were analyzed by immunoblotting with an anti-PIM-1 antibody (Figure 1C). To ascertain whether the endogenous RPS19 was able to interact with PIM-1, we also performed the reverse pull-down assay using the GST-PIM-1 affinity resin; in this case the bound proteins were analyzed by immunoblotting with a RPS19 polyclonal antibody (Figure 1D). Taken together, these results confirm that RPS19 and PIM-1 interact each other, and suggest that they form a stable complex in living cells. Since PIM-1 is a serine/threonine kinase, we evaluated whether RPS19 is phosphorylated by PIM-1 in an *in vitro* kinase assay. The results shown in Figure 2 demonstrate that RPS19 is a substrate for PIM-1 activity *in vitro* and suggest that their interaction may be of functional significance.

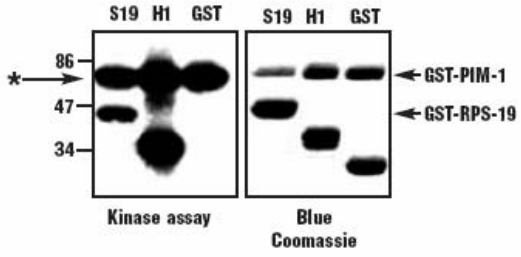

Figure 2. PIM-1 phosphorylates RPS19. GST-RPS19 and GST-PIM-1 were expressed in *E. coli* and affinity purified. Eluted GST-PIM-1 protein was used in the kinase assay, using as substrate either GST-RPS19 or histone-1 (positive control) or GST proteins (negative control). Phosphorylated proteins were separated by 10% SDS-PAGE and visualized by autoradiography (left panel). Coomassie staining (right panel) shows the proportion of recombinant protein used in the kinase assay. Data are representative of three independent experiments. *Autophosphorylation.

DBA natural mutants alter the binding with PIM-1

Various kinds of RPS19 mutations are found in DBA patients and many completely suppress the expression of the allele.[14,18,19] To determine whether DBA-associated mutations affect the binding of RPS19 to PIM-1, we analyzed the DBA missense mutants R56Q, R62W, R101H and an in-frame insertion, 53_54insAGA, by pull-down experiments. Lysates from 293T cells transfected with wild-type *RPS19* or mutant cDNAs were incubated with the GST-PIM-1 affinity resin and bound proteins analyzed by immunoblotting. The results, representative of several independent experiments, are shown in Figure 3A. All the mutant proteins bind to PIM-1, but with different strengths. In particular, whereas R101H showed reduced binding, R62W and R56Q showed increased binding, as compared to the

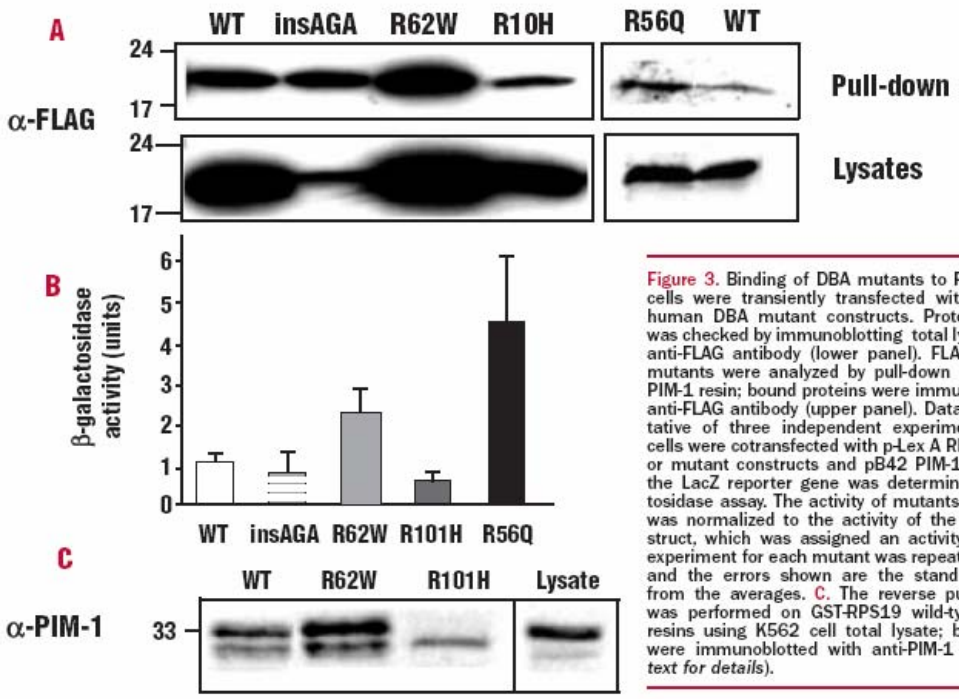

Figure 3. Binding of DBA mutants to PIM-1. A. 293T cells were transiently transfected with wild-type or human DBA mutant constructs. Protein expression was checked by immunoblotting total lysates with the anti-FLAG antibody (lower panel). FLAG-RPS19 DBA mutants were analyzed by pull-down assay on GST-PIM-1 resin; bound proteins were immunoblotted with anti-FLAG antibody (upper panel). Data are representative of three independent experiments. B. Yeast cells were cotransfected with p-Lex A RPS19 wild-type or mutant constructs and pB42 PIM-1. Activation of the LacZ reporter gene was determined by β-galactosidase assay. The activity of mutants in each assay was normalized to the activity of the wild-type construct, which was assigned an activity of 1.0. Each experiment for each mutant was repeated nine times, and the errors shown are the standard deviations from the averages. C. The reverse pull-down assay was performed on GST-RPS19 wild-type or mutant resins using K562 cell total lysate; bound proteins were immunoblotted with anti-PIM-1 antibody (*see text for details*).

wild-type protein. We also employed a semi-quantitative yeast β-galactosidase assay to evaluate these differences, as reported by other authors with other interactors.[33] The results (Figure 3B) show that the R101H mutant significantly reduced the interaction ($p<0.01$), whereas the R56Q and R62W mutants increased it ($p<0.01$). This behavior was shown in many independent experiments and was not due to differences in protein expression in yeast cells, as checked by western blot analysis (*data not shown*). Nevertheless, to exclude the possibility that stoichiometric differences among the RPS19 proteins could have affected their binding to PIM-1, we performed reverse pull-down assays using either the GST-RPS19 wild-type or R62W or R101H affinity resins. Equal amounts of K562 whole cell extract were incubated with equivalent amounts of GST-RPS19 affinity resins and bound endogenous PIM-1 was detected by immunoblotting with anti-PIM-1 antiserum (Figure 3C). In these conditions, too, compared to the wild-type protein, R101H showed reduced binding, whereas R62W showed increased binding. The results confirmed those observed in previous experiments and illustrate differences in the ability of the RPS19 proteins to interact with PIM-1.

At this stage, we do not know whether the mutations affect the on/off rate of the interaction because of structural differences or altered intracellular distribution of RPS19 proteins. Further analyses are needed to ascertain the functional role of these differences.

PIM-1 interacts with polysomes

To check whether RPS19 and PIM-1 interact on the ribosome, we analyzed the sedimentation profile of cytoplasmic extracts from 293T cells. Extracts were fractionated on a linear sucrose gradient to separate polysomes (fractions 1-5), 80S ribosomes, 60S and 40S ribosomal subunits and ribosome-free cytosol (as indicated in Figure 4A). Collected fractions were subjected to SDS-PAGE and immunoblot analysis with specific antibodies. Preliminary experiments on HEK 293 cells transiently transfected with pHA-PIM-1 indicated that at least part of the tagged PIM-1 was associated with polysomes and 40S ribosomal subunit (*not shown*).

We then repeated the analysis on untransfected cells with antibodies against PIM-1, RPS19, and a known cytosolic serine-threonine kinase, S6K1,[34] which phosphorylates another ribosomal protein, RPS6. The results (Figure 4B) indicate that S6K1 sediments in cytosolic ribosome-free fractions whereas RPS19 is distributed in fractions 1 to 9 (polysomes to 40S subunit), as expected. Interestingly, most PIM-1 distributes together with polysomes, as well as in 80S and 40S fractions, demonstrating that the interaction with RPS19 occurs on ribosomal particles. A lower molecular weight band recognized by anti-PIM-1 antibodies was visible in the cytosolic ribosome-free fractions. This could be a PIM-1 isoform reported by other authors in the nucleus and the cytoplasm.[35,36] However it constitutes a small fraction of the total cytoplasmic PIM-1. Therefore our results are

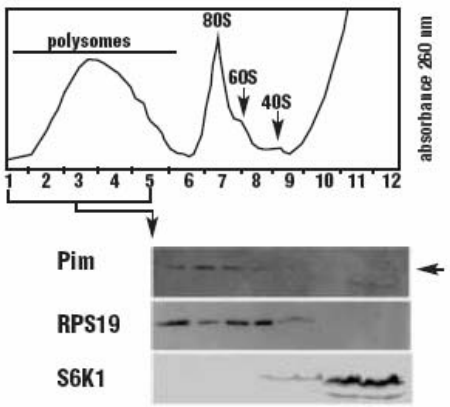

Figure 4. PIM-1 associates with ribosomes. A. Cytoplasmic extracts from 293T cells were fractionated onto a 5-65% sucrose gradient. The absorbance profile and the polysomal and ribosomal fractions are indicated. B. Fraction aliquots were precipitated by trichloroacetic acid and analyzed by western blot using antibodies against PIM-1, RPS19, and S6 kinase-1. Only 1/10 of fractions 11 and 12 was analyzed. Arrow indicates a slower migrating PIM-1 isoform (see *text*).

consistent with the possibility that the RPS19-PIM-1 reaction in the cytoplasm takes place on translationally active ribosomes. However, since both RPS19 and PIM-1 are also located in the nucleus, these data cannot rule out the possibility that the interaction takes place in the nucleus, as well.

Mutation screening of PIM-1 in DBA patients

To check whether *PIM-1* is a candidate gene for DBA forms not due to *RPS19* mutations, we performed mutational screening in 99 DBA patients and identified two missense mutations: P311T (C→A) and C17Y (G→A). These mutations were not found in 50 normal controls.

The patient heterozygous for P311T has an intra-atrial defect (ostium secundum type), was diagnosed in infancy, is transfusion-dependent and a steroid non-responder. Her reportedly healthy parents are not available for mutation analyses. We, therefore, analyzed the mutant's ability to bind RPS19 and to phosphorylate either RPS19 or histone-1, in pull-down or *in vitro* phosphorylation assays, respectively. These abilities were retained by the mutant PIM-1 (*data not shown*).

Mutation C17Y was found in a family which included two DBA patients: the mother and one of her two daughters. The affected mother is very short (<2SD) but without malformations. She was transfusion-dependent as a child and is now steroid-dependent. The affected daughter was anemic in infancy and responded to prednisone. After a few years, her hemoglobin levels normalized and she is now in complete remission. Her sister and father have always had normal hemoglobin levels. The C17Y mutation was carried by the affected daughter and her healthy father (both were heterozygotes); thus it does not segregate with the disease. Since there is a definite phenotypic variation between the mother and daughter, it is possible that C17Y is a phenotype modifier and reduces the severity of the disease. However, we did not observe a difference in binding strength to RPS19 between the C17Y mutant and wild-type protein in a pull-down assay (*data not shown*). We also searched for mutations in 17 patients who carried a mutation in RPS19 to test the hypothesis of *PIM-1* being a *modifier gene*, i.e. one capable of modifying the DBA phenotype and thus explaining the variable expressivity and/or incomplete penetrance of this disease. No mutations were identified in these patients.

Discussion

DBA is rare, but is important in hematology as a paradigm of an intrinsic genetic disorder of the committed erythroid progenitor. Many of its clinical and pathogenic aspects are still unclear. Mutations in the *RPS19* gene account for about 25% of cases.[4] DBA is the first and so far the only human disease known to be due to a structural ribosomal protein defect. However, the link between *RPS19* and erythropoiesis remains to be clarified. A generic deficiency of protein synthesis or a defect of a distinct, so far unknown, physiologic function of *RPS19* have been proposed.[13] These hypotheses are not mutually exclusive.

We employed a yeast two-hybrid screen to look for cellular partners that could link *RPS19* to biological pathways involved in erythropoiesis. Screening of a human fetal liver cDNA library identified the PIM-1 oncoprotein as a prominent RPS19 interactor. Our data also show that RPS19 interacts with PIM-1 both *in vitro* and in living cells, including the erythroleukemia-derived K562 cell line. *In vitro* this interaction leads to RPS19 phosphorylation. The functional role of the interaction in living cells is also suggested by the observation that in human 293T cells PIM-1 interacts with polysomes, the 80S and the small ribosomal subunit.

The proto-oncogene *pim-1* (MIM164960) was first isolated in mouse T-cell lymphomas as a preferred integration site of the Moloney leukemia virus.[37] It encodes for a serine/threonine kinase with autophosphorylating activity and a very short half-life.[31,38] PIM-1 is ubiquitously expressed in mammalian tissues, but is strongly induced as an early response gene by cytokines having hemopoietin-type receptors,[39-43] such as erythropoietin.[44,45] Ligand-mediated activation of these receptors rapidly activates one or more members of the Jak family of receptor-associated tyrosine kinases. Once acti-

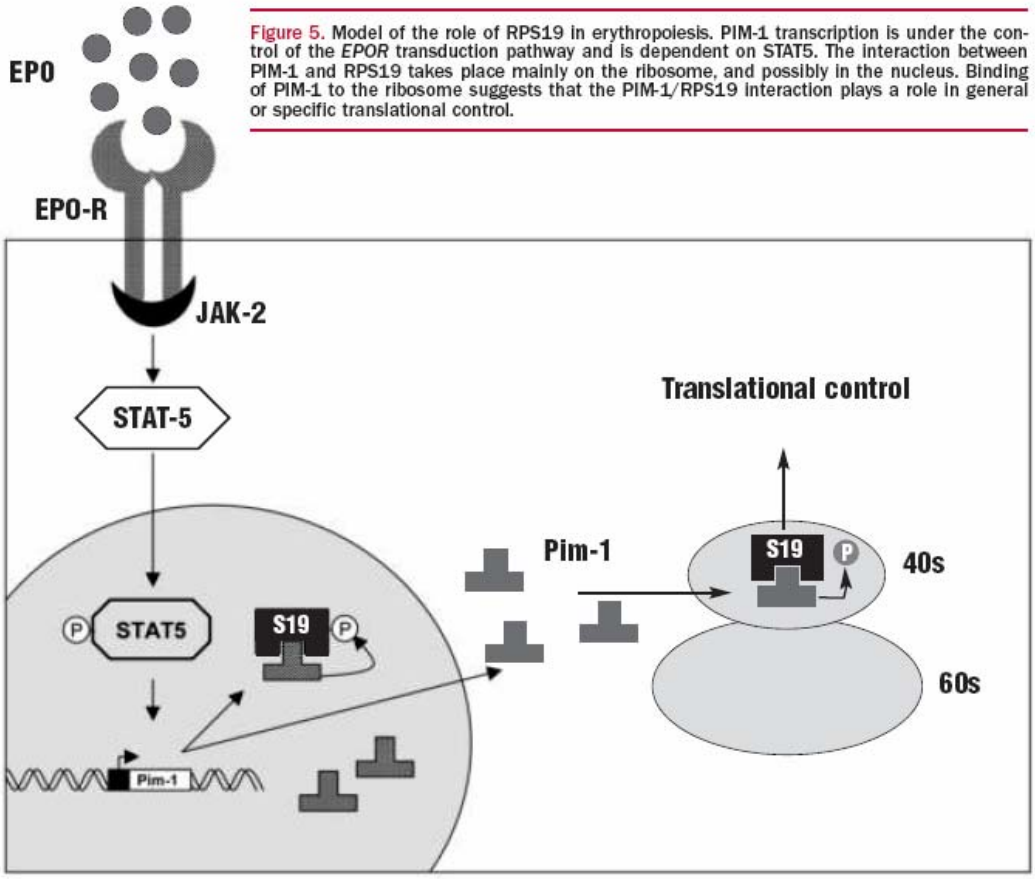

Figure 5. Model of the role of RPS19 in erythropoiesis. PIM-1 transcription is under the control of the *EPOR* transduction pathway and is dependent on STAT5. The interaction between PIM-1 and RPS19 takes place mainly on the ribosome, and possibly in the nucleus. Binding of PIM-1 to the ribosome suggests that the PIM-1/RPS19 interaction plays a role in general or specific translational control.

vated, these kinases phosphorylate members of the signal transducers and activators of transcription (STAT) family of transcription factors. Activated STAT dimerize, translocate to the nucleus and bind specifically to promoter regions of responsive genes. In the erythroid lineage, PIM-1 expression is correlated with the JAK2/STAT5-mediated mitogenic response to erythropoietin.[45] Since it is rapidly induced after cytokine stimulation, PIM-1 has been thought to play a significant role in the transduction of mitogenic signals from cytokines. In agreement with this hypothesis, the proliferative response to cytokines, in particular to interleukin-3, is impaired in *pim-1* null mice.[46] Confocal microscopy has revealed dynamic redistribution of *pim-1* during the cell cycle: it moves from the nucleus to the cytoplasm in interphase.[47] PIM-1 has also been associated with protection of hematopoietic cells from apoptosis induced by genotoxic stress or growth factor withdrawal.[48] Its role in erythropoiesis is also suggested by the observation that mice defective for *pim-1* have smaller red cells, whereas those hyperexpressing it display macrocytosis.[48,50] Its effect on erythropoiesis is supposed to be redundant in mice, since *pim-1*$^{-/-}$ mice show a mild phenotype.[49] On the other hand, hyperexpression of *pim-1* is involved in the development of myeloid leukemias and lymphomas.[50-53] Its effect on proliferation and on apoptosis protection are probably involved in tumorigenesis.[54] These effects are mediated by interactions with multiple substrates, as for other serine-threonine kinases.[35,36,55-64]

We have shown that RPS19 is another interactor for PIM-1. *In vitro* this interaction leads to RPS19 phosphorylation. Several other ribosomal proteins, such as RPS6 and RPL13, undergo phosphorylation by serine-threonine kinases.[65,66] Phosphorylation of RPS6 is considered to have a role in cell cycle control, whereas RPL13 phosphorylation is involved in a specific translational control. The binding of PIM-1 to the ribosome suggests that the PIM-1/RPS19 interaction plays a role in general or specific translational control (Figure 5).

We do not know whether the PIM-1/RPS19 interaction also takes place in the nucleus. However, the fact that in our assay a cytosolic protein which phosphorylates RPS6 (S6K1) was not detected in the ribosomal fractions indicates that the PIM-1/RPS19 association is more stable than a simple kinase-target interaction. The question of the place of *PIM-1* in the pathogenesis of DBA was investigated by determining whether the

PIM-1/RPS19 interaction is altered by RPS19 DBA mutants, and by looking for PIM-1 mutations in DBA patients. To ascertain whether four DBA mutants altered the PIM-1/RPS19 interaction, we used both a pull-down and a yeast β-galactosidase assay. Three mutants (R101H, R62W, and R56Q) showed a altered binding (Figure 3).

Reduced or increased binding may be supposed to disrupt the finely-tuned regulation of the many activities of PIM-1. R101H and *null RPS19* mutations would both impair its possible role in translational control and leave PIM-1 available for other interactions. Since DBA patients are at risk of malignancies,[1] this could be due to the increased availability of the oncoprotein PIM-1. By contrast, mutations that increase the strength of the interaction (R62W, R56Q) might sequester both PIM-1 and RPS19 and make them less available for their other functions, including ribosome biogenesis. Both hypotheses need to be assessed with other experiments. Lastly, mutational screening of *PIM-1* in 116 DBA patients led to the identification of two missense mutations. These do not seem to alter the interaction with RPS19 dramatically. These mutations do not affect important PIM-1 domains.[67,68] However, since they were not found in 50 normal controls, they are not common polymorphisms. Even if our data show that *PIM-1* is not a major DBA gene, its missense mutations may subtly modulate the phenotype in those patients who carry them.

As to the pathogenesis of DBA, our data cannot be used to discriminate between the two hypotheses which consider DBA as a ribosome biogenesis defect or due to the loss of a second function for *RPS19*. It is likely that both mechanisms co-operate to induce the erythroid defect. However, our data show that the function implicated by PIM-1 binding is still connected with the ribosome and that RPS19 may have more than a merely structural role. In conclusion, our study demonstrates that RPS19 is a new interactor of PIM-1. A link between hematopoietic growth factor signaling and *RPS19* has been identified for the first time and may be involved in the pathogenesis of DBA.

ACh: performed most of the experiments reported in the paper; ID, CS: developed the project, designed the experimental procedures and coordinated them; all other authors participated, with the following specific contributions: LG helped ACh to prepare the necessary constructs, she also performed the mutant pull-down assays in 293T cells; ACa performed the yeast two-hybrid system, which identified PIM-1 as a RPS19 interactor; AA performed all the experiments in K562 cells; PS performed the β-galactosidase assay in yeast; EG, AB performed mutation detection analyses of PIM-1 in the 116 DBA patients; EG also performed mutation detection analysis of RPS19 on half of the DBA patients; FL and MA performed the sucrose gradient fractionation assay and the relative western blotting analyses; ND diagnosed the disease and performed mutation detection analysis of RPS19 on half of the DBA patients; UD participated in the design of the experimental work focused on the definition of protein-protein interactions; UR diagnosed DBA in half of the DBA patients, provided their clinical data, coordinated the mutation detection analyses. Figures 1,2,3, and 5 were prepared by ACh, figure 4 was prepared by FL. ID takes primary responsibility for the paper. The authors declare that they have no potential conflict of interest.

This work was supported by Telethon Grant E619 and GGP02434 to ID and FL; FIRB grant 2001 to ID; MURST grants to ID and UR Cariplo and Compagnia San Paolo grants. We thank S. Biffo, F. Di Cunto, C. Camaschella and C. Dompè for their helpful discussion and/or technical advice.

Manuscript received April 1, 2005. Accepted September 6, 2005.

References

1. Alter BP. Bone marrow failure syndromes in children. Pediatr Clin North Am 2002; 49:973-88.
2. Nathan DG, Clarke BJ, Hillman DG, Alter BP, Housman DE. Erythroid precursors in congenital hypoplastic (Diamond-Blackfan) anemia. J Clin Invest 1978; 61: 489-98.
3. Halperin DS, Freedman MH. Diamond-Blackfan anemia: etiology, pathophysiology, and treatment. Am J Pediatr Hematol Oncol 1989;11:380-94.
4. Campagnoli MF, Garelli E, Quarello P, Carando A, Varotto S, Nobili B, et al. Molecular basis of Diamond-Blackfan anemia: new findings from the Italian registry and a review of the literature. Haematologica 2004;89:480-9.
5. Bagnara GP, Zauli G, Vitale L, Rosito P, Vecchi V, Paolucci G, et al. In vitro growth and regulation of bone marrow enriched CD34+ hematopoietic progenitors in Diamond-Blackfan anemia. Blood 1991;78:2203-10.
6. Ohene-Abuakwa Y, Orfali KA, Marius C, Ball SE. Two-phase culture in Diamond Blackfan anemia: localization of erythroid defect. Blood 2005;105:838-46.
7. Abkowitz JL, Sabo KM, Nakamoto B, Blau CA, Martin FH, Zsebo KM, et al. Diamond-Blackfan anemia: in vitro response of erythroid progenitors to the ligand for c-kit. Blood 1991;78:2198-202.
8. Olivieri NF, Grunberger T, Ben-David Y, Ng J, Williams DE, Lyman S, et al. Diamond-Blackfan anemia: heterogenous response of hematopoietic progenitor cells in vitro to the protein product of the steel locus. Blood 1991;78:2211-5.
9. Dianzani I, Garelli E, Crescenzio N, Timeus F, Mori PG, Varotto S, et al. Diamond-Blackfan anemia: expansion of erythroid progenitors in vitro by IL-9, but exclusion of a pathogenetic role for the IL-9 gene and the hemopoietic gene cluster on chromosome 5q. Exp Hematol 1997;25:1270-7.
10. Dianzani I, Garelli E, Dompè C, Crescenzio N, Locatelli F, Schilirò G, et al. Mutations in the erythropoietin receptor gene are not a common cause of Diamond-Blackfan anemia. Blood 1996;87: 2568-72.
11. Spritz RA, Freedman MH. Lack of mutations of the MGF and KIT genes in Diamond-Blackfan anemia. Blood 1993; 81:3165.
12. Vlachos A, Federman N, Reyes-Haley C, Abramson J, Lipton JM. Hematopoietic stem cell transplantation for Diamond-Blackfan anemia: a report from the Diamond-Blackfan anemia registry. Bone Marrow Transplant 2001;27:381-6.
13. Draptchinskaia N, Gustavsson P, Andersson B, Pettersson M, Willig TN, Dianzani I, et al. The gene encoding ribosomal protein S19 is mutated in Diamond-Blackfan anaemia. Nat Genet 1999;21:169-75.
14. Willig T-N, Draptchinskaia N, Dianzani I, Ball S, Niemeyer C, Ramenghi U, et al. Mutations in ribosomal protein S19 gene and Diamond Blackfan Anemia: wide variations in phenotypic expression. Blood 1999;94:4294-306.
15. Gazda H, Lipton JM, Willig T-N, Ball S, Niemeyer CM, Tchernia G, et al. Evidence for linkage of familial Diamond-Blackfan anemia to chromosome 8p23.3-p22 and for non-19q non-8p disease. Blood 2001;97:2145-50.
16. Kongsuwan K, Yu Q, Vincent A, Frisardi MC, Rosbash M, Lengyel JA, Merriam J. A Drosophila Minute gene encodes a ribosomal protein. Nature 1985;317:555-8.
17. Cramton SE, Laski FA. String of pearls encodes *Drosophila* ribosomal protein S2, has Minute-like characteristics, and is required during oogenesis. Genetics 1994;137:1039-48.
18. Chatr-aryamontri A, Angelini M, Garelli E, Tchernia G, Ramenghi U, Dianzani I, et al. Nonsense-mediated and nonstop decay of ribosomal protein S19 mRNA in Diamond-Blackfan anemia. Hum Mutat

2004; 24:526-33.
19. Gazda HT, Zhong R, Long L, Niewiadomska E, Lipton JM, Ploszynska A, et al. RNA and protein evidence for haploinsufficiency in Diamond-Blackfan anaemia patients with RPS19 mutations. Br J Haematol 2004;127:105-13.
20. Da Costa L, Tchernia G, Gascard P, Lo A, Meerpohl J, Niemeyer C, et al. Nucleolar localization of RPS19 protein in normal cells and mislocalization due to mutations in the nucleolar localization signals in 2 Diamond-Blackfan anemia patients: potential insights into pathophysiology. Blood 2003;101:5039-45.
21. Cretien A, Da Costa LM, Rince P, Proust A, Mohandas N, Gazda H, et al. Subcellular localization and protein expression level of twelve ribosomal protein S19 mutants identified in DBA patients. American Society of Hematology Annual Meeting, December 6-9. 2003; San Diego, USA[abstract 717].
22. Da Costa L, Narla G, Willig T-N, Peters LL, Parra M, Fixler J, et al. Ribosomal protein S19 expression during erythroid differentiation. Blood 2003; 101:318-24.
23. Hamaguchi I, Ooka A, Brun A, Richter J, Dahl N, Karlsson S. Gene transfer improves erythroid development in ribosomal protein S19-deficient Diamond-Blackfan anemia. Blood 2002;100:2724-31.
24. Flygare J, Kiefer T, Miyake K, Utsugisawa T, Hamaguchi I, Da Costa L, et al. Deficiency of ribosomal protein S19 in CD34+ cells generated by siRNA blocks erythroid development and mimics defects seen in Diamond-Blackfan anemia. Blood 2004; 105:4627-34.
25. Wool IG. Extraribosomal functions of ribosomal proteins. Trends Biochem Sci 1996;21:164-5.
26. Soulet F, Al Saati T, Roga S, Amalric F, Bouche G. Fibroblast growth factor-2 interacts with free ribosomal protein S19. Biochem Biophys Res Commun 2001; 289:591-6.
27. Nishiura H, Tanase S, Sibuya Y, Nishimura T, Yamamoto T. Determination of the cross-linked residues in homo-dimerization of S19 ribosomal protein concomitant with the exhibition of monocyte chemotactic activity. Lab Invest 1999;79: 915-23.
28. Coates PJ, Hall PA. The yeast two-hybrid system for identifying protein-protein interactions. J Pathol 2003; 199: 4-7
29. Gietz D, St Jean A, Woods RA, Schiestl RH. Improved method for high efficiency transformation of intact yeast cells. Nucl Acid Res 1992;20:1425.
30. den Dunnen JT, Antonarakis SE. Mutation nomenclature extensions and suggestions to describe complex mutations: a discussion. Hum Mutat 2000; 15: 7-12.
31. Hoover D, Friedmann M, Reeves R, Magnuson NS. Recombinant human pim-1 protein exhibits serine/threonine kinase activity. J Biol Chem 1991; 266:14018-23.
32. Koeffler HP, Golde DW. Human myeloid leukemia cell lines: a review. Blood 1980; 56:344-50.
33. Akey DT, Zhu X, Dyer M, Li A, Sorensen A, Blackshaw S, Fukuda-Kamitani T, et al. The inherited blindness associated protein AIPL1 interacts with the cell cycle regulator protein NUB1. Hum Mol Genet 2002;11:2723-33.
34. Pullen N, Thomas G. The modular phosphorylation and activation of p70s6k. FEBS Lett 1997;410:78-82.
35. Wang Z, Bhattacharya N, Meyer MK, Seimiya H, Tsuruo T, Magnuson NS. Pim-1 negatively regulates the activity of ptp-u2s phosphatase and influences terminal differentiation and apoptosis of monoblastoid leukemia cells. Arch Biochem Biophys 2001;390:9-18.
36. Wang Z, Bhattacharya N, Mixter PF, Wei W, Sedivy J, Magnuson NS. Phosphorylation of the cell cycle inhibitor p21Cip1/WAF1 by Pim-1 kinase. Biochim Biophys Acta 2002; 1593:45-55.
37. Cuypers HT, Selten G, Quint W, Zijlstra M, Maandag ER, Boelens W, et al. Murine leukemia virus-induced T-cell lymphomagenesis: integration of proviruses in a distinct chromosomal region. Cell 1984;37:141-50.
38. Stewart BE, Rice RH. Differentiation-associated expression of the proto-oncogene pim-1 in cultured human keratinocytes. J Invest Dermatol 1995; 105: 699-703.
39. Dautry F, Weil D, Yu J, Dautry-Varsat A. Regulation of pim and myb mRNA accumulation by interleukin-2 and interleukin-3 in murine hematopoietic cell lines. J Biol Chem 1988;263:17615-20.
40. Wingett D, Reeves R, Magnuson NS. Stability changes in pim-1 proto-oncogene mRNA after mitogen stimulation of normal lymphocytes. J Immunol 1991; 147:3653-9.
41. Lilly M, Le T, Holland P, Hendrickson SL. Sustained expression of the pim-1 kinase is specifically induced by cytokines whose receptors are structurally related. Oncogene 1992;7:727-2.
42. Cosman, D. The hematopoietic receptor superfamily. Cytokine 1992;5:95-106.
43. Horseman ND, Yu-Lee LY. Transcriptional regulation by the helix bundle peptide hormones: growth hormone, prolactin, and hematopoietic cytokines. Endocr Rev 1994;15:627-49.
44. Joneja B, Wojchowski, DM. Mitogenic signaling and inhibition of apoptosis via the erythropoietin receptor Box-1 domain. J Biol Chem 1997; 272: 11176-84.
45. Joneja B, Chen HC, Seshasayee D, Wrentmore AL, Wojchowski DM. Mechanisms of stem cell factor and erythropoietin proliferative co-signaling in FDC2-ER cells. Blood 1997; 90:3533-45.
46. Domen J, van der Lugt NM, Laird PW, Saris CJ, Clarke AR, Hooper ML, et al. Impaired interleukin-3 response in Pim-1-deficient bone marrow-derived mast cells. Blood 1993;82:1445-52.
47. Bhattacharya N, Wang Z, Davitt C, McKenzie IF, Xing PX, Magnuson NS. Pim-1 associates with protein complexes necessary for mitosis. Chromosoma 2002;111:80-95.
48. Pircher TJ, Zhao S, Geiger JN, Wojchowski DM. Pim kinase protects hematopoietic FDC cells from genotoxin-induced death. Oncogene 2000; 19: 3684-92.
49. Laird PW, van der Lugt NM, Clarke A, Domen J, Linders K, Berns A. In vivo analysis of Pim-1 deficiency. Nucl Acid Res 1993;21:4750-5.
50. van der Houven van Oordt CW, Schouten TG, van Krieken JH, van Dierendonck JH, van der Eb AJ, Breuer ML. X-ray-induced lymphomagenesis in E mu-pim-1 transgenic mice: an investigation of the co-operating molecular events. Carcinogenesis 1998;19:847-53.
51. Breuer M, Wientjens E, Verbeek S, Slebos R, Berns A. Carcinogen-induced lymphomagenesis in pim-1 transgenic mice: dose dependence and involvement of myc and ras. Cancer Res 1991;51:958-63.
52. Nagarajan L, Louie E, Tsujimoto Y, ar-Rushdi A, Huebner K, Croce CM. Localization of the human pim oncogene (PIM) to a region of chromosome 6 involved in translocations in acute leukemias. Proc Natl Acad Sci USA 1986;83:2556-60.
53. Amson R, Sigaux F, Przedborski S, Flandrin G, Givol D, Telerman A. The human protooncogene product p33pim is expressed during fetal hematopoiesis and in diverse leukemias. Proc Natl Acad Sci USA 1989;86:8857-61.
54. Bachmann M, Möröy T. The serine/threonine kinase Pim-1. Int J Biochem Cell Biol 2005;37:726-30.
55. Mochizuki T, Kitanaka C, Noguchi K, Muramatsu T, Asai A, Kuchino Y. Physical and functional interactions between Pim-1 kinase and Cdc25A phosphatase. Implications for the Pim-1 mediated activation of the c-Myc signaling pathway. J Biol Chem 1999; 274: 18659-66.
56. Bachmann M, Hennemann H, Xiang Xing P, Hoffmann I, Moroy T. The oncogenic serine/threonine kinase Pim-1 phosphorylates and inhibits the activity of Cdc25C-associated kinase 1 (C-TAK1) a novel role for pim-1 at the G2/M cell cycle checkpoint. J Biol Chem 2004; 279: 48319-28.
57. Leverson JD, Koshinen PJ, Orrico FC, Rainio EM, Jalkanen KJ, Dash AB, et al. Pim-1 kinase and p-100 cooperate to enhance c-Myb activity. Mol Cell 1998; 2:417-25.
58. Koike N, Maita H, Taira T, Ariga H, Iguchi-Ariga SM. Identification of heterochromatin protein 1 (HP1) as a phosphorylation target by Pim-1 kinase and the effect of phosphorylation on the transcriptional repression function of HP1. FEBS Lett 2000;467:17-21.
59. Maita H, Harada Y, Nagakubo D, Kitaura H, Ikeda M, Tamai K, et al. PAP-1, a novel target protein of phosphorylation by pim-1 kinase. Eur J Biochem 2000; 267:5168-78.
60. Rainio EM, Sandholm J, Koskinen PJ. Cutting edge: Transcriptional activity of NFATc1 is enhanced by the Pim-1 kinase. J Immunol 2002;168:1524-27.
61. Ishibashi Y, Maita H, Yano M, Koike N, Tamai K, Ariga H, et al. Pim-1 translocates sorting nexin 6/TRAF4-associated factor 2 from cytoplasm to nucleus. FEBS Lett 2001;506:33-8.
62. Chen XP, Losman JA, Cowan S, Donahue E, Fay S, Vuong BQ, et al. Pim serine/threonine kinases regulate the stability of Socs-1 protein. Proc Natl Acad Sci USA 2002;99:2175-80.
63. Peltola KJ, Paukku K, Aho TL, Ruuska M, Silvennoinen O, Koskinen PJ. Pim-1 kinase inhibits STAT5-dependent transcription via its interactions with SOCS1 and SOCS3. Blood 2004; 103:3744-50.
64. Mizuno K, Shirogane T, Shinohara A, Iwamatsu A, Hibi M, Hirano T. Regulation of Pim-1 by Hsp90. Biochem Biophys Res Commun 2001;281:663- 9.
65. Volarevic S, Thomas G. Role of S6 phosphorylation and S6 kinase in cell growth. Prog Nucleic Acid Res Mol Biol 2001; 65:101-27.
66. Mazumder B, Sampath P, Seshadri V, Maitra RK, DiCorleto PE, Fox PL. Regulated release of L13a from the 60S ribosomal subunit as a mechanism of transcript-specific translational control. Cell 2003;115:187-98.
67. Qian KC, Wang L, Hickey ER, Studts J, Barringer K, Peng C, et al. Structural basis of constitutive activity and a unique nucleotide binding mode of human Pim-1 kinase. J Biol Chem 2005; 280:6130-7.
68. Jacobs MD, Black J, Futer O, Swenson L, Hare B, Fleming M, et al. Pim-1 ligand-bound structures reveal the mechanism of serine/threonine kinase inhibition by LY294002. J Biol Chem 2005;280:13728-34.

Chapter 3

Analysis of the RPS19 interactome

After the identification of PIM-1, our search for molecular interactors of RPS19 proceeded using a different strategy. We purified RPS19 binding proteins by a pull-down experiment and we analyzed them by coupling monodimensional electrophoresis and mass spectrometry. The binding of RPS19 with some of its putative interactors was validated with immunoprecipitation and western blot, and the reliability of this approach was ascertained. We found 159 proteins, most nucleolar, even if we used a whole cell extract. Many of these proteins interact with each other and they are likely to partecipate with RPS19 in one or more multiprotein complexes. We identified several ribosomal proteins, RNA helicases and other components of the 90S preribosome, the early ribonucleoproteic precursor of both ribosomal subunits. Among them there were proteins of the box C/D small nucleolar ribonucleoprotein (snoRNP), such as fibrillarin and NOP56, and proteins of the H/ACA box snoRNP, and in particular dyskerin, whose mutations are responsible for dyskeratosis congenita. Both these snoRNP complexes are required for rRNA maturation and ribosome biogenesis, pointing out the connection between RPS19 and these processes. RPS19 interactome also includes some splicing factors and transcription factors, as well as some translation regulators, such as IGF2BP1 and STAU1; these data suggest the existence of additional functional roles for RPS19.

The proteomic analysis of RPS19 interactors by mass spectrometry has been performed in collaboration with the laboratory directed by Prof. Margherita Ruoppolo in the Department of Biochemistry and Medical Biotechnologies, University Federico II, Napoli.

Supplemental Material can be found at:
http://www.mcponline.org/cgi/content/full/M600156-MCP200/DC1

Analysis of the Ribosomal Protein S19 Interactome*[S]

Stefania Orrù‡§, Anna Aspesi¶, Marta Armiraglio¶, Marianna Caterino§‖, Fabrizio Loreni**, Margherita Ruoppolo§‖, Claudio Santoro¶‡‡, and Irma Dianzani¶‡‡§§

Ribosomal protein S19 (RPS19) is a 16-kDa protein found mainly as a component of the ribosomal 40 S subunit. Its mutations are responsible for Diamond Blackfan anemia, a congenital disease characterized by defective erythroid progenitor maturation. Dysregulation of RPS19 has therefore been implicated in this defective erythropoiesis, although the link between them is still unclear. Two not mutually exclusive hypotheses have been proposed: altered protein synthesis and loss of unknown functions not directly connected with the structural role of RPS19 in the ribosome. A role in rRNA processing has been surmised for the yeast ortholog, whereas the extracellular RPS19 dimer has a monocyte chemotactic activity. Three proteins are known to interact with RPS19: FGF2, complement component 5 receptor 1, and a nucleolar protein called RPS19-binding protein. We have used a yeast two-hybrid approach to identify a fourth protein: the serine-threonine kinase PIM1. The present study describes our use of proteomics strategies to look for proteins interacting with RPS19 to determine its functions. Proteins were isolated by affinity purification with a GST-RPS19 recombinant protein and identified using LCMS/MS analysis coupled to bioinformatics tools. We identified 159 proteins from the following Gene Ontology categories: NTPases (ATPases and GTPases; five proteins), hydrolases/helicases (19 proteins), isomerases (two proteins), kinases (three proteins), splicing factors (five proteins), structural constituents of ribosome (29 proteins), transcription factors (11 proteins), transferases (five proteins), transporters (nine proteins), DNA/RNA-binding protein species (53 proteins), other (one dehydrogenase protein, one ligase protein, one peptidase protein, one receptor protein, and one translation elongation factor), and 13 proteins of still unknown function. Proteomics results were validated by affinity purification and Western blotting. These interactions were further confirmed by co-immunoprecipitation using a monoclonal RPS19 antibody. Many interactors are nucleolar proteins and thus are expected to take part in the RPS19 interactome; however, some proteins suggest additional functional roles for RPS19. *Molecular & Cellular Proteomics 6:382–393, 2007.*

RPS19[1] is a structural component of the ribosomal 40 S subunit. It was considered to have only a structural role until its loss-of-function mutations were identified in patients with a rare hematological disease, Diamond-Blackfan anemia (DBA) (OMIM 105650) (1–3). DBA is characterized by defective erythroid progenitor maturation and is the first human disease due to mutations in a structural ribosomal protein. Dysregulation of RPS19 has thus been surmised as the cause of this defective erythropoiesis, although the link between them is still unclear. The finding that most RPS19 mutations suppress the expression of the allele has suggested that haploinsufficiency is the main cause of the defect (4, 5). However, some patients carry missense mutations in the RPS19 gene. Deficient nucleolar localization may lead to abnormal ribosome incorporation and has been found for four missense mutants (6, 7)[2]; this means that the disease mechanism may not be univocal.

RPS19 expression is increased during the intense proliferation at the start of erythropoiesis compared with the maturation of precursors at its close (8). Enhanced erythroid burst-forming unit formation after overexpression of a wild type transgene in CD34+ bone marrow cells from DBA patients (9) and depressed *in vitro* erythropoiesis when RPS19 is knocked down (10) are other illustrations of its role.

Like other ribosomal proteins (RPs), RPS19 translocates from the cytoplasm to the nucleus where it participates in ribosome biogenesis. In yeast its absence is associated with

From the §Centro di Ingegneria Genetica (CEINGE) Advanced Biotechnologies scarl, 80131 Napoli, Italy, ‡Faculty of Movement Sciences, Università di Napoli "Parthenope" and Fondazione SDN Napoli (Istituto di Ricerca Diagnostica e Nucleare), 80133 Napoli, Italy, ‖Department of Biochemistry and Medical Biotechnologies, Università di Napoli "Federico II," 80131 Napoli, Italy, **Department of Biology, Università "Tor Vergata," 00133 Roma, Italy, and ¶Interdisciplinary Research Center of Autoimmune Diseases (IRCAD) and Department of Medical Sciences, Università del Piemonte Orientale, 28100 Novara, Italy

Received, April 27, 2006, and in revised form, September 12, 2006
Published, MCP Papers in Press, December 6, 2006, DOI 10.1074/mcp.M600156-MCP200

[1] The abbreviations used are: RPS19, ribosomal protein S19; RP, ribosomal protein; GATA1, globin transcription factor 1; DBA, Diamond-Blackfan anemia; HPRD, Human Protein Reference Database; FGF, fibroblast growth factor; PCV, packed cell volume; NCL, nucleolin; μLC, microcapillary LC; NCBI, National Center for Biotechnology Information; IGF2BP1, insulin-like growth factor 2-binding protein 1; MCM, minichromosome maintenance-deficient protein; RNP, ribonucleoprotein; OMIM, Online Mendelian Inheritance in Man.

[2] F. Loreni, manuscript in preparation.

abnormal rRNA cleavage and defective 40 S biogenesis (11, 12). It has recently been suggested that defective erythropoiesis in DBA is due to the faulty protein synthesis particularly evident in progenitors whose RPS19 levels are lower than in other tissues (13, 14).

We have used a yeast two-hybrid system to show that RPS19 binds PIM1, a ubiquitous serine-threonine kinase whose expression can be induced in erythropoietic cells by several growth factors, such as erythropoietin (15). We also showed that in human 293T cells PIM1 interacts with ribosomes and may be involved in translational control (15). A role in translational control of specific transcripts has been shown for other ribosomal proteins (*i.e.* RPL13 and RPL26) (16, 17).

It thus appears that RPS19, in addition to its structural role in the ribosome, is involved in ribosome biogenesis, specifically in rRNA processing and possibly in translation. These functions are probably assisted by interaction with different protein substrates.

In the study now reported, we used functional proteomics procedures to look for proteins interacting with RPS19 (18) and thus secure additional information regarding its function and regulation. We identified 159 RPS19-associated proteins. These included many ribosomal proteins and proteins with a known role in ribosome biogenesis. Furthermore the identification of proteins with other functions, such as translational control and splicing, indicates that RPS19 may also be involved in RNA processing/metabolism and translational control.

EXPERIMENTAL PROCEDURES

Cell Culture and Whole Cell Extract—Human erythroleukemia K562 cells (ATCC number CCL-243) were cultured in RPMI 1640 medium (Sigma) supplemented with 10% fetal bovine serum (Invitrogen), 100 units/ml penicillin, and 0.1 mg/ml streptomycin at 37 °C with 5% CO_2.

To prepare whole cell extract, 10^8 K562 cells were harvested and resuspended in 4 packed cell volumes (PCVs) of ice-cold buffer H (10 mM Tris-HCl, pH 7.9, 10 mM KCl, 2 mM EDTA, 20 μg/ml leupeptin, 8 μg/ml pepstatin A, 0.2 units/ml aprotinin, 2 mM PMSF, 5 mM DTT, 2 mM sodium metabisulfite). Cells were disrupted with 4 PCVs of a solution containing 50% glycerol and 25% sucrose and 1 PCV of saturated ammonium sulfate. Cell debris were removed by centrifugation at 35,000 rpm for at least 3 h, and proteins were precipitated with 0.33 g/ml ammonium sulfate. The protein pellet was resuspended in 1 ml of TM 0.0 buffer (50 mM Tris-HCl, pH 7.9, 12.5 mM $MgCl_2$, 1 mM EDTA, 1 mM DTT, 1 mM PMSF) and stored at −20 °C.

Expression and Purification of Fusion Proteins—The human RPS19 cDNA was amplified by RT-PCR (15) and cloned into pGEX-4T-1 (Amersham Biosciences) to generate plasmid pGEX-RPS19. As a further control we used a pGST-NTGATA1 construct that encodes for a GST fusion protein with the N-terminal domain of the human GATA1 transcription factor (19).

GST, GST-RPS19, and GST-GATA fusion proteins were expressed in *Escherichia coli* cells, strain BL21, by induction with 0.5 mM isopropyl 1-thio-β-D-galactopyranoside for 1 h at 37 °C. Bacteria were resuspended in PBS containing 1% Triton X-100, 1 mM EDTA, 1 mM PMSF, 1 μg/ml leupeptin, 1 μg/ml aprotinin, and 1 μg/ml pepstatin. Bacterial extracts were sonicated and centrifuged to remove cell debris. GST proteins were purified by affinity binding to GST·Bind™ resin (Novagen, Madison, WI). Protein samples were separated by SDS-PAGE and compared with known concentrations of bovine serum albumin after Coomassie Brilliant Blue staining.

Affinity Purification—Whole cell extract was preincubated with GST resin (300 μg of recombinant protein) for 1 h at 4 °C. Unbound proteins were then incubated with the same quantity and volume of GST-RPS19 resin overnight at 4 °C on a rocker. The resin was extensively washed with TM 0.1 buffer (0.1 M KCl in TM 0.0 buffer), and bound proteins were eluted with TM 0.5 buffer (0.5 M KCl in TM 0.0 buffer) and precipitated with 20% trichloroacetic acid. The pellets were washed twice with acetone, dried, and used for mass spectrometry. This experiment was repeated six times to provide enough samples.

Monoclonal Antibody against RPS19—Immunization and screening for putative monoclonal antibodies have been carried out according to Cianfriglia *et al.* (20). Briefly BALB/c mice (age, 12 weeks) were repeatedly intraperitoneally injected (five times) with 30 μg of purified GST-human RPS19 (the first injection was diluted with Freund's complete adjuvant; the second injection, after 10 days, was diluted with Freund's incomplete adjuvant; the other boosters, every 4 days, were with saline solution). Hybrid cells were obtained by fusion of myeloma cells (SP2/0-AG-14) with polyethylene glycol (Sigma) and were screened by ELISA with recombinant GST-RPS19. Positive clones were expanded, and the supernatant was analyzed by Western blotting. Highly positive hybridomas were cloned by limiting dilution, and the stable line C3 was selected for the production of antibody specific for RPS19. The heavy chain isotype of C3 monoclonal antibody is IgG1 with κ light chains as determined by a mouse hybridoma subtyping kit (Roche Applied Science).

Validation by Western Blot and Co-immunoprecipitation—To validate the MS/MS results, new preparations of GST-RPS19 pulldowns were subjected to Western blot analysis. Antibodies specific for PIM1 (Upstate, Charlottesville, VA), insulin-like growth factor 2-binding protein 1 (IGF2BP1) (IMP1), minichromosome maintenance-deficient protein 6 (MCM6), DDX5, and nucleolin (NCL) (C23) (Santa Cruz Biotechnology, Santa Cruz, CA) were used according to the manufacturer's instructions. Monoclonal anti-STAU1 antibody was a gift from Dr. Luc DesGroseillers (21) (University of Montreal, Montreal, Canada) and used at a dilution of 1:1000. The polyclonal antibody against DKC1 was a gift from Philip Mason (Washington University, St. Louis, MO) (22) and used at a dilution of 1:5000. All immunoblot detections were carried out using horseradish peroxidase-conjugated secondary antibodies and enhanced chemiluminescence (Amersham Biosciences) with the exception of the nucleolin blots where an alkaline phosphatase-conjugated secondary antibody was used (Sigma).

For co-immunoprecipitation analyses, 0.5% Triton X-100 was added to K562 whole cell extracts, prepared as described above. Extracts were precleared by incubation with protein G-agarose (Sigma) on a rocker for 1 h at 4 °C.

The supernatant was incubated with an anti-RPS19 monoclonal antibody (hybridoma supernatant) and with protein G-agarose on a rocker at 4 °C for 16 h. As a negative control, we used an anti-hemagglutinin monoclonal antibody (Santa Cruz Biotechnology).

Immunocomplexes were pelleted by centrifugation, extensively washed with Washing Buffer (TM 0.1 + 0.5% Triton X-100), resuspended in SDS-PAGE Sample Buffer (750 mM Tris-HCl, pH 8.8, 5% SDS, 40% glycerol, 10% β-mercaptoethanol), and subjected to Western blot analysis using antibodies specific for PIM1, IGF2BP1, MCM6, DDX5, STAU1, DKC1, and NCL.

SDS-PAGE, In-gel Digestion, Peptide Mapping, and Mass Spectrometry—The six pellets obtained by affinity purification were resuspended in SDS-PAGE sample buffer and pooled for one-dimensional electrophoresis. The total volume for each sample (GST and GST-RPS19) was 50 μl. The two protein mixtures were fractionated by 8–18% SDS-PAGE. Molecular masses of protein bands were esti-

mated by using Precision Plus All Blue protein standards (Bio-Rad). Protein electrophoretic patterns were then visualized using GelCode Blue Stain Reagent (Pierce).

The GST-RPS19 and GST gel lanes were cut to create 65 2-mm slices per lane. Each slice was crushed and washed first with acetonitrile and then with 0.1 M ammonium bicarbonate. Protein samples were reduced by incubation in 10 mM dithiothreitol for 45 min at 56 °C and alkylated with 55 mM iodoacetamide in 0.1 M ammonium bicarbonate for 30 min at room temperature in the dark as described previously (23). The gel particles were then washed with 0.1 M ammonium bicarbonate and acetonitrile. Enzymatic digestions were carried out with modified trypsin (Sigma) (10 ng/μl) in 50 mM ammonium bicarbonate, pH 8.5, at 4 °C for 45 min. The enzymatic solution was then removed. A new aliquot of the buffer solution was added to the gel particles and incubated at 37 °C for 18 h. A minimum reaction volume sufficient for complete rehydration of the gel was used. Peptides were extracted by washing the gel particles in acetonitrile at 37 °C for 15 min and lyophilized.

The peptide extract volumes were divided in two to inject the peptide mixtures two times. The analysis were performed by μLCMS/MS with a Q-TOF hybrid mass spectrometer (Waters, Milford, MA) equipped with a Z-spray source and coupled on line with a capLC chromatography system (Waters) or alternatively by using the LC/MSD Trap XCT Ultra (Agilent Technologies, Palo Alto, CA) equipped with a 1100 HPLC system and a chip cube (Agilent Technologies). After loading, the peptide mixture (7 μl in 0.5% TFA) was first concentrated and washed (i) at 1 μl/min onto a C_{18} reverse-phase precolumn (Waters) or (ii) at 4 μl/min in a 40-nl enrichment column (Agilent Technologies chip) with 0.1% formic acid as the eluent. The sample was then fractionated on a C_{18} reverse-phase capillary column (75 μm × 20 cm in the Waters system, 75 μm × 43 mm in the Agilent Technologies chip) at a flow rate of 200 nl/min with a linear gradient of eluent B (0.1% formic acid in acetonitrile) in A (0.1% formic acid) from 5 to 60% in 50 min. Elution was monitored on the mass spectrometers without any splitting device. Peptide analysis was performed using data-dependent acquisition of one MS scan (mass range from 400 to 2000 *m/z*) followed by MS/MS scans of the three most abundant ions in each MS scan. Dynamic exclusion was used to acquire a more complete survey of the peptides by automatic recognition and temporary exclusion (2 min) of ions from which definitive mass spectral data had been acquired previously. Moreover a permanent exclusion list of the most frequent peptide contaminants (keratins and trypsin doubly and triply charged peptides: 403.20, 517.00, 519.32, 525.00, 532.90, 559.32, 577.30, 587.86, 616.85, 618.23, 721.75, 745.90, 747.32, 758.43, 854.30, 858.43, 896.30, and 1082.06) was included in the acquisition method to focus the analyses on significant data.

Data Analysis—Raw data from μLCMS/MS analyses were converted into a Mascot format text to identify proteins by means of the Matrix Science software (24). The protein search was governed by the following parameters: non-redundant protein sequence database (NCBInr, January 24, 2006 download, 3,229,765 sequences), specificity of the proteolytic enzyme used for the hydrolysis (trypsin), taxonomic category of the sample (*Homo sapiens*), no protein molecular weight was considered, up to one missed cleavage, cysteines as *S*-carbamidomethylcysteines, unmodified N- and C-terminal ends, methionines both unmodified and oxidized, putative pyro-Glu formation by Gln, precursor peptide maximum mass tolerance of 150 ppm, and a maximum fragment mass tolerance of 300 ppm. In the experience of the authors' laboratory all the MS/MS spectra displaying a Mascot score (24) higher than 38 show a good signal/noise ratio leading to an unambiguous interpretation of the data. Individual MS/MS spectra for peptides with a Mascot score (24) equal to 38 were inspected manually and only included in the statistics if a series of at least four continuous y or b ions were observed.

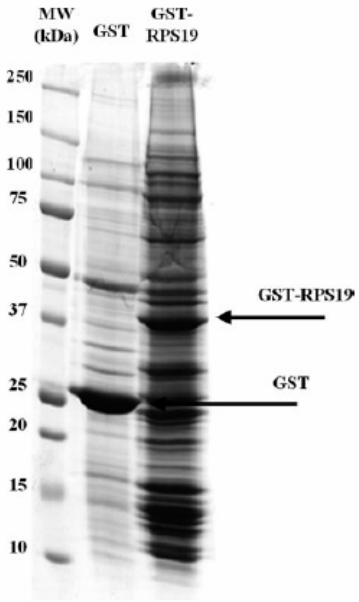

FIG. 1. **GST-RPS19 affinity purification.** Proteins from K562 whole cell extract were affinity-purified using GST or GST-RPS19 resins. Bound proteins were eluted, resolved on an 8–18% SDS-polyacrylamide gel, and stained with colloidal Coomassie.

In Silico Analysis—A list of primary (direct) and secondary (indirect) protein-protein interactions of RPS19 was created using the web-available Human Protein Reference Database (www.hprd.org). In April 2006, the database contained 20,097 human protein entries, 33,710 documented protein-protein interactions, and 171,677 links to the PubMed literature. Primary interactions of RPS19 were screened for protein interactors to define an *in silico* interaction map with the indirect protein partners. This map was then compared with the RPS19 protein partners identified in this study. In addition a list of primary interactions was created by HPRD for each identified protein.

Lastly the list of RPS19 protein partners was compared with the Nucleolar Proteome Database (www.lamondlab.com/NoPDB) (25) and with the Pre-Ribosomal Network yeast database (www.pre-ribosome.de/Home.html) (26). Ortholog *Saccharomyces cerevisiae* gene names were determined using the web-available database Ensembl (www.ensembl.org).

RESULTS

Identification of RPS19-interacting Proteins—To determine the RPS19 interactome in K562 cells, we performed LCMS/MS analysis of proteins purified by pulldown experiments on a GST-RPS19 affinity resin. The proteins eluted from the GST-RPS19 or the negative control GST resins were fractionated by 13-cm 8–18% SDS-PAGE and revealed by colloidal Coomassie stain (Fig. 1). SDS-PAGE indicated that the RPS19-associated proteins span a broad molecular weight range. The two major bands at 26 kDa (Fig. 1, *lane GST*) and at 43 kDa (Fig. 1, *lane GST-RPS19*) correspond to the bait proteins as verified by Western blotting with anti-GST antisera (data not shown). To check the efficiency of the

pulldown experiments, aliquots of the proteins eluted from the GST or the GST-RPS19 resins were analyzed by Western blotting using an anti-PIM1 antibody. PIM1 (*i.e.* the positive control) was identified in the GST-RPS19 lanes only (see Fig. 4).

The procedure described under "Experimental Procedures" gave 65 peptide mixture samples from each lane. The peptide extract volumes were divided in two to analyze peptide mixtures two times by μLCMS/MS. These duplicates showed a high level of reproducibility where in all cases identifications from the first analysis were confirmed from the second one. Peptide mixtures deriving from the GST lane constituted our control for the analysis of GST-RPS19 lane and were therefore always injected before the peptides from the GST-RPS19 lane. Mass spectrometry data were then analyzed with the Mascot software on the NCBI human protein sequence database. To select proteins that interact specifically with RPS19, we subtracted species common to the GST and GST-RPS19 lanes (Fig. 1). These proteins are shown in Supplemental Table 1.

Table I displays the complete list of RPS19 protein interactors identified in this study. Proteins are grouped according to their known function, and for each identification the human gene name, the corresponding protein name, and the ortholog *S. cerevisiae* gene name is reported. Supplemental Table 2 reports for each protein entry the identified peptides together with their sequences, the observed mass errors on the precursor peptides, the Mascot score for each peptide, and the protein sequence coverage expressed as the number of amino acids spanned by the identified peptides divided by the sequence length. All protein species identified by a single peptide were further checked. First the peptide sequence stretch, manually verified, was searched on the Basic Local Alignment Search Tool (BLAST) software at the NCBI web site (ncbi.nlm.nih.gov/blast) against human taxonomy. When other matches were possible, the candidate was removed from the list. The remaining single peptide protein species were added to the list only when involved in protein complexes known to interact with mRNA/rRNA or reported to interact with one of the proteins identified in this study (27–32). Fig. 2 (*A–D*) shows the MS full scan, the MS/MS scan, and the amino acid sequence relative to four identified RPS19-associated proteins: IGF2BP1 (Fig. 2*A*), MCM6 (Fig. 2*B*), DDX5 (Fig. 2*C*), and STAU1 (Fig. 2*D*). STAU1 is an example of protein species identified by a single peptide. Supplemental Fig. S3 shows additional examples like CCT2 (A), DDX17 (B), and NOLA3 (C).

The 159 human proteins identified in this study were divided into Gene Ontology functional groups as shown in Fig. 3*A*: NTPases (ATPases and GTPases, five proteins), hydrolases/helicases (19 proteins), isomerases (two proteins), kinases (three proteins), splicing factors (five proteins), structural constituents of ribosome (29 proteins), transcription factors (11 proteins), transferases (five proteins), transporters (nine proteins), DNA/RNA-binding protein species (53 proteins), other (one dehydrogenase protein, one ligase protein, one peptidase protein, one receptor protein, and one elongation factor), and 13 proteins of still unknown function. They were also grouped according to their Gene Ontology cellular localization (Fig. 3*B*) and the biological processes in which they are involved (Fig. 3*C*). Moreover according to the Human Nucleolar Database, 101 are nucleolar proteins (Supplemental Table 3); many of these are part of the 90 S preribosome as assessed by comparison with the yeast Pre-Ribosomal Network (Supplemental Table 4).

Among the interactors we identified RPS8, a ribosomal protein found in a previous yeast two-hybrid study.[3] In the same study we also revealed PIM1 (15), which was not detected in the proteomics analysis despite its presence in the eluate from GST-RPS19 resin (Fig. 4) and in the immunoprecipitate obtained with the anti-RPS19 monoclonal antibody (Fig. 5). The difference is presumably ascribable to the sensitivity limitations of proteomics analysis compared with antibody-based assays.

Validation of MS/MS Data by Western Blotting and Immunoprecipitation—To corroborate the authenticity of the proteins identified by MS/MS, we confirmed the presence of representative proteins in the eluates from GST-RPS19 resins by immunoblotting: the serine-threonine kinase PIM1, IGF2BP1, MCM6, the DEAD box polypeptide 5 (DDX5), Staufen (STAU1), dyskerin (DKC1), and NCL (Fig. 4).

Affinity purification was also performed using as negative controls a GST-GATA1 protein and different amounts of the GST protein. The bound proteins were eluted from the resins and analyzed by Western blot using specific antibodies for three selected interactors (DDX5, DKC1, and NCL). All these negative controls confirmed the specificity of the interaction between RPS19 and the proteins analyzed (Supplemental Fig. S1).

In addition, we performed immunoprecipitations using K562 lysates and a monoclonal antibody to RPS19 to show that the same interactions occur in living cells. Immunoprecipitated proteins were resolved by SDS-PAGE and analyzed by Western blotting with specific antibodies (Fig. 5 and Supplemental Fig. S2). In Fig. 5 we omitted the results regarding the positive co-precipitation of STAU1 because the close co-migration of the immunoglobulin heavy chains affects the quality of the data (as shown in Supplemental Fig. 2A). Supplemental Fig. S2, A, B, and C, shows the whole image of the co-immunoprecipitation assay.

In Silico Analysis of RPS19-interacting Proteins and Comparison with in Vitro Strategies

We carried out an *in silico* proteomics analysis of proteins known to directly or indirectly interact with RPS19. Examination of the publicly available databases HPRD and PubMed showed that four proteins interact with RPS19 directly and

[3] A. Aspesi, M. Armiraglio, M. C. Santoro, and I. Dianzani, unpublished data.

TABLE I
Identification of RPS19-interacting proteins by tandem mass spectrometry
dsRNA, double-stranded RNA; GPI, glycosylphosphatidylinositol; snoRNP, small nucleolar RNP; HLA, human leukocyte antigen.

Gene (Ref.)	Protein	Yeast gene
NTPase activity		
GTPBP4 (28, 29, 47)	GTP-binding protein NGB (G protein binding CRFG)	*NOG1*
PSMC5	Proteasome 26 S ATPase subunit 5	*RPT6*
PSMC6	Proteasome 26 S ATPase subunit 6	*RPT4*
RAB11B	RAB11B member RAS oncogene family	*YPT31*
XAB1	XPA-binding protein 1, GTPase	*NPA3*
Hydrolase/helicase activity		
DDX5 (28–30, 47)	Growth-regulated nuclear 68 protein (DEAD box polypeptide 5)	*DBP2*
DDX17 (28, 30)	DDX17 protein	
DDX18 (28, 29, 47)	RNA helicase (DEAD box polypeptide 18)	*HAS1*
DDX21 (28, 29, 47)	RNA helicase II/Gu protein (DEAD box polypeptide 21)	
DDX24 (29, 47)	DEAD box polypeptide 24	*MAK5*
DDX3X (28)	DEAD box, X isoform (DEAD box polypeptide 3)	
DDX41	DEAD box protein abstrakt	
DDX50 (28, 29)	DEAD box polypeptide 50 (nucleolar protein GU2)	
DDX54 (28, 29)	ATP-dependent RNA helicase (DEAD box polypeptide 54)	*DBP10*
DHX9 (28, 29, 31)	RNA helicase A (DEAH box polypeptide 9)	
DHX15 (28, 29, 47)	DEAH box polypeptide 15	*PRP43*
DHX36	DEAH box polypeptide 36	
MCM2	MCM2 minichromosome maintenance-deficient 2, mitotin (*S. cerevisiae*)	*MCM2*
MCM6	p105MCM (MCM6 minichromosome maintenance-deficient 6)	*MCM6*
MCM7	p85MCM protein (MCM7 minichromosome maintenance-deficient 7)	*CDC47*
RUVBL2 (25)	RuvB-like 2	*RVB2*
SKIV2L2 (28, 29)	Superkiller viralicidic activity 2-like 2 (*S. cerevisiae*)	*MTR4*
SMARCA5	SWI/SNF-related, matrix-associated, actin-dependent regulator of chromatin, subfamily a, member 5	*ISW2*
XRN2 (29)	Dhm1-like protein (5′–3′ exoribonuclease 2)	*RAT1*
Isomerase activity		
DKC1 (28, 29)	Cbf5p homolog (dyskerin)	*CBF5*
PPIH	Peptidyl-prolyl isomerase H	
Kinase activity		
CSNK2A1 (25, 29)	Casein kinase 2, α 1 polypeptide	
SRP72	Signal recognition particle 72	*SRP72*
PRKCQ	Δ^2-Isopentenylpyrophosphate transferase-like protein (protein kinase C, θ)	
Splicing factor activity		
SF3B1	Splicing factor 3b, subunit 1, 155 kDa	*HSH155*
SF3B2	Splicing factor 3b, subunit 2, 145 kDa	*CUS1*
SF3B3	Splicing factor 3b, subunit 3, 130 kDa	*RSE1*
SFRS9 (28)	Splicing factor Arg/Ser-rich 9	
SFRS10	Splicing factor Arg/Ser-rich 10	
Structural constituent of ribosome		
RPL10A (25, 28, 29)	60 S ribosomal protein L10a	*RPL1B*
RPL14 (28, 29, 32)	60 S ribosomal protein L14	*RPL4B*
RPL24	60 S ribosomal protein L24	*RPL24A*
RPL27A (25, 28, 29)	60 S ribosomal protein L27a	*RPL28*
RPL3 (25, 28, 29)	60 S ribosomal protein L3	*RPL3*
RPL4 (25, 28, 29)	60 S ribosomal protein L4	*RPL4B*
RPL6 (25, 28, 29, 31, 32)	60 S ribosomal protein L6	*RPL6B*
RPL7 (25, 28, 29)	60 S ribosomal protein L7	
RPL7A (25, 28, 29, 32)	60 S ribosomal protein L7a	*RPL8B*
RPL8 (25, 28)	60 S ribosomal protein L8	*RPL2A*
RPL9 (25, 28, 29)	60 S ribosomal protein L9	*RPL9B*
RPLP0 (28, 29, 31, 32)	60 S ribosomal protein P0	*RPP0*
RPLP1	60 S acidic ribosomal protein P1 isoform 1	*RPP1A*
RPLP2 (25)	60 S acidic ribosomal protein P2	*RPP2B*
RPS10 (25)	40 S ribosomal protein S10	*RPS10A*
RPS14 (25, 29)	40 S ribosomal protein S14	*RPS14B*
RPS16 (25, 28)	40 S ribosomal protein S16	*RPS16A*
RPS2 (25, 32)	40 S ribosomal protein S2	*RPS2*

TABLE I— *continued*

Gene (Ref.)	Protein	Yeast gene
RPS23 (25)	40 S ribosomal protein S23	*RPS23A*
RPS24 (25)	40 S ribosomal protein S24	*RPS24B*
RPS26 (28)	40 S ribosomal protein S26	*RPS26B*
RPS3	40 S ribosomal protein S3	*RPS3*
RPS4X (25, 28, 29)	40 S ribosomal protein S4, X-linked	*RPS4A*
RPS5 (25, 28, 29)	40 S ribosomal protein S5	*RPS5*
RPS6 (31, 32)	40 S ribosomal protein S6	*RPS6B*
RPS7 (25)	40 S ribosomal protein S7	*RPS7A*
RPS8 (25, 28, 31, 32)	40 S ribosomal protein S8	*RPS8B*
RPSA (28)	Ribosomal protein SA	*RPS0A*
RSL1D1 (29)	PBK1 protein	
Transcription factor		
BAZ1B (25)	Bromodomain adjacent to zinc finger domain, 1B	
HNRPD (25, 30)	Heterogeneous nuclear ribonucleoprotein D2	
ILF2 (28–30)	Interleukin enhancer binding factor 2	
ILF3 (29, 30, 32)	Nuclear factor associated with dsRNA NFAR-2	
NKRF (29)	Transcription factor NRF	
PURA	Purine-rich element-binding protein A	
TAF15 (25)	TLS protein (TBP-associated factor 15)	*NPL3*
TRIM28 (25)	Tripartite motif-containing 28	
UBTF (28)	Upstream binding transcription factor, RNA 4 polymerase I	
XPO5	Exportin 5	*MSN5*
YBX1	DNA-binding protein B	
Transferase activity		
FDFT1	Farnesyl-diphosphate farnesyltransferase	*ERG9*
FTSJ3 (29, 47)	FtsJ homolog 3 (*E. coli*)	*SPB1*
NAT10 (29)	*N*-Acetyltransferase 10 (FLJ10774)	
NOL1 (28, 29, 47)	Proliferating cell nuclear protein p120 (NOL protein 1)	*NOP2*
ZC3HAV1	Zinc finger CCCH type, antiviral 1	
Transporter activity		
COPA	Coatomer protein complex, subunit α	*COP1*
COPB2	Coatomer protein complex, subunit β 2	*SEC27*
CSE1L	CSE1 chromosome segregation 1-like (yeast)	*CSE1*
IPO4	Importin 4	*KAP123*
IPO7	Importin 7	
NPEPL1	Aminopeptidase-like 1	
STAU1	Staufen protein	
SSR4	Signal sequence receptor δ	
XPO1	Exportin 1 (CRM1 homolog yeast)	*CRM1*
DNA/RNA/protein binding capacity		
AATF (25, 28, 29)	Ded protein (apoptosis-antagonizing transcription factor)	*BFR2*
ACTR1B	ARP1 actin-related protein 1 homolog B, centractin β	
C1orf77	DKFZP547E1010 protein	
CCT2 (25, 29)	Chaperonin containing TCP1, subunit 2 (β)	*CCT2*
CCT8	Chaperonin containing TCP1, subunit 8 (θ)	*CCT8*
CEBPZ (28, 29, 47)	CCAAT/enhancer-binding protein ζ	*MAK21*
CENPC1	Centromere protein C 1	
COPG	Coatomer protein complex, subunit γ 1	*SEC21*
DHX30	DEAH (Asp-Glu-Ala-His) box	
DNAJC9	DnaJ homolog, subfamily C, member 9	
FBL (28, 29, 47)	Fibrillarin, U3 small nucleolar interacting protein 1	*NOP1*
FUSIP1 (29)	FUS-interacting protein (serine/arginine-rich) 1	
GNB2L1 (25)	Guanine nucleotide-binding protein (G protein), β polypeptide 2-like 1	
HIST1H1C (25)	Histone H1b	
HIST1H1D (25)	Histone H1 member 3	
HIST1H2AK (25)	H2A histone family	
HIST1H2BL (25, 29)	H2B histone family, member C	
HIST1H2BO (25)	Histone 1, H2bo	
HIST2H4 (28)	Histone 2 H4	
HNRPA2B1 (25, 28–30)	Heterogeneous nuclear ribonucleoprotein A2/B1	
HNRPA3 (30)	Heterogeneous nuclear ribonucleoprotein A3	

TABLE I— *continued*

Gene (Ref.)	Protein	Yeast gene
HNRPC (25, 28, 30)	Heterogeneous nuclear ribonucleoprotein C	
HNRPDL (25)	Heterogeneous nuclear ribonucleoprotein D-like (A + U-rich element RNA binding factor)	
HNRPF	Heterogeneous nuclear ribonucleoprotein F	
HNRPR (25)	Heterogeneous nuclear ribonucleoprotein R	
HNRPU (25, 30–32)	Heterogeneous nuclear ribonucleoprotein U (scaffold attachment factor A)	
HNRPUL2	Heterogeneous nuclear ribonucleoprotein U-like 2	
HP1BP3	HP1-BP74	
IGF2BP1	IGF-II mRNA-binding protein 1	
IGF2BP3	Koc1 (IGF-II mRNA-binding protein 3)	
IMP3 (28)	U3 snoRNP protein 3 homolog	*IMP3*
ITGB4BP (25, 28, 29)	Integrin β4-binding protein	*TIF6*
LYAR (28, 29)	Hypothetical protein FLJ20425	*YCR087C-A*
NCL (28, 29, 31, 32)	Nucleolin	*NSR1*
NIP7 (29)	60 S ribosome subunit biogenesis protein Nip7 homolog (*S. cerevisiae*)	*NIP7*
NOLA1 (25, 28)	Nucleolar protein family A member 1 (H/ACA small nucleolar RNPs)	*GAR1*
NOL5A (25, 28, 29, 47)	hNop56	*SIK1*
PABPC3 (30)	Poly(A)-binding protein	
PAK1IP1 (25, 29)	PAK/PLC-interacting protein 1	*MAK11*
PNN	Pinin, desmosome-associated protein	
PPP2R1A	PPP2R1A (Ser/Thr protein phosphatase 2A)	
RAB1B	RAB1B member RAS oncogene family	
RAP1B	RAP1B member RAS oncogene family	*RSR1*
RBM19 (28, 29)	RNA binding motif 19	*MRD1*
RBMX (28)	RNA binding motif protein, X-linked (heterogeneous nuclear ribonucleoprotein G)	
RNPC2	RNA-binding region-containing protein 2	
SART3	Squamous cell carcinoma antigen recognized by T cells 3	
SNRPA1 (25, 28)	Small nuclear ribonucleoprotein polypeptide A′ (U2 small nuclear ribonucleoprotein polypeptide A′)	
SNRPG (25)	Small nuclear ribonucleoprotein polypeptide G	*SMX2*
SNRPN	Small nuclear ribonucleoprotein polypeptide N	
SRP68	Signal recognition particle 68	*SRP68*
SURF6 (25, 28)	Surfeit protein 6	*RRP14*
SYNCRIP (30)	NS1-associated protein	
Other function		
Dehydrogenase activity		
DPYD	Dehydropyrimidine dehydrogenase	*GLT1*
Ligase activity		
MARS	Methionine-tRNA synthetase	*MES1*
Peptidase activity		
SEC11L1	Signal peptidase complex 18 kDa	*SEC11*
Receptor activity		
REEP6	Receptor accessory protein 6	
Translation elongation factor activity		
EEF1B2	Eukaryotic translation elongation factor 1 β 2	
Unknown function		
EBNA1BP2 (25, 28, 29)	EBNA1-binding protein 2	*EBP2*
GPIAP1	GPI-anchored protein p137 precursor	
HDCMA18P	Hypothetical protein DKFZp564K112.1 (HDCMA18P)	
LOC389217	Similar to SET protein (phosphatase 2A inhibitor I2PP2A) (I-2PP2A) (template-activating factor I) (TAF-I) (HLA-DR-associated protein II) (PHAPII) (inhibitor of granzyme A-activated DNase) (IGAAD)	
MGC3731	Hypothetical protein LOC79159	
NOC2L (28, 29)	Nucleolar complex-associated 2 homolog (*S. cerevisiae*; hypothetical protein DKFZp564C186.1)	*NOC2*
NOC3L (29)	Nucleolar complex-associated 3 homolog (*S. cerevisiae*)	*NOC3*
NOL10 (28, 29)	Nucleolar protein 10 (hypothetical protein FLJ14075)	*ENP2*
NOLA3 (25)	Nucleolar protein family A, member 3	*NOP10*
PES1 (25, 28, 29, 47)	Pescadillo homolog 1 containing BRCT domain	*NOP7*
RBM12B	RNA binding motif protein 12B	
RP13-36C9.1	Cancer/testis antigen CT45–2	
SYNGR2	Synaptogyrin 2	

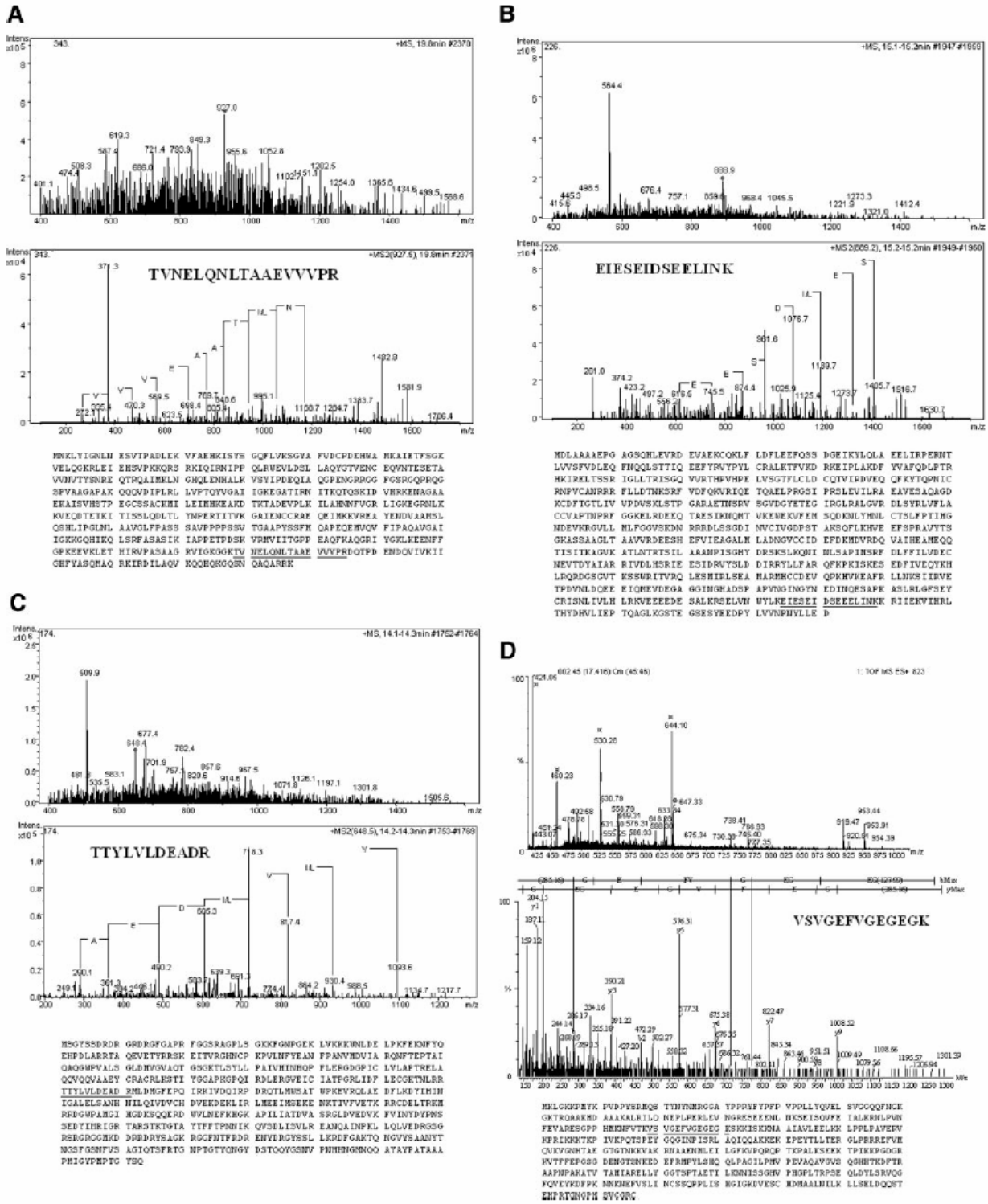

FIG. 2. **Protein identification by tandem mass spectrometry.** MS full scan, MS/MS scan, and amino acid sequence of IGF2BP1 (*A*), MCM6 (*B*), DDX5 (*C*), and STAU1 (*D*) are shown. Each MS/MS spectrum shows the predicted peptide sequence and the tryptic identified fragment. In protein sequences identified peptides are *underlined*. ♦, *m/z* signal fragmented. In *D*, ¤ indicates peaks fragmented in previous scans.

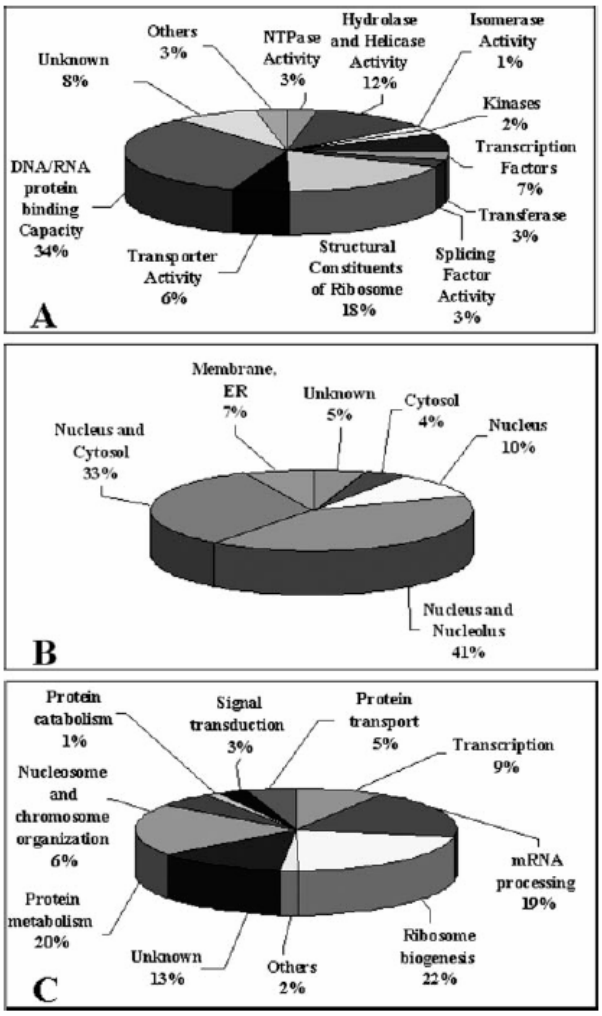

FIG. 3. **Classification of the identified proteins according to Gene Ontology molecular function (*A*), cellular localization (*B*), and biological processes (*C*).** *ER*, endoplasmic reticulum.

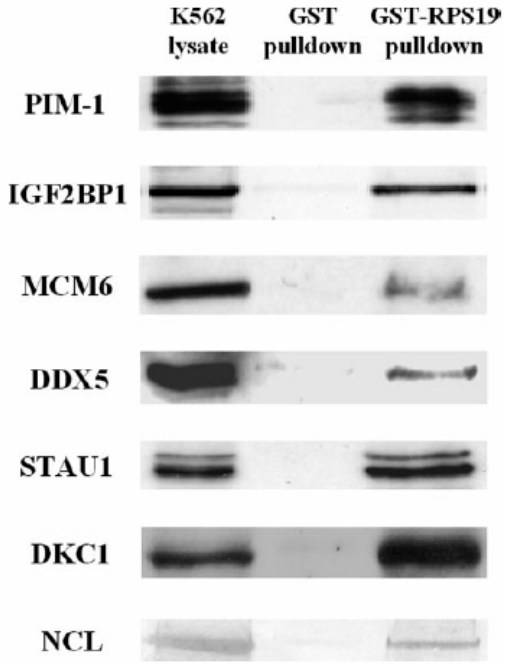

FIG. 4. **GST-RPS19 pulldown.** Proteins from K562 whole cell extracts were affinity-purified with GST and GST-RPS19 resins. Total lysates (*K562 lysate*) and bound proteins eluted from the GST control resin (*GST*) or the GST-RPS19 resin (*GST-RPS19*) were analyzed by Western blotting with antibodies specific to the indicated proteins. All blots were revealed by the chemiluminescence method except for NCL, which was revealed by alkaline phosphatase.

that 32 interact indirectly (Table II).

The already known primary interactors of RPS19 reported in the *in silico* analysis were not identified in this proteomics study. However, they were identified interacting with RPS19 in very particular conditions. In the case where FGF2 was reported to interact with free RPS19, in fact the GST pulldown experiment was performed with only the cytoplasmic extracts of NIH3T3 or ECV304 cells (33). In the case of complement component 5 receptor, the protein-protein interaction was reported in extracts of a rheumatoid arthritis synovial lesion when a covalent dimer of RPS19 by transglutamination occurs (34). In the case of RPS19-binding protein the specific antibody is not available (35) to perform an antibody-based assay to complement mass spectrometric data.

Our analysis shows that several proteins identified in this study interact with each other. DDX5, PES1, DDX21, GTPBP4, NOL5A, and NCL, for example, interact with RPL4, RPL6, RPL7a, RPL10a, RPLP0, and RPS3. Their relationship with RPS19, however, is not illustrated in the HPRD database nor in the literature, and they are therefore new RPS19 partners.

DISCUSSION

This study represents the first global, high throughput functional proteomics approach to identify the proteins that interact with RPS19. Our analysis of the GST-RPS19 pulldown revealed 159 proteins, most of them not previously known to associate with RPS19. On the other hand, *in silico* analysis and PubMed data show that many proteins interact with each other. They may thus participate with RPS19 in the same multiprotein complex or complexes.

It is known that ribosomal proteins are involved at different stages of ribosome biogenesis and/or in distinct translation steps (36). In particular, they have been thought to play a central role in rRNA processing, protein assembly, RNA folding, transport of the ribosomal precursors, stabilization of the subunit structure, and/or interaction with other factors required for either ribosome biogenesis or translation (37–39). Their involvement in cotranslational processes, such as the interaction with protein folding factors at the exit tunnel of the

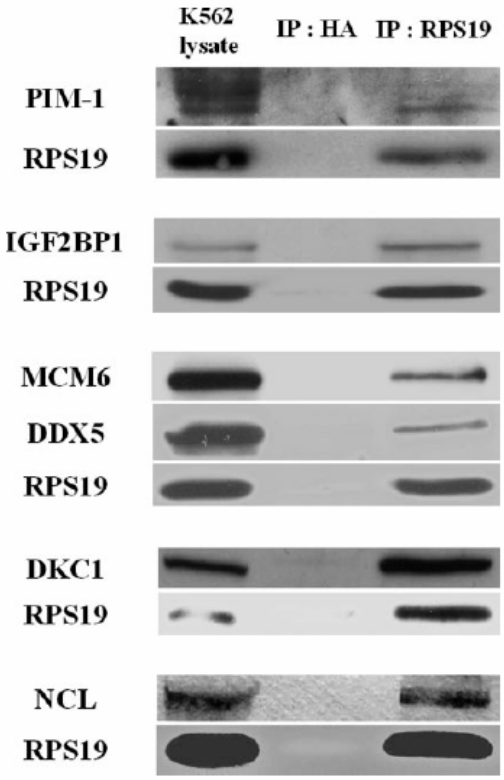

FIG. 5. **Co-immunoprecipitation.** Proteins from K562 cell lysates were immunoprecipitated with a monoclonal anti-RPS19 or an anti-hemagglutinin antibody as negative control. Immunocomplexes were fractionated by SDS-PAGE, blotted on nitrocellulose, and revealed by the specific antibodies. All blots were revealed by the chemiluminescence method except for NCL, which was revealed by alkaline phosphatase. *IP*, immunoprecipitate; *HA*, hemagglutinin.

ribosome (40, 41), cotranslational translocation (42, 43), and important enzymatic activities for ribosome function, *e.g.* the mRNA helicase activity of bacterial ribosomes (44), has also been proposed.

Interestingly most proteins reported in this study, such as nucleolar or ribosomal proteins, play a role in processes related to RPS19. It should be stressed that we used a total cell lysate and not a nuclear extract and that the complex formation was extracellular. Nevertheless proteins abundant in cytoplasm were not found. This suggests that the structure of the recombinant RPS19 protein is functionally suitable to recruit multiple cellular partners.

Comparison with the Human Nucleolar Database showed that two-thirds of the RPS19 interactome is composed of nucleolar proteins (Supplemental Table 3). As expected, a large group of interactors includes other structural ribosomal proteins. RPS19 is part of the 40 S ribosomal subunit: we have found 14 proteins that share this location (*i.e.* S2, S3, S4X, S5, S6, S7, S8, S10, S14, S16, S23, S24, S26, and SA). Many proteins belong to the pre-40 S nucleolar complex

TABLE II
Identification of RPS19-interacting proteins by in silico proteomics

Primary	
RPS19	
	Complement component 5 receptor 1
	Fibroblast growth factor 2
	PIM1
	RPS19-binding protein
Secondary	
Complement component 5 receptor 1	
	Complement component 5
	RPS19
	GNAI2
	G protein-coupled receptor 77
Fibroblast growth factor 2	
	Apoptosis inhibitor 5
	Protein-arginine *N*-methyltransferase 1
	FGF receptor 1
	RPS19
	CD44
	Vitronectin
	Chemokine, CXC motif, ligand 13
	Glypican 4
	Translokin
	Casein kinase II, α 1[a]
	RPL6[a]
	FGF receptor 2
	FGF receptor 4
	Syndecan 3
	FGF-binding protein 1
	Perlecan
	Platelet factor 4
	Glypican 3
	Casein kinase 2, α 2
PIM1	
	NFATC1
	Sorting nexin 6
	p100
	EBNA2 coactivator p100
	HP1 β
	Nuclear mitotic apparatus protein 1
	HP1 γ
	Dynactin 1
	Dynein
	CDC 25A
	Cyclin-dependent kinase inhibitor 1A
	Protein tyrosine phosphatase U2
	HSP90A
	SNX6

[a] Proteins identified in this study.

(Supplemental Table 4). We have also found 11 proteins belonging to the 60 S subunit (L3, L4, L6, L7, L7a, L8, L9, L10a, L14, L24, and L27a).

The identification of RPs belonging to the small and the large subunits suggests that we have purified components of the preribosome (90 S), the structure formed before processing of the pre-rRNA. The subsequent cut at a specific site (A2) divides these subunits. The preribosome is a highly dynamic structure that comprises more than 150 non-ribosomal proteins with various activities, including nucleases, RNA helicases, GTPases, AAA ATPases, kinases, etc. (for reviews, see Refs. 45 and 46). We have, indeed, found 23 of 31 proteins with orthologs in the yeast preribosome network that belong to the 90 S subunit. Many interactors are shared between

RPS19 and parvulin, a peptidyl-prolyl isomerase involved in early ribosome biogenesis (*i.e.* L3, L4, L6, L7, L7a, L8, L10a, L14, S3, S4X, S6, S8, and DDX18) (47).

The interaction with most of the RPs essential for the transport of the small subunit from the nucleus to the cytoplasm (*i.e.* RPS10, RPS26, RPS3, and RPS2) and to the exportin XPO (known to control the 40 S and 60 S export) suggests a role for RPS19 in this process. This is in agreement with two recent reports of its involvement in the early processing of rRNA (11) and possibly in its export from the nucleus (12). Concordantly the greater portion of the RPS19-interacting proteins identified in this study includes proteins involved in pre-rRNA processing, such as RNA helicases, and major components of the box C-D small nucleolar RNAs (48, 49), such as fibrillarin and Nop56.

We also found major components of the H/ACA box small nucleolar RNP complex, *i.e.* dyskerin, NOLA1, and NOLA3. This complex (that includes a fourth protein, NOLA2) is required for the site-specific pseudouridylation of rRNA involved in the early stages of ribosome biogenesis (50). Both 18 S rRNA production and rRNA pseudouridylation are impaired if any one of the four proteins is depleted.

A further group of interactors includes proteins controlling protein synthesis, such as proteins involved in cotranslational translocation (42, 43) (such as signal recognition particle 68) and translation regulators, such as IGF2BP1 and STAU1. Other ribosomal proteins (*i.e.* RPL13 and RPL26) (16, 17) are known to regulate translation of specific transcripts. It is intriguing that RPS19 could have a similar role. Our previous studies showing interactions of PIM1 and RPS19 on the 40 S subunit suggested such a role (15).

Lastly this study identified proteins with more diverse cellular functions. These included proteins such as integrins, proteasome components, and kinases. Further studies are needed to clarify their involvement in the RPS19 interactome.

The scenario disclosed by our study clearly shows that RPS19 is definitely involved in RNA processing and metabolism and perhaps in translation control. Although it must be stressed that our results do not take the spatial-temporal dimension of RPS19 interactome into account, future experiments will be directed toward the comprehension of this point.

It is intriguing that among the direct or indirect RPS19 interactors we also found proteins involved in pathologies with phenotypes similar to DBA (14). These include the following: 1) DKC1, responsible for dyskeratosis congenita (OMIM 305000), that shares bone marrow failure with DBA; 2) RPL24, whose spontaneous defect in mice produces growth retardation and skeletal malformations (51); 3) TCOF1, responsible for the Treacher-Collins syndrome (OMIM 154500), which shares some malformations with DBA, and that interacts with NOL5A and UBTF; and 5) SBDS (OMIM 260400), responsible for the Schwachman-Diamond syndrome, that interacts with nucleolin. This suggests a link between the ribosomal diseases, possibly a common pathogenetic mechanism.

In short, we have identified several new protein interactions with RPS19. This should lead to a fuller understanding of its activities and a more complete picture of its cellular roles and/or regulation. A clearer understanding of the function of RPS19 could help to elucidate the pathogenesis of DBA.

Acknowledgments—Drs. Luc DesGroseillers and Philip Mason are thanked for the gifts of the STAU1 and DKC1 antibodies, respectively.

* This work was supported by Telethon GGP02434 (to I. D.), COFIN grants (to I. D. and M. R.), Compagnia di San Paolo (to C. S.), and the Diamond-Blackfan Anemia Foundation (to I. D.). The costs of publication of this article were defrayed in part by the payment of page charges. This article must therefore be hereby marked "*advertisement*" in accordance with 18 U.S.C. Section 1734 solely to indicate this fact.

S The on-line version of this article (available at http://www.mcponline.org) contains supplemental material.

‡‡ Both authors contributed equally to this work.

§§ To whom correspondence should be addressed: Dept. of Medical Sciences, Università del Piemonte Orientale, Via Solaroli 17, 28100 Novara, Italy. Tel.: 39-0321-660-644; Fax.: 39-0321-660-421; E-mail: irma.dianzani@med.unipmn.it.

REFERENCES

1. Campagnoli, M. F., Garelli, E., Quarello, P., Carando, A., Varotto, S., Nobili, B., Longoni, D., Pecile, V., Zecca, M., Dufour, C., Ramenghi, U., and Dianzani, I. (2004) Molecular basis of Diamond-Blackfan anemia, new findings from the Italian registry and a review of the literature. *Haematologica* **89,** 480–489
2. Draptchinskaia, N., Gustavsson, P., Andersson, B., Pettersson, M., Willig, T. N., Dianzani, I., Ball, S., Tchernia, G., Klar, J., Matsson, H., Tentler, D., Mohandas, N., Carlsson, B., and Dahl, N. (1999) The gene encoding ribosomal protein S19 is mutated in Diamond-Blackfan anaemia. *Nat. Genet.* **21,** 169–175
3. Willig, T. N., Draptchinskaia, N., Dianzani, I., Ball, S., Niemeyer, C., Ramenghi, U., Orfali, K., Gustavsson, P., Garelli, E., Brusco, A., Tiemann, C., Perignon, J. L., Bouchier, C., Cicchiello, L., Dahl, N., Mohandas, N., and Tchernia, G. (1999) Mutations in ribosomal protein S19 gene and Diamond Blackfan anemia, wide variations in phenotypic expression. *Blood* **94,** 4294–4306
4. Chatr-Aryamontri, A., Angelini, M., Garelli, E., Tchernia, G., Ramenghi, U., Dianzani, I., and Loreni, F. (2004) Nonsense-mediated and nonstop decay of ribosomal protein S19 mRNA in Diamond-Blackfan anemia. *Hum. Mutat.* **24,** 526–533
5. Gazda, H. T., Zhong, R., Long, L., Niewiadomska, E., Lipton, J. M., Ploszynska, A., Zaucha, J. M., Vlachos, A., Atsidaftos, E., Viskochil, D. H., Niemeyer, C. M., Meerpohl, J. J., Rokicka-Milewska, R., Pospisilova, D., Wiktor-Jedrzejczak, W., Nathan, D. G., Beggs, A. H., and Sieff, C. A. (2004) RNA and protein evidence for haplo-insufficiency in Diamond-Blackfan anaemia patients with RPS19 mutations. *Br. J. Haematol.* **127,** 105–113
6. Da Costa, L., Tchernia, G., Gascard, P., Lo, A., Meerpohl, J., Niemeyer, C., Chasis, J. A., Fixler, J., and Mohandas, N. (2003) Nucleolar localization of RPS19 protein in normal cells and mislocalization due to mutations in the nucleolar localization signals in 2 Diamond-Blackfan anemia patients, potential insights into pathophysiology. *Blood* **101,** 5039–5045
7. Cretien, A., Da Costa, L. M., Rince, P., Proust, A., Mohandas, N., Gazda, H., Niemeyer, C., Delaunay, J., and Tchernia, G. (2003) Subcellular localization and protein expression level of twelve ribosomal protein S19 mutants identified in DBA patients, in *American Society of Hematology Annual Meeting, San Diego, December 6–9, 2003*, Abstr. 717, American Society of Hematology, Washington, D. C.
8. Da Costa, L., Narla, G., Willig, T. N., Peters, L. L., Parra, M., Fixler, J., Tchernia, G., and Mohandas, N. (2003) Ribosomal protein S19 expres-

sion during erythroid differentiation. *Blood* **101,** 318–324
9. Hamaguchi, I., Ooka, A., Brun, A., Richter, J., Dahl, N., and Karlsson, S. (2002) Gene transfer improves erythroid development in ribosomal protein S19-deficient Diamond-Blackfan anemia. *Blood* **100,** 2724–2731
10. Flygare, J., Kiefer, T., Miyake, K., Utsugisawa, T., Hamaguchi, I., Da Costa, L., Richter, J., Davey, E. J., Matsson, H., Dahl, N., Wiznerowicz, M., Trono, D., and Karlsson, S. (2005) Deficiency of ribosomal protein S19 in CD34+ cells generated by siRNA blocks erythroid development and mimics defects seen in Diamond-Blackfan anemia. *Blood* **105,** 4627–4634
11. Léger-Silvestre, I., Caffrey, J. M., Dawaliby, R., Alvarez-Arias, D. A., Gas, N., Bertolone, S. J., Gleizes, P. E., and Ellis, S. R. (2005) Specific role of yeast homologs of the Diamond-Blackfan anemia associated Rps19 protein in ribosome synthesis. *J. Biol. Chem.* **280,** 38177–38185
12. Ferreira-Cerca, S., Poll, G., Gleizes, P. E., Tschochner, H., and Milkereit, P. (2005) Roles of eukaryotic ribosomal proteins in maturation and transport of pre-18S rRNA and ribosome function. *Mol. Cell* **20,** 263–275
13. Ellis, S. R., and Massey, A. T. (2006) Diamond Blackfan anemia, A paradigm for a ribosome-based disease. *Med. Hypotheses* **66,** 643–648
14. Liu, J. M., and Ellis, S. R. (2006) Ribosomes and marrow failure, coincidental association or molecular paradigm? *Blood* **107,** 4583–4588
15. Chiocchetti, A., Gibello, L., Carando, A., Aspesi, A., Secco, P., Garelli, E., Loreni, F., Angelini, M., Biava, A., Dahl, N., Dianzani, U., Ramenghi, U., Santoro, C., and Dianzani, I. (2005) Interactions between RPS19, mutated in Diamond-Blackfan anemia, and the PIM-1 oncoprotein. *Haematologica* **90,** 1453–1462
16. Mazumder, B., Sampath, P., Seshadri, V., Maitra, R. K., DiCorleto, P. E., and Fox, P. L. (2003) Regulated release of L13a from the 60S ribosomal subunit as a mechanism of transcript-specific translational control. *Cell* **115,** 187–198
17. Takagi, M., Absalon, M. J., McLure, K. G., and Kastan, M. B. (2005) Regulation of p53 translation and induction after DNA damage by ribosomal protein L26 and nucleolin. *Cell* **123,** 49–63
18. Monti, M., Orrù, S., Pagnozzi, D., and Pucci, P. (2005) Interaction proteomics. *Biosci. Rep.* **25,** 45–56
19. Secco, M., Cotella, D., and Santoro, C. (2003) Selection of peptides with affinity for the N-terminal domain of GATA-1: identification of a potential interacting protein. *Biochem. Biophys. Res. Commun.* **305,** 1061–1066
20. Cianfriglia, M., Mariani, M., Armellini, D., Massone, A., Lafata, M., Presentini, R., and Antoni, G. (1986) Methods for high frequency production of soluble antigen-specific hybridomas; specificities and affinities of the monoclonal antibodies obtained. *Methods Enzymol.* **121,** 193–210
21. Dugre-Brisson, S., Elvira, G., Boulay, K., Chatel-Chaix, L., Mouland, A. J., and DesGroseillers, L. (2005) Interaction of Staufen1 with the 5′ end of mRNA facilitates translation of these RNAs. *Nucleic Acids Res.* **33,** 4797–4812
22. Mochizuki, Y., He, J., Kulkarni, S., Bessler, M., and Mason, P. J. (2004) Mouse dyskerin mutations affect accumulation of telomerase RNA and small nucleolar RNA, telomerase activity, and ribosomal RNA processing. *Proc. Natl. Acad. Sci. U. S. A.* **101,** 10756–10761
23. Orrù, S., Caputo, I., D'Amato, A., Ruoppolo, M., and Esposito, C. (2003) Proteomics identification of acyl-acceptor and acyl-donor substrates for transglutaminase in human intestinal epithelial cell line: implications for celiac disease. *J. Biol. Chem.* **278,** 31766–31777
24. Perkins, D. N., Pappin, D. J., Creasy, D. M., and Cottrell J. S. (1999) Probability-based protein identification by searching sequence databases using mass spectrometry data. *Electrophoresis* **20,** 3551–3567
25. Lam, Y. W., Trinkle-Mulcahy, L., and Lamond, A. I. (2005) The nucleolus. *J. Cell Sci.* **118** 1335–7
26. Milkereit, P., KuÊhn, H., Gas, N., and Tschochner, H. (2003) The pre-ribosomal network *Nucleic Acids Res.* **31,** 799–804
27. Andersen, J. S., Lam, Y. W., Leung, A. K., Ong, S. E., Lyon, C. E., Lamond, A. I., and Mann M. (2005) Nucleolar proteome dynamics. *Nature* **433,** 77–83
28. Andersen, J. S., Lyon, C. E., Fox, A. H., Leung, A. K. L., Lam, Y. W., Steen, H., Mann, M., and Lamond, A. I. (2002) Directed proteomic analysis of human nucleolus. *Curr. Biol.* **12,** 1–11
29. Scherl, A., Couté, Y., Déon, C., Callé, A., Kindbeiter, K., Sanchez, J. C., Greco, A., Hochstrasser, D., and Diaz, J. J. (2002) Functional proteomic analysis of human nucleolus. *Mol. Biol. Cell* **13,** 4100–4109
30. Elvira, G., Wasiak, S., Blandford, V., Tong, X. K., Serrano, A., Fan, X., Del Rayo Sanchez-Carbente, M., Servant, F., Bell, A. W., Boismenu, D., Lacaille, J. C., McPherson, P. S., Desgroseillers, L., and Sossin, W. S. (2006) Characterization of an RNA granule from developing brain. *Mol. Cell. Proteomics* **5,** 635–651
31. Villacé, P., Mariòn, R. M., and Ortìn, J. (2004) The composition of staufen-containing RNA granules from human cells indicates their role in the regulated transport and translation of messenger RNAs. *Nucleic Acids Res.* **32,** 2411–2420
32. Brendel, C., Rehbein, M., Kreienkamp, H. J., Buck, F., Richter, D., and Kindler, S. (2004) Characterization of Staufen 1 ribonucleoprotein complexes. *Biochem. J.* **384,** 239–246
33. Soulet, F., Al Saati, T., Roga, S., Amalric, F., and Bouche, G. (2001) Fibroblast growth factor-2 interacts with free ribosomal protein S19. *Biochem. Biophys. Res. Commun.* **289,** 591–596
34. Shibuya, Y., Shiokawa, M., Nishiura, H., Nishimura, T., Nishino, N., Okabe, H., Takagi, K., and Yamamoto, T. (2001) Identification of receptor-binding sites of monocyte chemotactic S19 ribosomal protein dimer. *Am. J. Pathol.* **159,** 2293–2301
35. Maeda, N., Toku, S., Kenmochi, N., and Tanaka, T. (2006) A novel nucleolar protein interacts with ribosomal protein S19q. *Biochem. Biophys. Res. Commun.* **339,** 41–46
36. Leger-Silvestre, I., Milkereit, P., Ferreira-Cerca, S., Saveanu, C., Rousselle, J. C., Choesmel, V., Guinefoleau, C., Gas, N., and Gleizes, P. E. (2004) The ribosomal protein Rps15p is required for nuclear exit of the 40S subunit precursors in yeast. *EMBO J.* **23,** 2336–2347
37. Blaha, G. (2004). Structure of the ribosome, in *Protein Synthesis and Ribosome Structure* (Nierhaus, K. H., and Wilson, D. N., eds) pp. 53–84, Wiley-VCH, Weinheim, Germany
38. Nierhaus, K. H. (2004). Assembly of the prokaryotic ribosome, in *Protein Synthesis and Ribosome Structure* (Nierhaus, K. H., and Wilson, D. N., eds) pp. 85–106, Wiley-VCH, Weinheim, Germany
39. Dresios, J., Panopoulos, P., and Synetos, D. (2006) Eukaryotic ribosomal proteins lacking a eubacterial counterpart, important players in ribosomal function. *Mol. Microbiol.* **59,** 1651–1663
40. Kramer, G., Rauch, T., Rist, W., Vorderwulbecke, S., Patzelt, H., Schulze-Specking, A., Ban, N., Deuerling, E., and Bukau, B. (2002) L23 protein functions as a chaperone docking site on the ribosome. *Nature* **419,** 171–174
41. Pool, M. R., Stumm, J., Fulga, T. A., Sinning, I., and Dobberstein, B. (2002) Distinct modes of signal recognition particle interaction with the ribosome. *Science* **297,** 1345–1348
42. Beckmann, R., Spahn, C. M., Eswar, N., Helmers, J., Penczek, P. A., Sali, A., Frank, J., and Blobel, G. (2001) Architecture of the protein conducting channel associated with the translating 80S ribosome. *Cell* **107,** 361–372
43. Clemons, W. M., Jr., Menetret, J. F., Akey, C. W., and Rapoport, T. A. (2004) Structural insight into the protein translocation channel. *Curr. Opin. Struct. Biol.* **14,** 390–396
44. Takyar, S., Hickerson, R. P., and Noller, H. F. (2005) mRNA helicase activity of the ribosome. *Cell* **120,** 49–58
45. Fatica, A., and Tollervey, D. (2002) Making ribosomes. *Curr. Opin. Cell Biol.* **14,** 313–318
46. Fromont-Racine, M., Senger, B., Saveanu, C., and Fasiolo, F. (2003) Ribosome assembly in eukaryotes. *Gene (Amst.)* **313,** 17–42
47. Fujiyama, S., Yanagida, M., Hayano, T., Miura, Y., Isobe, T., and Takahashi, N. (2002) Isolation and proteomic characterization of human Parvulin-associating preribosomal ribonucleoprotein complexes. *J. Biol. Chem.* **277,** 23773–23780
48. Gautier, T., Berges, T., Tollervey, D., and Hurt, E. Nucleolar (1997) KKE/D repeat proteins Nop56p and Nop58p interact with Nop1p and are required for ribosome biogenesis. *Mol. Cell. Biol.* **17,** 7088–7098
49. Lafontaine, D. L. J., and Tollervey, D. (2000) Synthesis and assembly of the box C1D small nucleolar RNPs. *Mol. Cell. Biol.* **20,** 2650–2659
50. Wang, C., and Meier, U. T. (2004) Architecture and assembly of mammalian H/ACA small nucleolar and telomerase ribonucleoproteins. *EMBO J.* **23,** 1857–1867
51. Oliver, E. R., Saunders, T. L., Tarlé, S. A., and Glaser, T. (2004) Ribosomal protein L24 defect in Belly spot and tail (Bst), a mouse Minute. *Development* **31,** 3907–3920

Supplementary Figure S1. **Affinity purification including a negative control.** Proteins from K562 whole cell extracts were affinity-purified with GST, GST-RPS19 and GST-GATA resins. In the lane named GST 5x pulldown we used a quantity of GST protein five fold higher than in the GST-pulldown lane. Total lysates (K562 lysate) and bound proteins eluted from the GST control resin (GST), the GST-RPS19 resin (GST-RPS19) or the GST-NTGATA1 resin (GST-GATA) were analysed by western blotting with antibodies specific to the three selected interactors, as indicated. All blots were revealed by the chemiluminescence method except the for NCL which was revealed by the alkaline-phosphatase.

Supplementary Figure S2. **Co-immunoprecipitation (whole images).** Proteins from K562 cell lysates were immunoprecipitated with a monoclonal anti-RPS19 or an anti-HA antibody as negative control. Immunocomplexes were fractionated by SDS-PAGE and blotted on nitrocellulose. After the transfer, the nitrocellulose was cut (dotted lines) and incubated with the indicated antibodies. All blots were revealed by the chemiluminescence method except for NCL which was revealed by the alkaline phosphatase. Single or double asterisk indicate immunoglobulin heavy or light chains, respectively. The differences in intensity depend on the antibody concentrations (the anti-RPS19 is a hybridoma supernatant) and exposures.

Supplementary Figure S3. **Protein identification by tandem mass spectrometry.** MS full scan, MS/MS scan and amino acid sequence of CCT2 (A), DDX17 (B), and NOLA3 (C). Each MS/MS spectrum shows the predicted peptide sequence and the tryptic identified fragment. ♦ m/z signal fragmented

Figure S1

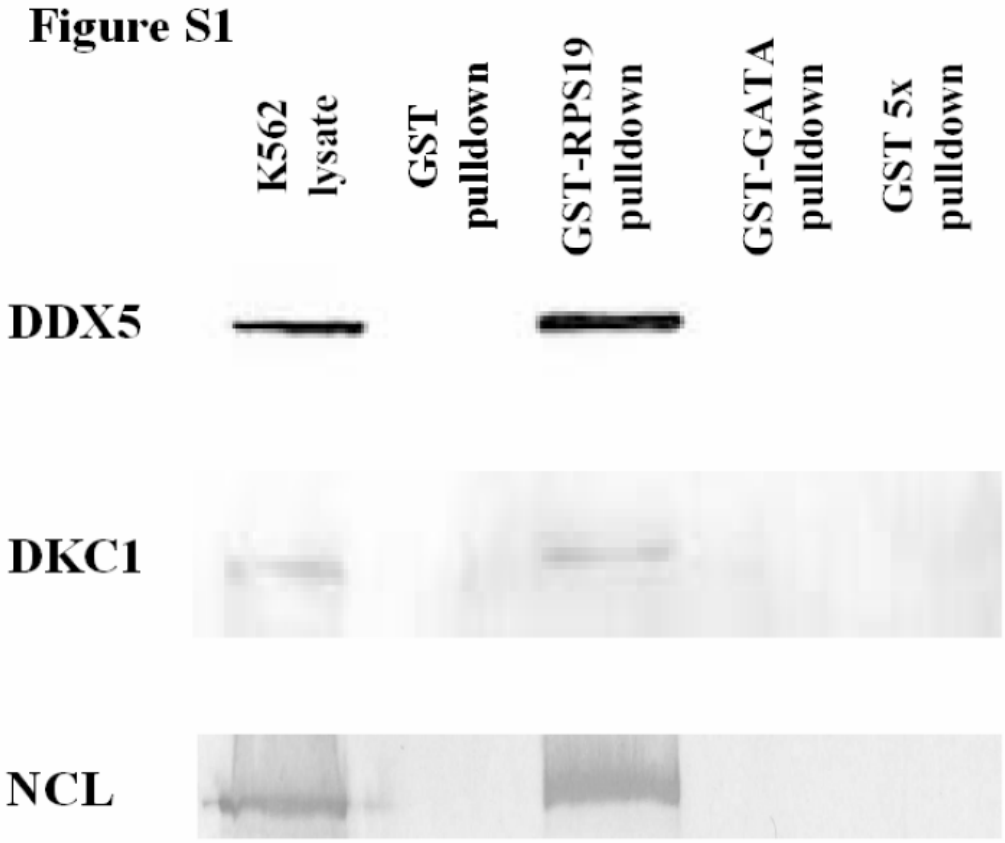
K562 lysate
GST pulldown
GST-RPS19 pulldown
GST-GATA pulldown
GST 5x pulldown
DDX5
DKC1
NCL

Figure S2A

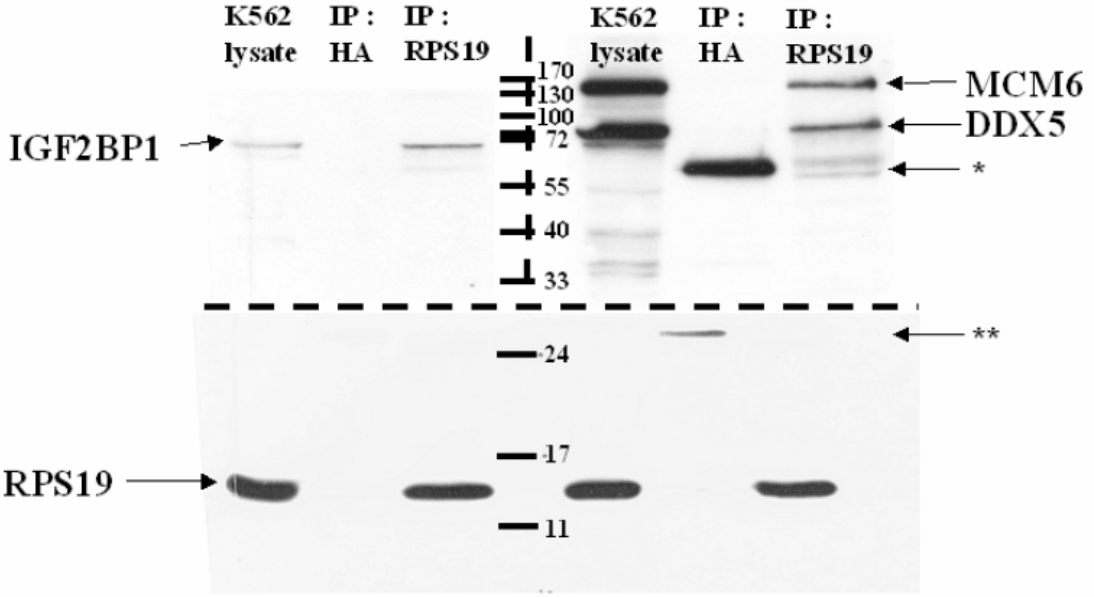

Figure S2B

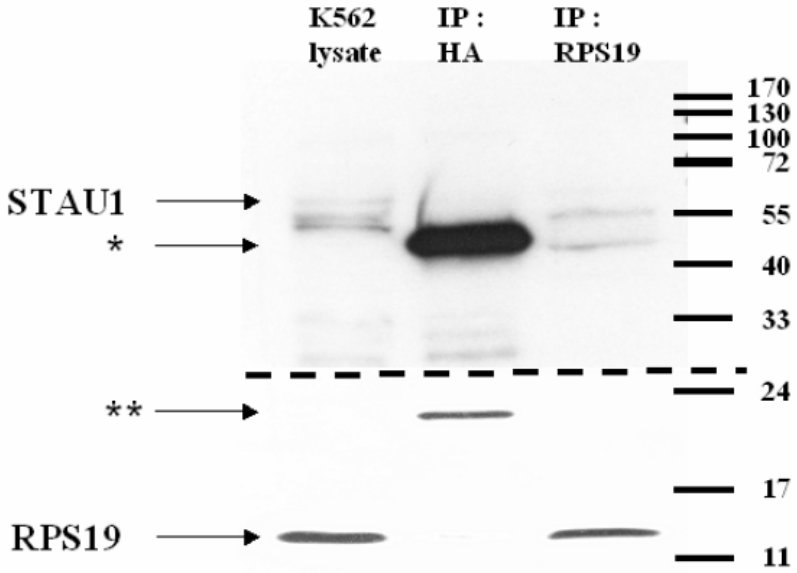

Figure S2C

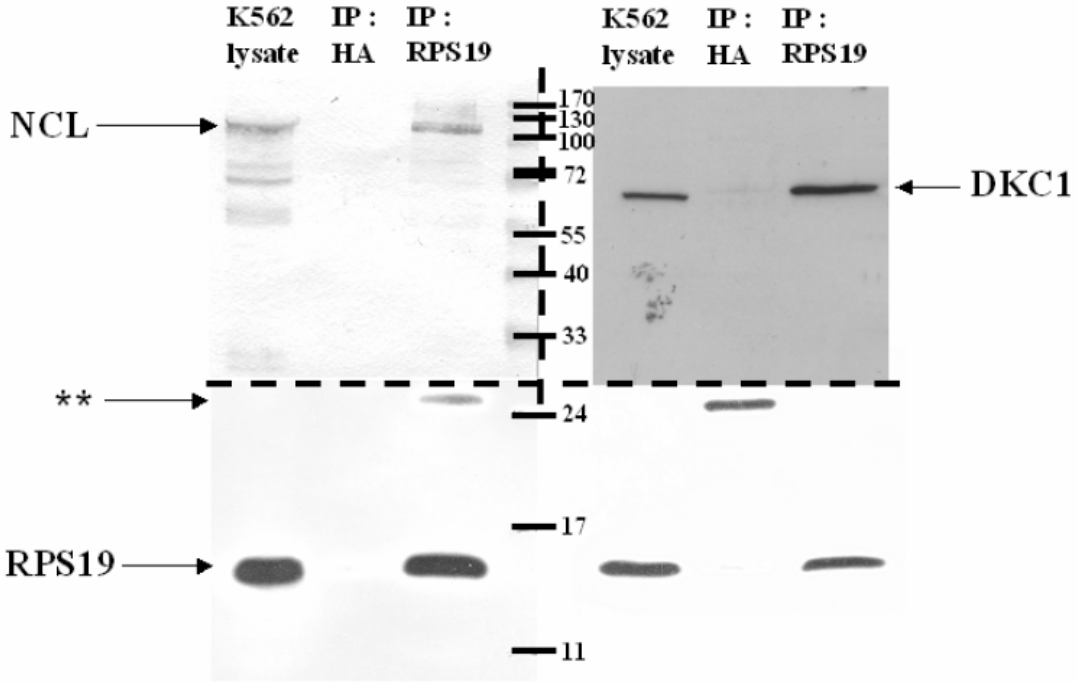
K562 lysate
IP : HA
IP : RPS19
K562 lysate
IP : HA
IP : RPS19
NCL
**
RPS19
DKC1
170
130
100
72
55
40
33
24
17
11

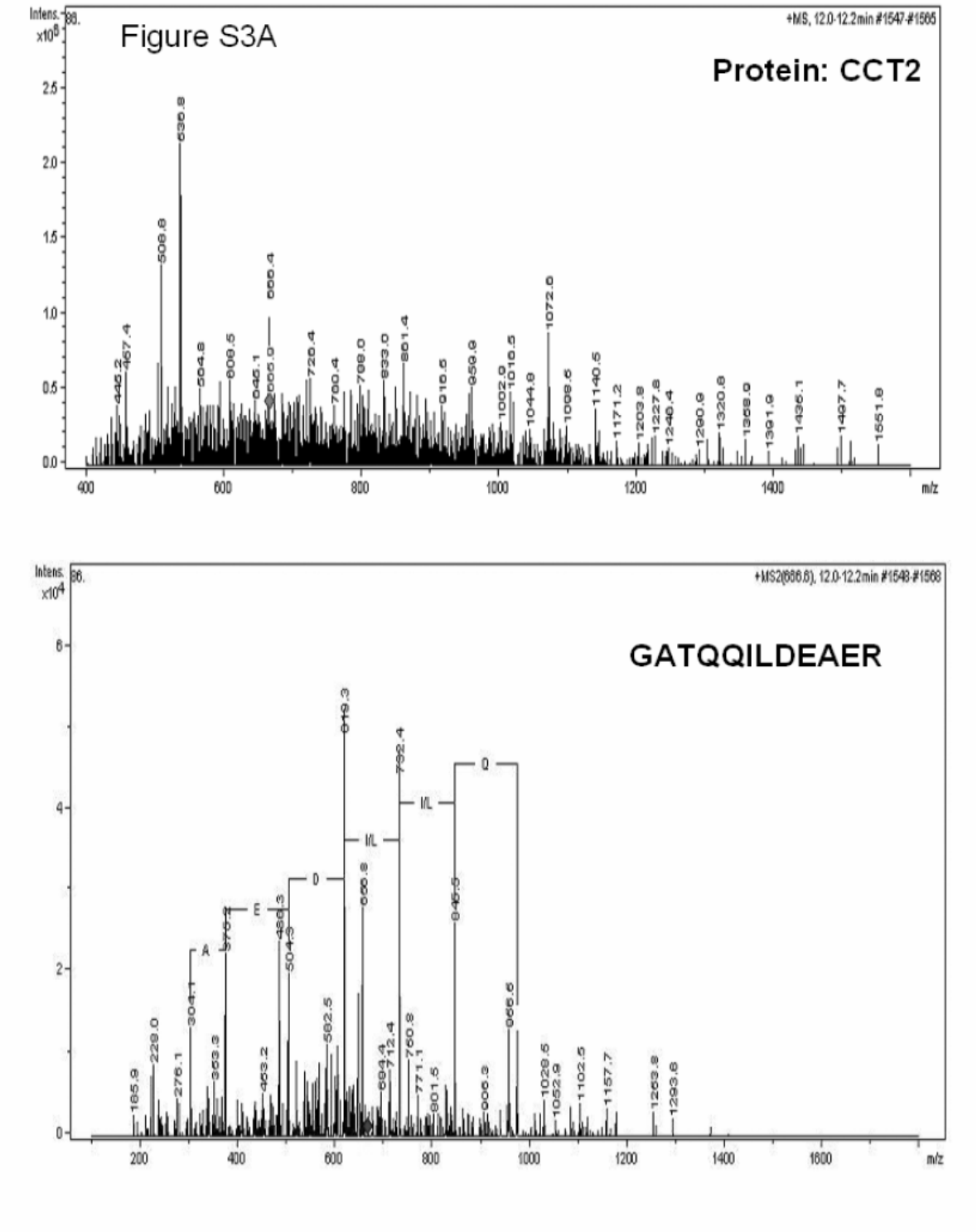
Figure S3A
Protein: CCT2
+MS, 12.0-12.2min #1547-#1565
Intens.
x10^6
GATQQILDEAER
+MS2(686.8), 12.0-12.2min #1548-#1568
Intens.
x10^4
m/z

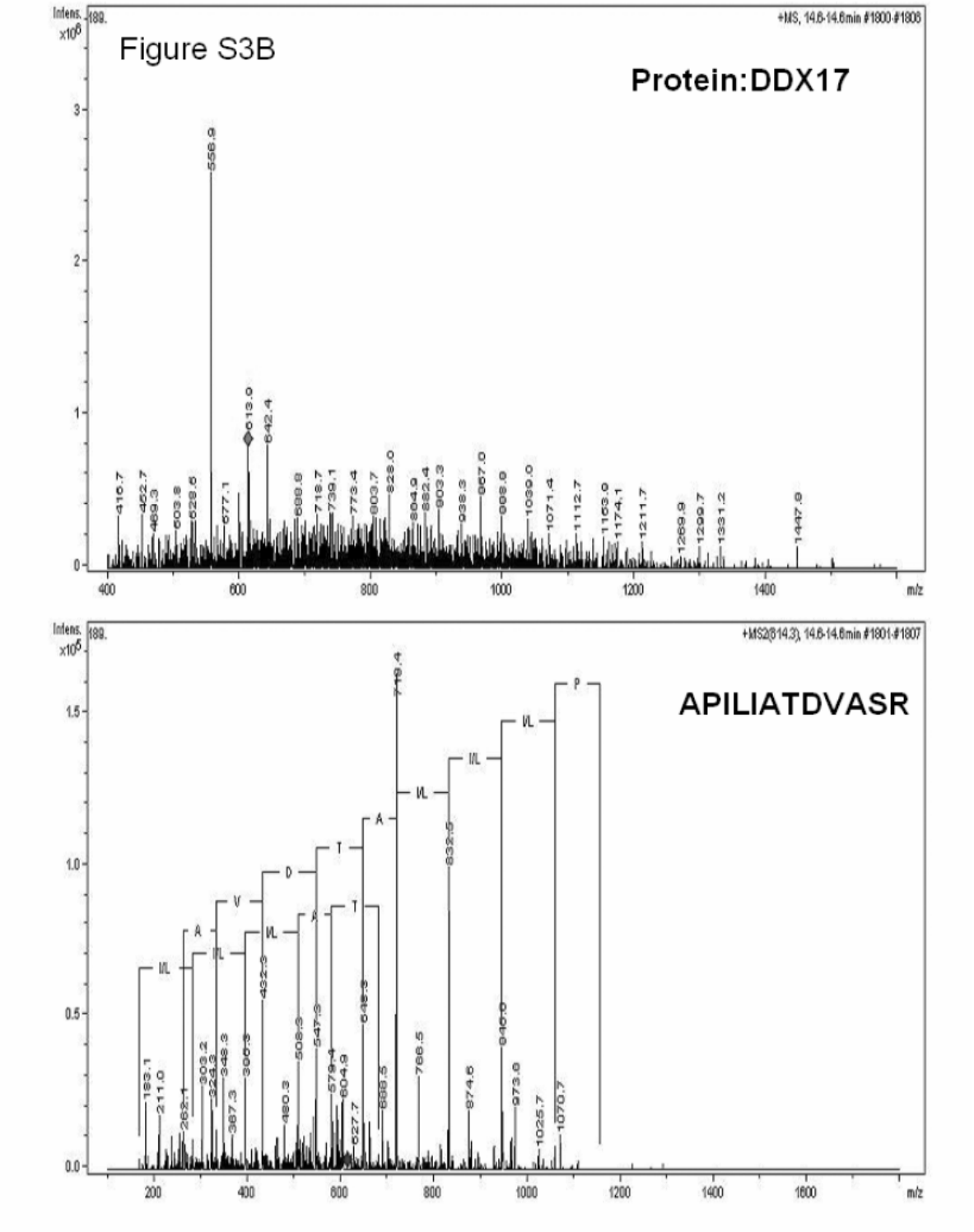
Figure S3B
Protein:DDX17
+MS, 14.6-14.6min #1800-#1806
Infens.
×10^6
189.
556.9
613.0
642.4
416.7
452.7
469.3
503.8
528.6
577.1
688.8
718.7
739.1
773.4
803.7
828.0
864.9
882.4
903.3
938.3
967.0
998.9
1039.0
1071.4
1112.7
1153.0
1174.1
1211.7
1269.9
1299.7
1331.2
1447.9
m/z
+MS2(814.3), 14.6-14.6min #1801-#1807
APILIATDVASR
P
I/L
I/L
I/L
A
T
T
D
V
A
I/L
I/L
719.4
766.5
632.5
946.6
874.6
973.6
1025.7
1070.7
432.3
518.3
547.3
578.4
604.9
627.7
688.5
480.3
506.3
367.3
348.3
324.2
303.2
262.1
211.0
189.1
m/z

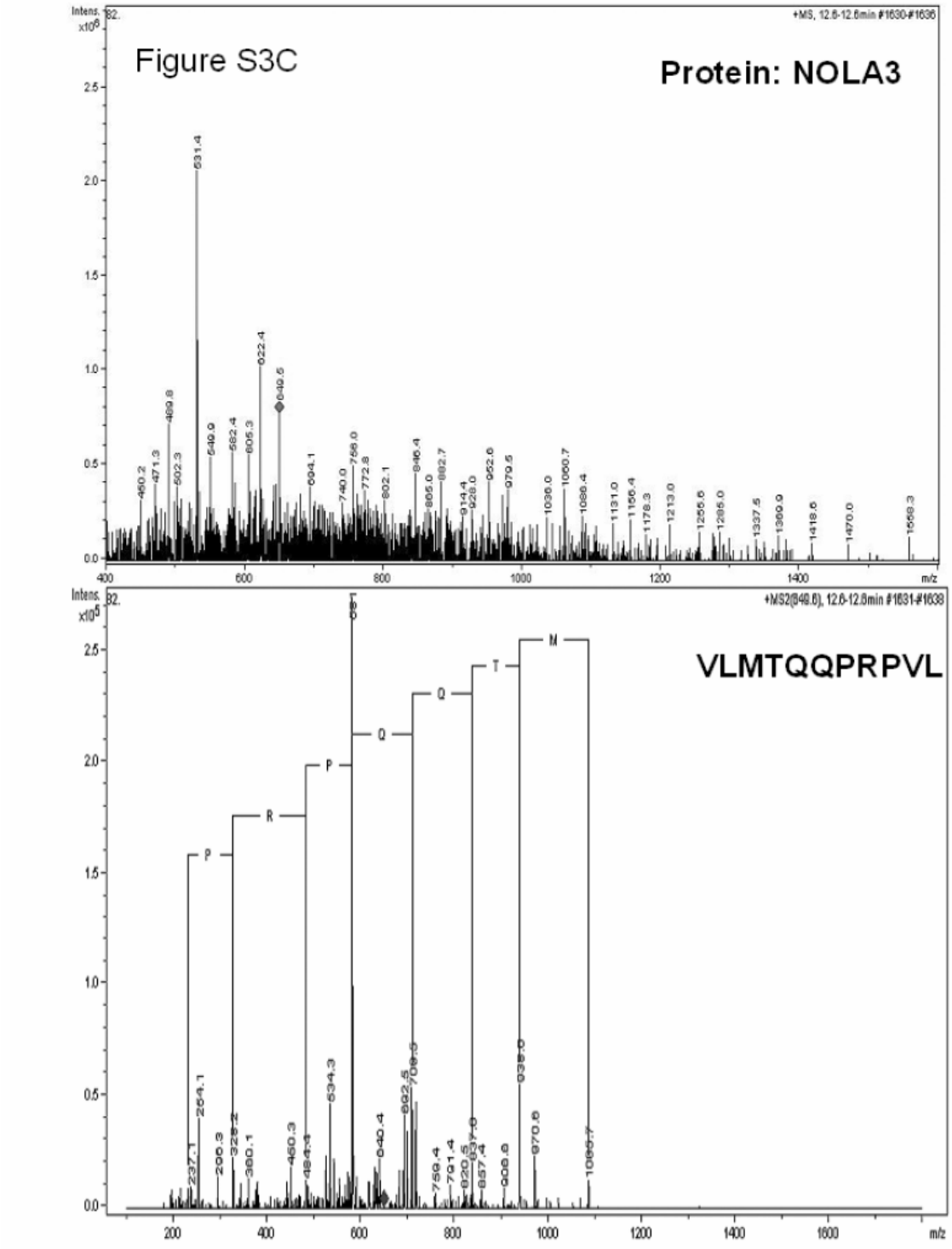
Figure S3C
Protein: NOLA3
+MS, 12.6-12.8min #1630-#1636
Intens.
x10^6
82.
531.4
622.4
649.6
469.8
549.9
582.4
605.3
450.2
471.3
502.3
644.1
740.0
756.0
772.8
802.1
846.4
865.0
892.7
914.4
928.0
952.6
979.5
1036.0
1050.7
1086.4
1131.0
1156.4
1176.3
1213.0
1255.6
1285.0
1337.5
1369.9
1418.6
1470.0
1558.3
m/z
+MS2(649.6), 12.6-12.8min #1631-#1638
Intens.
x10^5
82.
VLMTQQPRPVL
P
R
P
Q
Q
T
M
881.1
254.1
237.1
295.3
328.2
360.1
460.3
484.4
534.3
640.4
692.5
709.5
759.4
791.4
820.5
837.6
857.4
909.6
938.5
970.6
1085.7
m/z

Supplemental Table 1. Analysis of GST control lane by tandem mass spectrometry

GENE	IDENTIFIED PEPTIDE SEQUENCE	MASS ERROR (ppm)	MASCOT SCORE	SEQUENCE COVERAGE
ACTB	DLTDYLMK	4	38	14%
	QEYDESGPSIVHR	53	40	
	EITALAPSTMK	85	38	
	DLYANTVLSGGTTMYPGIADR	5	38	
BXDC2	ILIFSSR	132	48	15%
	FVLNLIK	121	50	
	LFVINEVCEMK	90	57	
	FLVQNIHTLAELK	105	38	
	NFQIIEEDAALVEIGPR	142	38	
DCD	ENAGEDPGLAR	35	40	20%
	DAVEDLESVGK	43	38	
DDB1	LFMLLLEK	114	50	1%
EEF1G	KLDPGSEETQTLVR	52	38	11%
	LDPGSEETQTLVR	21	38	
	ALIAAQYSGAQVR	14	38	
	QAFPNTNR	53	38	
EGFR	MLLVDELR	120	38	1%
	ILMVGLDAAGK	90	53	
HBZ	ISTQADTIGTETLER	67	88	10%
HEJ1	EQYSAVIIAK	26	41	15%
HSPA6	TTPSYVAFTDTER	150	41	2%
HSPCB	DNSTMGYMMAK	116	75	1%
ITGAX	ESHVAMHR	110	45	2%
	IAPPASDFLAHIQK	80	40	
K-ALPHA-1	DVNAAIATIK	110	39	2%
KRT1	SLDLDSIIAEVK	150	52	4%
	WELLQQVDTSTR	150	51	
KRT14	QFTSSSSMK	85	94	8%
	VTMQNLNDR	63	73	
	MSVEADINGLR	142	80	
	CEMEQQNQEYK	120	47	
KRT19	VLDELTLAR	104	54	2%
KRT9	MTLDDFR	150	38	8%
	TLLDIDNTR	104	40	
	QEYEQLIAK	141	43	

	QVLDNLTMEK	69	38	
	VQALEEANNDLENK	2	54	
KTR10	DAEAWFNEK	90	91	5%
	LENEIQTYR	123	46	
	ALEESNYELEGK	107	83	
KTR15	IMATTIDNSR	72	107	5%
	QGVEADINGLR	80	50	
RGD1307877	LALDIEIATYR	1	74	3%
SPATA	AVAPSIIFFDELDALAVER	72	89	7%
TSR1	QIDAPGDPFPLNPR	68	70	7%
	LLHIVGYGDFQMK	72	38	
	LEEMFPDEVDTPR	63	42	
	LLLLDTQQEAGMLLR	46	83	
TUBB4	LAVNMVPFPR	74	40	10%
	ISVYYNEATGGK	53	39	
	IMNTFSVVPSPK	89	38	
	AILVDLEPGTMDSVR	123	41	
ZNF561	SFTNFSQLYAPVK	110	130	3%

2

Supplemental table 2. Identification of RPS19 interacting proteins by tandem mass spectrometry

GENE	IDENTIFIED PEPTIDE SEQUENCE	MASS ERROR (ppm)	MASCOT SCORE	SEQUENCE COVERAGE
NTPase activity				
GTPBP4	LPTIDPNTR	107	38	12%
	LALGQINIAK	125	38	
	QSLEYLEQVR	138	38	
	TLLLCGYPNVGK	147	50	
	ADVDVQPYAFTTK	149	40	
PSMC5	GVCTEAGMYALR	89	38	20%
	VDPLVSLMMVEK	123	71	
	GVCTEAGMYALR	150	65	
	VPDSTYEMIGGLDK	110	50	
	VHVTQEDFEMAVAK	100	40	
	TMLELLNQLDGFEATK	125	38	
PSMC6	EMFNYAR	91	38	1%
RAB11B	DHADSNIVIMLVGNK	112	42	7%
XAB1	SMSLVLDEFYSSLR	120	83	4%
Hydrolase/helicase activity				
DDX5	QVSDLISVLR	107	40	10%
	APILIATDVASR	88	45	
	TTYLVLDEADR	96	50	
	RLMEEIMSEKENK	140	39	
	TGTAYTFFTPNNIK	110	46	
DDX17	APILIATDVASR	98	38	2%
DDX18	NGTGVLILSPTR	12	53	9%
	EPLYVGVDDDK	150	44	
	LGNGINIIVATPGR	50	78	
	SAEAQKLGNGINIIVATPGR	144	38	
DDX21	DFSDITKK	112	38	42%
	LHGELQDR	140	38	
	TIIFCETK	150	38	
	IGVPSATEIIK	150	38	
	EQLGEEIDSK	150	39	
	APQVLVLAPTR	133	40	
	TAITVEHLAIK	106	38	
	NGIDILVGTPGR	147	48	
	GVTFLFPIQAK	150	38	
	STYEQVDLIGK	122	38	
	TFSFAIPLIEK	110	38	
	RIGVPSATEIIK	128	38	
	EAQELSQNSAIK	136	45	
	EQLGEEIDSKVK	139	39	
	GRAPQVLVLAPTR	140	48	

	STYEQVDLIGKK	142	40	
	EEYQLVQVEQK	150	38	
	NGSFGVLVATNVAAR	147	40	
	LLDSVPPTAISHFK	109	38	
	EGAFSNFPISEETIK	138	49	
	NEEPSEEEIDAPKPK	127	40	
	WQLSVATEQPELEGPR	111	40	
	TFHHVYSGKDLIAQAR	105	38	
	LLDSVPPTAISHFKQSAEK	148	38	
	GLDIPEVDLVIQSSPPKDVESYIHR	109	40	
DDX24	DKLDILGAAETGSGK	95	76	2%
DDX3X	VGSTSENITQK	146	38	4%
	VRPCVVYGGADIGQQIR	147	40	
DDX41	SGNTGIATTFINK	150	44	2%
DDX50	VLVLAPTR	111	44	5%
	VLVATNVAAR	145	38	
	LSSNAVSQITR	107	50	
	TFSFAIPLIER	57	48	
DDX54	LLVEFAR	147	41	27%
	TSFFLVR	141	48	
	ELALQTLK	144	39	
	TIPVILDGK	129	48	
	AGLTEPVLIR	146	39	
	ATIFEINASSR	124	74	
	LVHVAVEMSLK	117	47	
	SGGFQSMGLSYPVFK	74	40	
	LPGGHQTVLFSATLPK	144	38	
	LQSVEYVVFDEADR	78	45	
	TIPVILDGKDVVAMAR	106	38	
	EMDLVGLGLHPLFSSR	150	38	
	LFEMGFAEQLQEIIAR	84	69	
	AKEMDLVGLGLHPLFSSR	96	38	
	GLDIPLLDNVINYSFPAK	112	38	
	MEDQFAALHENPDIIIATPGR	5	54	
	VPQSVVDEEDSGLQSTLEASLELR	85	49	
DHX9	LGGIGQFLAK	119	40	21%
	MLNMIR	105	43	
	LNMATLR	113	38	
	MGGEEAEIR	115	38	
	MTPSYEIR	106	38	
	LSMSQLNEK	96	40	
	DFVNYLVR	146	38	
	VFDPVPVGVTK	138	38	
	DVVQAYPEVR	59	40	
	TPLHEIALSIK	122	38	
	AAMEALVVEVTK	133	38	
	KVFDPVPVGVTK	93	39	
	LAAQSCALSLVR	146	40	
	YPSPFFVFGEK	127	38	
	SFIAEMTIYIK	120	38	
	ETPFELIEALLK	135	39	

	YQILPLHSQIPR	143	38	
	GISHVIVDEIHER	106	38	
	QPAIISQLDPVNER	150	40	
	VQSDGQIVLVDDWIK	111	38	
	ELDALDANDELTPLGR	52	38	
	GMTLVTPLQLLLFASK	109	38	
	QLYHLGVVEAYSGLTK	96	42	
	AIEPPPLDAVIEAEHTLR	30	38	
	KFESEILEAISQNSVVIIR	3	40	
	NELMYQLEQDHDLQAILQER	7	38	
	LGGIGQFLAKAIEPPPLDAVIEAEHTLR	150	38	
	DINTDFLLVVLR	142	38	
DHX15	EVDDLGPEVGDIK	148	54	2%
DHX36	ELDILLQEK	146	38	3%
	NLQSDVLMTVVK	108	63	
	ASLLDDYQLPEILR	110	69	
MCM2	VAVGELTDEDVK	149	38	6%
	QLVAEQVTYQR	147	49	
	DTVDPVQDEMLAR	112	53	
	YDPSLTFSENVDLTEPIISR	148	81	
MCM6	YLQLAEELIRPER	147	46	7%
	EIESEIDSEEELINK	17	76	
	LFLDFLEEFQSSDGEIK	143	45	
MCM7	AGILTTLNAR	150	38	4%
	SITVLVEGENTR	147	47	
RUVBL2	TTEMETIYDLGTK	20	70	3%
SKIV2L2	ALFATETFAMGINMPAR	110	38	2%
SMARCA5	FEYLLK	147	48	14%
	EILFYR	139	43	
	FDWFLK	116	39	
	DIDILNSAGK	147	44	
	YLVIDEAHR	117	52	
	LDSIVIQQGR	106	61	
	FITDNTVEER	33	64	
	KANYAVDAYFR	83	62	
	TLQTISLLGYMK	130	45	
	LRLDSIVIQQGR	122	38	
	LGFDKENVYDELR	150	38	
	ESEITDEDIDGILER	121	70	
	TPEEVIEYSAVFWER	43	62	
	NFTMDTESSVYNFEGEDYR	34	61	
XRN2	TGGYLTESGYVNLQR	88	38	6%
	ELTMASLPFTFDVER	115	38	
	AALEEVYPDLTPEETR	102	38	
	VQMIMLAVGEVEDSIFK	105	35	
Isomerase activity				
DKC1	LHNAIEGGTQLSR	140	41	6%

5

	ALETLTGALFQRPPLIAAVK	150	38	
PPIH	IIDGLLVMR	105	61	10%
	IELFADVVPK	115	69	
Kinase activity				
CSNK2A1	ALDYCHSMGIMHR	112	55	4%
SRP72	LTNAEGVEFK	144	43	10%
	VLANNSLSFEK	147	38	
	GTQGATAGASSELDASK	135	63	
	TVSSPPTSPRPGSAATVSASTSNIIPPR	146	38	
PRKCQ	AKGQSLQDPFLNALR	6	41	2%
Splicing factor activity				
SF3B1	TEILPPFFK	76	43	8%
	QLVDTTVELANK	145	42	
	LLVDVDESTLSPEEQK	122	38	
	ILVVIEPLLIDEDYYAR	113	40	
	MVMETIEKIMGNLGAADIDHK	107	38	
	AAGLATMISTMRPDIDNMDEYVR	109	55	
SF3B2	YGPPPSYPNLK	150	40	3%
	GIEKPPFELPDFIK	150	38	
SF3B3	SVAGGFVYTYK	126	55	11%
	LTISSPLEAHK	147	39	
	IVPGQFLAVDPK	93	38	
	FLAVGLVDNTVR	123	53	
	ILELLRPDPNTGK	150	38	
	TVLDPVTGDLSDTR	107	67	
	ITLETDEDMVTEIR	42	90	
	NENQLIIFADDTYPR	83	46	
	ELAAEMAAAFLNENLPESIFGAPK	114	60	
SFRS9	HGLVPFAFVR	144	44	10%
	IYVGNLPTDVR	24	38	
SFRS10	VDFSITK	150	38	12%
	YGPIADVSIVYDQQSR	133	7	
Structural costituent of Ribosome				
RPL10A	DTLYEAVR	20	46	10%
	KYDAFLASESLIK	74	50	
RPL14	GTAAAAAAAAAAAAK	60	96	18%
	VAYVSFGPHAGK	113	50	
	LVAIVDVIDQNR	15	68	
RPL24	VFQFLNAK	148	52	13%
	TAMAAAKAPTK	97	70	
RPL27A	TGAAPIIDVVR	99	71	7%
RPL3	HGSLGFLPR	20	38	2%

RPL4	NIPGITLLNVSK	142	44	3%
RPL6	YYPTEDVPR	147	51	3%
RPL7	ASINMLR	145	38	31%
	KVLQLLR	138	38	
	SVNELIYK	145	38	
	EVPAVPETLK	129	38	
	SVNELIYKR	71	38	
	IALTDNALIAR	76	47	
	AGNFYVPAEPK	92	38	
	KAGNFYVPAEPK	5	42	
RPL7A	AGVNTVTTLVENK	148	76	7%
RPL8	AVVGVVAGGGR	85	61	5%
RPL9	TILSNQTVDIPENVDITLK	90	49	10%
RPLP0	EDLTEIR	131	38	2%
RPLP1	AAGVNVEPFWPGLFAK	117	41	14%
RPLP2	LASVPAGGAVAVSAA	50	38	31%
RPS10	IAIYELLFK	135	64	5%
RPS14	IEDVTPIPSDSTR	14	46	9%
RPS16	DILIQYDR	122	38	40%
	ALVAYYQK	90	38	
	TATAVAHCK	84	38	
	GPLQSVQVFGR	75	38	
	VNGRPLEMIEPR	150	38	
	GGGHVAQIYAIR	95	38	
8				
RPS2	GTGIVSAPVPK	68	60	11%
RPS23	VANVSLLALYK	67	87	8%
RPS24	QMVIDVLHPGK	54	69	22%
	TTGFGMIYDSLDYAK	60	70	
RPS26	GHVQPIR	100	70	17%
	LHYCVSCAIHSK	98	49	
RPS3	ELTAVVQK	34	38	30%
	KFVADGIFK	68	42	
	TEIIILATR	150	57	
	AELNEFLTR	54	49	
	ELAEDGYSGVEVR	56	57	
	KPLPDHVSIVEPK	144	43	
	DEILPTTPISEQK	41	38	
RPS4X	LSNIFVIGK	131	51	18%
	YALTGDEVK	90	38	

7

	TIRYPDPLIK	150	38	
	TDITYPAGFMDVISIDK	5	50	
RPS5	QAVDVSPLR	10	44	4%
RPS6	LIEVDDER	20	56	8%
	DIPGLTDTTVPR	39	61	
RPS7	AIIIFVPVPQLK	60	41	6%
RPS8	LTPEEEEILNK	8	47	5%
RPSA	LLVVTDPR	150	50	25%
	SDGIYIINLK	70	52	
	FAAATGATPIAGR	33	51	
	AIVAIENPADVSVISS	46	70	
	FLAAGTHLGGTNLDFQMEQYTYK	15	38	
RSL1D1	FFTTPSK	72	38	33%
	SPNPSTPR	128	40	
	LLFVKTEK	41	38	
	QLDKEQVR	10	38	
	RLLPSLIGR	19	38	
	VPVSVNLLSK	5	42	
	AVDALLTHCK	18	38	
	KVPVSVNLLSK	84	44	
	TVSQIISLQTLK	37	38	
	DDVAPESGDTTVK	8	43	
	TVSQIISLQTLKK	41	38	
	LLSSFDFFLTDAR	26	100	
	EINDCIGGTVLNISK	110	50	
	ATNESEDEIPQLVPIGK	54	38	
	DEPNSTPEKTEQFYR	5	39	
Transcription factor				
BAZ1B	GGLGYVEETSEFEAR	150	75	1%
HNRPD	IFVGGLSPDTPEEK	74	78	12%
	EYFGGFGEVESIELPMDNK	9	74	
ILF2	VLQSALAAIR	67	90	25%
	KLDPELHLDIK	150	38	
	ILPTLEAVAALGNK	70	77	
	VKPAPDETSFSEALLK	23	69	
	INNVIDNLIVAPGTFEVQIEEVR	150	38	
	AQDPSEVLTMLTNETGFEISSSDATVK	150	51	
ILF3	AYAALAALEK	118	63	14%
	LFPDTPLALDANK	127	83	
	VADNLAIQLAAVTEDK	36	63	
	EPPLSLTIHLTSPVVR	78	52	
	VLAGETLSVNDPPDVLDR	89	55	
	VADNLAIQLAAVTEDKYEILQSVDDAAIVIK	57	46	
NKRF	DIEQIIR	131	44	13%
	EIPPADIPK	150	42	
	INYTYMLTR	92	43	

	LLTDGYACEVR	131	52	
	TNPEYIYAPLK	84	54	
	VILESEVIAEAVGVK	130	64	
PURA	FFFDVGSNK	94	65	11%
	LIDDYGVEEEPAELPEGTSLTVDNK	33	59	
TAF15	GEATVSFDDPPSAK	150	44	2%
TRIM28	LSPPYSSPQEFAQDVGR	139	46	2%
UBTF	DYEVELLR	122	39	13%
	KKDYEVELLR	148	38	
	HPELNISEEGITK	82	40	
	ITLTELILDAQEHVK	143	38	
XPO5	DPLLLAIIPK	145	45	3%
	LFSSVTFETVEESK	62	61	
	QGETQTELVMFILLR	62	70	
YBX1	GAEAANVTGPGGVPVQGSK	53	57	10%
	SVGDGETVEFDVVEGEK	5	105	
Transferase activity				
FDFT1	ALDTLEDDMTISVEK	86	71	6%
	AIIYQYMEEIYHR	140	94	
FTSJ3[29,47]	FQFLQK	150	38	13%
	EVEVQAK	102	54	
	TSVTDFLR	150	48	
	AANPVDFLSK	141	42	
	DLIDNSFNR	128	38	
	AEAVVNTVDISER	150	53	
	ILDPEGLALGAVIASSK	78	79	
	SDDDGFEIVPIEDPAK	51	38	
	LTEVQDDKEEEEEENPLLVPLEEK	138	38	
NAT10	SMDLSEYIIR	150	38	4%
	LDYLGVSYGLTPR		41	
	LGQAELVVIDEAAAIPLPLVK		41	
NOL1	GVNLDPLGK	119	39	14%
	DLAQALINR	137	60	
	IQDIVGILR	145	51	
	GADSELSTVPSVTK	137	38	
	VLLDAPCSGTGVISK	46	44	
	LGVTNTIISHYDGR	131	50	
	ELLLSAIDSVNATSK	30	78	
	LVPTGLDFGQEGFTR	72	53	
	SPEAKPLPGKLPKGAVQTAGK	137	47	
ZC3HAV1	ASLEDAPVDDLTR	150	44	2%
Transporter activity				
COPA	MHSLLIK	63	38	13%
	VWDISGLR	105	38	
	TALNLFFK	147	44	

	GFFEGTIASK	150	47	
	VLTIDPTEFK	106	51	
	TLDLPIYVTR	126	56	
	NLSPGAVESDVR	105	55	
	EYIVGLSVETER	86	55	
	DADSITLFDVQQK	54	65	
	SILLSVPLLVVDNK	126	61	
	GITGVDLFGTTDAVVK	113	51	
	VTTVTEIGKDVIGLR	69	59	
	LLELGPKPEVAQQTR	71	56	
	ASNLENSTYDLYTIPK	8	43	
COPB2	GSNNVALGYDEGSIIVK	121	75	3%
CSE1L	TGNIPALVR	128	50	14%
	VIVPNMEFR	149	62	
	SANVNEFPVLK	144	58	
	DAAIYLVTSLASK	126	49	
	ALTLPGSSENEYIMK	60	52	
	LVLDAFALPLTNLFK	66	38	
	YGALALQEIFDGIQPK	68	53	
	AADEEAFEDNSEEYIR	42	66	
	LLQTDDEEEAGLLELLK	98	86	
IPO4	QGCTVAEK	121	67	2%
	LLMASPTR	90	65	
IPO7	ETENDDLTNVIQK	110	64	3%
	ENIVEAIIHSPELIR	117	68	
NPEPL1	YHAAVLTNSAEWEAACVK	58	44	3%
STAU1	VSVGEFVGEGEGK	38	43	3%
SSR4	FFDEESYSLLR	112	69	6%
XPO1	YVVGLIIK	121	38	7%
	IYLDMLNVYK	148	45	
	EFAGEDTSDLFLEER	40	84	
	LLSEEVFDFSSGQITQVK	46	62	
	MAKPEEVLVVENDQGEVVR	14	40	
DNA/RNA/protein binding capacity				
AATF	DKGGPEFSSALK	150	41	2%
ACTR1B	DWNDMER	120	67	2%
C1orf77	LGRPIGALAR	91	69	10%
CCT2	GATQQILDEAER	112	58	2%
CCT8	DIDEVSSLLR	118	46	2%
CEBPZ	ALLVQVVNK	133	40	10%
	EQIDTLFK	127	39	
	QTLLLRPGGK	122	38	
	MLSALLTGVNR	148	38	
	QAMFLNLVYK	65	39	

10

	LYQHEINLFK	150	38	
	ELLITDLLPDNR	136	40	
	DKQNIFEFFER	109	40	
	EESQIPVDEVFFHR	69	38	
	KLETEETVPETDVETK	59	40	
CENPC1	VSDEEDK	58	80	3%
	QMPPVGSK	89	55	
	ILATDVSSK	95	95	
COPG	SIATLAITTLLK	148	69	5%
	SLEELPVDIILASVG	32	51	
	LLLLDTVTMQVTAR	126	95	
DHX30	IPQLLLER	100	51	17%
	ALTQFPLPK	120	39	
	VPGFMYPVK	123	38	
	EYLTTLGQR	92	50	
	AVAGWEEVLR	148	76	
	LQSDDILPLGK	146	48	
	AIFQQPPVGVR	99	38	
	TPLENLVLQAK	98	47	
	EHYLEDILAK	130	38	
	ATISLSDSDLLR	77	53	
	MVPFQVPEILR	89	40	
	DVNTDFLLILLK	128	72	
	GVLMAGLYPNLIQVR	90	44	
	AVDEAVILLQEIGVLDQR	121	55	
	DSGPLSDPITGKPYVPLLEAEEVR	23	38	
	WQDRSSRENYLEENLLYAPSLR	132	38	
DNAJC9	ELGLDEGVDSLK	150	41	8%
	ISLEDIQAFEK	150	43	
FBL	TNIIPVIEDAR	120	62	11%
	NLVPGESVYGEK	150	38	
	VSISEGDDKIEYR	150	52	
FUSIP1	DAEDALHNLDR	8	57	6%
GNB2L1	DVLSVAFSSDNR	99	66	4%
HIST1H1C	ALAAAGYDVEK	63	42	12%
	SETAPAAPAAPAPAEK	40	40	
HIST1H1D	ALAAAGYDVEK	72	46	10%
	ASGPPVSELITK	125	57	
HIST1H2AK	NDEELNK	110	38	5%
HIST1H2BL	LLLPGELAK	112	38	7%
HIST1H2BO	QVHPDTGISSK	123	50	17%
	AMGIMNSFVNDIFER	90	53	
HIST2H4	ISGLIYEETR	93	65	36%
	DNIQGITKPAIR	136	48	

	TVTAMDVVYALK	141	80	
	TVTAMDVVYALKR	142	38	
HNRPA2B1	DYFEEYGK	28	38	8%
	TLETVPLER	75	40	
	IDTIEIITDR	76	47	
HNRPA3	LFIGGLSFETTDDSLR	45	94	5%
HNRPC	VPPPPPIAR	22	58	9%
	SDVEAIFSK	70	51	
	KSDVEAIFSK	62	61	
HNRPDL	DLTEYLSR	70	46	3%
HNRPF	SSQEEVR	70	85	13%
	TEMDWVLK	98	90	
	VHIEIGPDGR	110	56	
	DLSYCLSGMYDHR	123	48	
	QSGEAFVELGSEDDVK	57	54	
HNRPR	LFVGSIPK	150	43	8%
	ENILEEFSK	150	46	
	TGYTLDVTTGQR	30	57	
	NLATTVTEEILEK	116	79	
	DLYEDELVPLFEK	12	48	
HNRPU	FIEIAAR	89	38	5%
	GYFEYIEENK	100	41	
	YNILGTNTIMDK	141	38	
	NFILDQTNVSAAAQR	78	97	
HNRPUL2	EEAYHSR	112	46	2%
	ANFSLPEK	109	38	
HP1BP3	SGASVVAIRK	101	40	9%
	GASGSFVVVQK	65	40	
	YIIHKYPSLELER	147	47	
	SSAVDPEPQVK	112	38	
IGF2BP1	MVIITGPPEAQFK	150	39	10%
	LLVPTQYVGAIIGK	149	50	
	TVNELQNLTAAEVVVPR	10	54	
	LYIGNLNESVTPADLEK	21	50	
IGF2BP3	ALQSGPPQSR	10	38	
	IPVSGPFLVK	5	38	
	QKPCDLPLR	9	51	
	DQTPDENDQVVVK	9	43	
	SITILSTPEGTSAACK	6	66	
IMP3	LYALGLVPTR	140	52	5%
ITGB4BP	ETEEILADVLK	31	63	4%
LYAR	FQNWMK	150	78	3%

	QQAWIQK	95	48	
NCL	ALELTGLK	145	38	17%
	TGISDVFAK	124	42	
	GIAYIEFK	131	41	
	NDLAVVDVR	110	68	
	EVFEDAAEIR	150	73	
	GFGFVDFNSEEDAK	147	38	
	FGYVDFESAEDLEK	73	75	
	GLSEDTTEETLKESFDGSVR	91	43	
	TLVLSNLSYSATEETLQEVFEK	28	67	
NIP7[29]	LHVTALDYLAPYAK	142	62	10%
NOLA1	FYIDPYK	105	38	13%
	VDEIFGQLR	18	38	
	VPYFNAPVYLENK	6	49	
NOL5A	VVSLSEYR	148	40	1%
PABPC3	IVATKPLYVALAQR	150	56	2%
PAK1IP1	GEQYVVIIQNK	142	61	12%
	FLSESVLAVAGDEEVIR	103	77	
	IDIYQLDTASISGTITNEK	14	83	
PNN	LLALSGPGGGR	140	38	5%
	IEFAEQINK	120	42	
	LTEVPVEPVLTVHPESK	117	42	
PPP2R1A	LSTIALALGVER	120	50	2%
RAB1B	QWLQEIDR	98	49	4%
RAP1B	LVVLGSGGVGK	85	40	6%
RBM19	NLPYTSTEEDLEK	117	38	5%
	ILGENEEEEDLAESGR	146	92	
	VLLPEGGITAIVEFLEPLEAR	127	64	
RBMX	ALEAVFGK	72	50	13%
	IVEVLLMK	137	59	
	LFIGGLNTETNEK	91	57	
	GFAFVTFESPADAK	60	61	
RNPC2	IESIQLMMDSETGR	116	36	8%
	TDASSASSFLDSDELER	16	94	
SART3	IQLIFER	150	38	4%
	SALQALEMDR	148	44	
	EFESAIVEAAR	133	85	
	LAEYQAYIDFEMK	12	60	
SNRPA1	SLTYLSILR	94	46	4%
SNRPG	HVQGILR	80	42	9%

SNRPN	VLGLVLLR	104	48	10%
	GENLVSMTVEGPPPK	19	52	
SRP68	ALLQQQPEDDSKR	133	39	2%
SURF6	LLQEALK	65	48	2%
SYNCRIP	LFVGSIPK	120	44	2%
	TGYTLDVTTGQR	30	57	
Other function				
Dehydrogenase activity				
DPYD	VKEALSPIK	120	43	1%
Ligase activity				
MARS	ITQDIFQQLLK	148	37	5%
	GFVLQDTVEQLR	145	62	
	FFGGYVPEMVLTPDDQR	5	40	
Peptidase activity				
SEC11L1	VGEIVVFR	107	70	4%
Receptor activity				
REEP6	NVKPSQTPQPK	150	77	6%
Translation elongation factor activity				
EEF1B2	SPAGLQVLNDYLADK	12	82	15%
	YGPADVEDTTGSGATDSK	28	74	
Unknown function				
EBNA1BP2[25,28,29]	DLEWVER	95	38	14%
	QAQAAVLAVLPR	150	40	
	LDVTLGPVPEIGGSEAPAPQNK	120	39	
GPIAP1	QILGVIDKK	150	38	1%
HDCMA18P	MGEEVIPLR	149	39	4%
	SSAVVELDLEGTR	147	38	
LOC389217	LSQMQNK	110	62	1%
MGC3731	DPLLSQR	120	72	3%
NOC2L	QLAIHLR	60	45	4%
	EIQLEISGK	106	38	
	LEDLNFPEIK	105	46	
NOC3L	LGQASLGVIK	142	76	8%
	SPLLPAVLEGLAK	137	54	
	FYLENLEQMVK	77	38	
	YSSEVATESPLDFTK	84	40	
	SMLMEQDPDVAVTVR	6	47	
NOL10	QLTFTLKR	150	40	2%
	LLEQQELR	146	38	
NOLA3	VLMTQQPRPVL	139	45	17%

PES1	GSATNYITR	20	56	1%
RBM12B	YAFVMFK	145	38	16%
	GVGLGEALVK	149	44	
	NFPFDVTK	144	38	
	NLSLSIDER	124	44	
	FLGTEVLLR	150	67	
	AENPYLFLR	142	41	
	DSSVELFLSSK	148	77	
	GLPYLVNEDDVR	145	56	
	LLGLPFIAGPVDIR	108	42	
	DPPIYSVGAFENFR	67	42	
	FFADFLLAEDDIYLLYDDK	90	40	
	FLYKDENRTR	43	40	
RP13-36C9.1	VAVDPETVFK	144	53	13%
	IFEMLEGVQGPTAVR	12	58	
SYNGR2	AGGSFDLR	90	42	4%

Supplemental Table 3. Nucleolar Interactors of RPS19

GENE	PROTEIN	YEAST GENE
MCM2	MCM2 minichromosome maintenance deficient 2, mitotin (*S. cerevisiae*)	MCM2
MCM6	p105MCM (MCM6 minichromosome maintenance deficient 6)	MCM6
MCM7	p85MCM protein (MCM7 minichromosome maintenance deficient 7)	CDC47
GTPBP4	GTP/binding protein NGB (G protein binding CRFG)	NOG1
DDX5	growth regulated nuclear 68 protein (DEAD box polypeptide 5)	DBP2
DDX17[28]	DDX17 protein	
DDX18	RNA helicase (DEAD box polypeptide 18)	HAS1
DDX21	RNA helicase II / Gu protein (DEAD box polypeptide 21)	
DDX24[29]	DEAD box polypeptide 24	MAK5
DDX3X	dead box , X isoform (DEAD box polypeptide 3)	
DDX41	DEAD box protein abstrakt	
DDX50	DEAD box polypeptide 50 (Nucleolar protein GU2)	
DDX54	ATP/dependent RNA helicase (DEAD box polypeptide 54)	DBP10
DHX9	RNA helicase A (DEAH box polypep. 9)	
DHX15	DEAH box polypeptide 15	PRP43

RUVBL2[25]	RuvB-like 2	RVB2
SMARCA5	SWI/SNF related, matrix associated, actin dependent regulator of chromatin, subfamily a, member 5	ISW2
XRN2	Dhm1-like protein (5'-3' exoribonuclease 2)	RAT1
DKC1	Cbf5p homolog (dyskerin)	
PPIH	peptidyl prolyl isomerase H	
CSNK2A1[25]	casein kinase 2, alpha 1 polypeptide	
SRP72	signal recognition particle 72	SRP72
SF3B2	splicing factor 3b, subunit 2, 145 kDa	CUS1
SFRS10	splicing factor arg/ser rich 10	
RPL10A[25,28,29]	60S ribosomal protein L10a	RPL1B
RPL14	60S ribosomal protein L14	RPL4B
RPL24	60S ribosomal protein L24	RPL24A
RPL27A[25,28,29]	60S ribosomal protein L27a	RPL28
RPL3[25,28,29]	60S ribosomal protein L3	RPL3
RPL4[25,28,29]	60S ribosomal protein L4	RPL4B
RPL6[25,28,29,32]	60S ribosomal protein L6	RPL6B
RPL7[25,29]	60S ribosomal protein L7	
RPL7A[25,28,29,31]	60S ribosomal protein L7a	RPL8B
RPL8[25,28]	60S ribosomal protein L8	RPL2A
RPL9[25,28]	60S ribosomal protein L9	RPL9B
RPLP2[25]	60S acidic ribosomal protein P2	RPP2B
RPS10[25]	40S ribosomal protein S10	RPS10A
RPS14[25,29]	40S ribosomal protein S14	RPS14B
RPS16[25]	40S ribosomal protein S16	RPS16A

RPS2[25,31]	40S ribosomal protein S2	RPS2
RPS23[25]	40S ribosomal protein S23	RPS23A
RPS24[25]	40S ribosomal protein S24	RPS24B
RPS4X[25]	40S ribosomal protein S4, X-linked	RPS4A
RPS5[25,28,29]	40S ribosomal proteinS5	RPS5
RPS6	40S ribosomal protein S6	RPS6B
RPS7[25]	40S ribosomal protein S7	RPS7A
RPS8[25,28,31]	40S ribosomal protein S8	RPS8B
RPSA	ribosomal protein SA	RPS0A
RSL1D1	PBK1 protein	
BAZ1B[25]	bromodomain adjacent to zinc finger domain, 1B	
HNRPD[25]	heterogeneous nuclear ribonucleoprotein D2	
ILF2[30]	interleukin enhancer binding factor 2	
ILF3[30]	nuclear factor associated with dsRNA NFAR-2	
TAF15[25]	TLS protein (TBP-associated factor 15)	NPL3
TRIM28[25]	tripartite motif-containing 28	
UBTF	upstream binding transcription factor, RNA polymerase I	
FTSJ3	FtsJ homolog 3 (*E. coli*)	SPB1
NOL1	proliferating cell nuclear protein p120 (NOL protein 1)	NOP2
XPO1	exportin 1 (CRM1 homolog yeast)	CRM1
AATF[25,28,29]	Ded protein (Apoptosis antagonizing transcription factor)	BFR2

CCT2[25,29]	chaperonin containing TCP1, subunit 2 (beta)	CCT2
CEBPZ	CCAAT/enhancer binding protein zeta	MAK21
COPG	coatomer protein complex, subunit gamma 1	SEC21
FBL	fibrillarin, U3 small nucleolar interacting protein 1	NOP1
GNB2L1[25]	Guanine nucleotide binding protein (G protein), beta polypeptide 2-like 1	
HIST1H1C[25]	Histone H1b	
HIST1H1D[25]	Histone H1 member 3	
HIST1H2AK[25]	Histone 1 H2Ak	
HIST1H2BL[25]	H2B histone family, member C	
HIST1H2BO[25]	Histone 1, H2bo	
HNRPA2B1[25,28,29]	Heterogeneous nuclear ribonucleoprotein A2/B1	
HNRPC[25,30]	Heterogeneous nuclear ribonucleoprotein C	
HNRPDL[25]	Heterogeneous nuclear ribonucleoprotein D-like (A+U-rich element RNA binding factor)	
HNRPF	heterogeneous nuclear ribonucleoprotein F	
HNRPR[25]	Heterogeneous nuclear ribonucleoprotein R	
HNRPU[25,30]	heterogeneous nuclear ribonucleoprotein U (scaffold attachment factor A)	
HP1BP3	HP1-BP74	
IMP3[28]	U3 snoRNP protein 3 homolog	IMP3
ITGB4BP[25,28,29]	integrin beta 4 binding protein	TIF6
NCL	Nucleolin	NSR1

NIP7[29]	60S ribosome subunit biogenesis	NIP7
NOLA1[25]	nucleolar protein family A member 1 (H/ACA small nucleolar RNPs)	GAR1
NOL5A[25,28]	hNop56	SIK1
PAK1IP1[25]	PAK/PLC-interacting protein 1	MAK11
RBM19	RNA binding motif 19	MRD1
RBMX[28]	RNA binding motif protein, X-linked (heterogeneous nuclear ribonucleoprotein G)	
RNPC2	RNA-binding region containing protein 2	
SART3	squamous cell carcinoma antigen recognised by T cells 3	
SNRPA1[25,28]	small nuclear ribonucleoprotein polypeptide A' (U2 small nuclear ribonucleoprotein polypeptide A')	
SNRPG[25]	small nuclear ribonucleoprotein polypeptide G	SMX2
SURF6[25,28]	surfeit protein 6	RRP14
SYNCRIP	NS1 associated protein	
EEF1B2	eukaryotic translation elongation factor 1 beta 2	
IPO4	importin 4	KAP123
EBNA1BP2[25,28,29]	EBNA1 binding protein 2	EBP2
MGC3731	hypothetical protein LOC79159	
NOC2L[28,29]	nucleolar complex associated 2 homolog (*S. cerevisiae*; hypothetical protein)	NOC2
NOC3L	nucleolar complex associated 3 homolog (*S. cerevisiae*)	NOC3

NOL10[29]	nucleolar protein 10 (hypothetical protein FLJ14075)	ENP2
NOLA3[25]	nucleolar protein family A, member 3	NOP10
PES1[25,28]	Pescadillo homolog 1 containing BRCT domain	NOP7

Supplemental Table 4. Interactors found in the Pre-Ribosome Database

GENE	PROTEIN	YEAST GENE	FOUND IN
AATF	Ded protein (Apoptosis antagonizing transcription factor)	BFR2	90S*, Pre 40S
COPG	Coatomer protein complex, subunit gamma 1	SEC21	Late 40S
DDX18	RNA helicase (DEAD box polypeptide 18)	HAS1	90S, Pre 60S, Late 60S
DDX24	DEAD box polypeptide 24	MAK5	90S, Pre 60S
DDX5	Growth regulated nuclear 68 protein (DEAD box polypeptide 5)	DBP2	90S, Late 40S, Late 60S
DDX54	ATP/dependent RNA helicase (DEAD box polypeptide 54)	DBP10	90S, Pre 60S
DHX15	DEAH box polypeptide 15	PRP43	90S, Pre 60S, Pre 40S
EBNA1BP2	EBNA1 binding protein 2	EBP2	90S, Pre 60S
FBL	Fibrillarin, U3 small nucleolar interacting protein 1	NOP1	90S, Pre 40S
FTSJ3	FtsJ homolog 3 (*E. coli*)	SPB1	90S, Pre 60S
GTPBP4	GTP/binding protein NGB (G protein binding CRFG)	NOG1	90S, Pre 60S, Late 60S
IMP3	U3 snoRNP protein 3 homolog	IMP3	90S, Pre 40S
IPO4	Importin 4	KAP123	Late 60S
ITGB4BP	Integrin beta 4 binding protein	TIF6	90S, Pre 60S, Late 60S
MCM2	Minichromosome maintenance deficient 2, mitotin (*S. cerevisiae*)	MCM2	90S

MCM6	p105MCM (MCM6 minichromosome maintenance deficient 6)	MCM6	Pre 60S
NIP7	60S ribosome subunit biogenesis protein Nip7 homolog (*S. cerevisiae*)	NIP7	90S, Pre 60S, Late 60S
NOC2L	Nucleolar complex associated 2 homolog (*S. cerevisiae*; hypothetical protein DKFZp564C186.1)	NOC2	90S, Pre 60S, Late 60S
NOC3L	Nucleolar complex associated 3 homolog (*S. cerevisiae*)	NOC3	90S, Pre 60S
NOL1	Proliferating cell nuclear protein p120 (NOL protein 1)	NOP2	90S, Pre 60S, Late 60S
NOL5A	Nucleolar protein family A member 1 (H/ACA small nucleolar RNPs)	SIK1	90S, Pre 40S
NOLA1	hNop56	GAR1	90S
PAK1IP1	PAK/PLC-interacting protein 1	MAK11	Late 60S
PES1	Pescadillo homolog 1 containing BRCT domain	NOP7	90S, Pre 60S, Late 60S
RBM19	RNA binding motif 19	MRD1	Pre 40S
RPL8	60S ribosomal protein L8	RPL2A	Late 60S
RPLP2	60S acidic ribosomal protein P2	RPP2B	90S, Pre 40S
RPS23	40S ribosomal protein S23	RPS23A	Late 60S
TAF15	TLS protein (TBP-associated factor 15)	NPL3	90S
XAB1	XPA binding protein 1, GTPase	NPA3	90S, Late 60S, Late 40S
XRN2	Dhm1-like protein (5'-3' exoribonuclease 2)	RAT1	Late 60S

*genes classified as "found in 90S" in the present table include those classified as "early-pre40S" and "early pre-60S" in the Database.

Chapter 4

RPS19 is required for the maturation of 40S ribosomal subunits

A previous study in *Saccharomyces cerevisiae* revealed that disruption of either of the yeast *RPS19* genes reduces proliferation and affects the production of mature 40S ribosomal subunits (Léger-Silvestre *et al.*, 2005). In the same work it has been demonstrated that yeast RPS19 is required for the proper maturation of the 18S rRNA, that is the RNA component of 40S ribosomal subunits. This is consistent with our finding that many proteins of RPS19 interactome are involved in ribosome biogenesis.

We decided to investigate rRNA processing in human cells defective for RPS19. We first used human erythroleukemia TF-1 cells transduced with inducible siRNA against RPS19. We showed that in these cells downregulation of RPS19 blocks the processing of the 21S precursor into the 18S mature form, whereas the maturation of the rRNAs of the large ribosomal subunit appears normal. Both northern blot and pulse and chase analysis revealed decrease of 18S RNA production and accumulation of 21S precursor. rRNA processing was also analyzed in $CD34^+$ and $CD34^-$ cells isolated from the bone marrow of some DBA patients. RPS19 mutated cells exhibit the same defect in 18S maturation we noticed in TF-1 silenced cells, but patients cells with wild type RPS19 do not show alteration in the 21S/18S ratio.

Moreover, RPS19 deficiency impairs the maturation of 40S subunits in TF-1 cells.

All experiments were performed in the Department of Biochemistry and Molecular Biology of the University of Louisville, KY, USA, during the year I spent working under the supervision of Dr Steve Ellis.

Human *RPS19*, the gene mutated in Diamond-Blackfan anemia, encodes a ribosomal protein required for the maturation of 40S ribosomal subunits

Johan Flygare,[1] Anna Aspesi,[2,3] Joshua C. Bailey,[3] Koichi Miyake,[1,4] Jacqueline M. Caffrey,[3] Stefan Karlsson,[1] and Steven R. Ellis[3]

[1]Department of Molecular Medicine and Gene Therapy, Lund Stem Cell Center, Lund University Hospital, Lund, Sweden; [2]Dipartimento di Scienze Mediche, Università del Piemonte Orientale, Novara, Italy; [3]Department of Biochemistry and Molecular Biology, University of Louisville, KY; [4]Department of Biochemistry and Molecular Biology, Nippon Medical School, Tokyo, Japan

Diamond-Blackfan anemia (DBA) typically presents with red blood cell aplasia that usually manifests in the first year of life. The only gene currently known to be mutated in DBA encodes ribosomal protein S19 (RPS19). Previous studies have shown that the yeast RPS19 protein is required for a specific step in the maturation of 40S ribosomal subunits. Our objective here was to determine whether the human RPS19 protein functions at a similar step in 40S subunit maturation. Studies where RPS19 expression is reduced by siRNA in the hematopoietic cell line, TF-1, show that human RPS19 is also required for a specific step in the maturation of 40S ribosomal subunits. This maturation defect can be monitored by studying rRNA-processing intermediates along the ribosome synthesis pathway. Analysis of these intermediates in CD34$^-$ cells from the bone marrow of patients with DBA harboring mutations in *RPS19* revealed a pre-rRNA–processing defect similar to that observed in TF-1 cells where RPS19 expression was reduced. This defect was observed to a lesser extent in CD34$^+$ cells from patients with DBA who have mutations in *RPS19*. (Blood. 2007;109:980-986)

Introduction

Diamond-Blackfan anemia (DBA) typically presents as a red blood cell aplasia that affects children in their first year of life. In addition to anemia, patients with DBA present with a heterogeneous mixture of congenital abnormalities.[1] Craniofacial abnormalities are observed in approximately 50% of patients with DBA, while other defects, including growth failure, thumb malformation, and cardiac and urogenital defects, are observed less frequently.

Approximately 25% of patients with DBA have mutations in the gene encoding ribosomal protein S19, 1 of 33 ribosomal proteins that together with 18S rRNA constitutes the 40S ribosomal subunit.[2-4] The etiology of the remaining cases of DBA is unknown. DBA is the first and only human disease known to be caused by mutations in a gene encoding a ribosomal protein. Interestingly, several other bone marrow (BM) failure syndromes have been linked to factors involved in ribosome synthesis.[5] These syndromes include dyskeratosis congenita (DC), cartilage hair hypoplasia (CHH), and Shwachman Diamond syndrome (SDS). The proteins and RNAs affected in these diseases include the *DKC1* gene in X-linked DC, which encodes a pseudouracil synthase,[6] dyskerin involved in rRNA modification, the gene *RMRP* involved in CHH, which participates in rRNA processing,[7] and *SBDS*, the gene affected in SDS which encodes a protein thought to function in RNA metabolism.[8-11] The exact role of a defect in ribosome synthesis in each of these marrow failure syndromes is obscured by the fact that some of these proteins and RNAs are part of complexes that have multiple functions within cells. Dyskerin is a component of a number of ribonucleoprotein complexes, including telomerase,[12-14] whereas RMRP is a component of an endoribonuclease involved in mRNA decay in addition to rRNA processing.[15]

The only other known function for ribosomal protein S19 (RPS19) is as a monocyte attractant, leaving open the possibility that the loss of a nonribosomal function for RPS19 is responsible for DBA.[16] However, the recent identification of reduced ribosomal protein gene expression in DBA patients with normal *RPS19* strongly favors a ribosome synthesis defect as the underlying cause of DBA.[17] Previous studies have shown that the yeast homologs of RPS19 are required for the maturation of the 3′ end of 18S rRNA and the formation of active 40S ribosomal subunits. 40S subunit precursors that accumulate in cells depleted of the yeast RPS19 proteins are retained in the nucleus and fail to recruit factors required for late steps in the maturation of 40S subunits.[18]

To investigate the role of the human RPS19 protein in rRNA processing and the maturation of 40S ribosomal subunits, we turned to the TF-1 erythroleukemia cell line in which expression of RPS19 was reduced using siRNAs directed against RPS19 mRNA.[19] Reduced expression of RPS19 in TF-1 cells preferentially affects erythroid differentiation and leads to increased apoptosis. Here we show that like the yeast RPS19 protein, human RPS19 is involved in the maturation of 40S ribosomal subunits and is required for specific steps in the maturation of the 3′ end of 18S rRNA. In light of the processing defect observed in TF-1 cells expressing siRNA against RPS19 mRNA, we examined pre-rRNA processing in CD34$^+$ and CD34$^-$ cells from patients with DBA. Our data indicate that patient cells exhibit an rRNA-processing defect similar to that observed in TF-1 cells. These data are the first to

Submitted July 28, 2006; accepted August 23, 2006. Prepublished online as *Blood* First Edition Paper, September 21, 2006; DOI 10.1182/blood-2006-07-038232.

The publication costs of this article were defrayed in part by page charge payment. Therefore, and solely to indicate this fact, this article is hereby marked "advertisement" in accordance with 18 USC section 1734.

show a pre-rRNA–processing defect in cells from patients with DBA who have mutations in *RPS19*, providing further support for the view that defects in ribosome synthesis may contribute to DBA.

Materials and methods

Cell lines and culture conditions

Construction of TF-1 cell lines expressing inducible siRNAs targeting RPS19 mRNA (TF-1 A and TF-1 B) and a scrambled control siRNA (TF-1 Sc) was described previously.[19] The TF-1 cell lines were maintained in RPMI media supplemented with 10% fetal bovine serum and antibiotics (100 IU/mL penicillin and 100 μg/mL streptomycin). Granulocyte-macrophage colony-stimulating factor (GM-CSF; 5 ng/mL) was added to the media to support growth of the cytokine dependent TF-1 cell lines. Doxycycline (DOX) was included in the culture medium at a concentration of 0.5 μg/mL to induce siRNA expression.

Mononuclear BM cell samples

BM samples were collected after informed consent from healthy donors and patients with DBA. Mononuclear BM cells were isolated using a Lymphoprep density gradient (Nycomed, Oslo, Norway). Midi MACS LS separation columns and the CD34 MicroBead Kit (Miltenyi Biotec, Auburn, CA) were used to separate $CD34^+$ and $CD34^-$ mononuclear BM cells. Cells were frozen in DMEM supplemented with 20% fetal calf serum and 10% dimethylsulfoxide and stored at −80°C. DBA patients 1 through 6 do not have mutations in the *RPS19* gene. We previously described patients DBA-7, DBA-8, and DBA-9 as patients 2, 1, and 4, respectively.[20] Patient DBA-7 has a chromosomal break in intron 3 on the *RPS19* gene, patient DBA-8 has a total deletion of the *RPS19* gene, and patient DBA-9 has a (TT157-158AA, 160 insertion CT) mutation encoding a truncated form of RPS19. Patients DBA-7 and DBA-8 were transfusion dependent and patient DBA-9 was in spontaneous remission at the time of the study. Patients DBA-7, DBA-8, and DBA-9 display impaired erythroid development in vitro, which can be improved by *RPS19* gene transfer, proving that the erythroid defect is a result of RPS19 deficiency.[21]

RNA analysis

Total RNA was isolated from TF-1 cells or patient samples using an RNaqueous small-scale RNA isolation kit from Ambion (Austin, TX). Total RNA was recovered from 0.5 to 1×10^6 cells following the manufacturer's instructions for isolating RNA from suspension cultures. 5 to 10 μg total RNA was fractionated on 1.5% formaldehyde agarose gels and transferred to Zetaprobe membrane (Biorad Inc, Hercules, CA). Membranes were washed overnight at 55°C with 2 × SSC (0.3M NaCl and 0.03M Na citrate [pH 7.0]) and 1% sodium dodecyl sulfate and prehybridized for a minimum of 4 hours with ULTRAhyb oligonucleotide hybridization buffer (Ambion). The oligonucleotides used were: α, 5′-ACCGGTCACGACTCGGCA-3′ (complementary to sequences 1786-1804 in ETS1 of the rRNA transcription unit); β, 5′-GCATGGCTTAATCTTTGAGACAAGCATAT-3′ (complementary to sequences 3681-2709 in 18S rRNA); γ, 5′-CCTCGCCCTCCGGGCTCCGTTAATGATC-3′ (complementary to sequences 5520-5547 spanning the boundary between 18S rRNA and internal transcribed sequence 1 [ITS1]); δ, 5′-TCTCCCTCCCGAGTTCTCGGCTCT-3′ (complementary to sequences 5687-5710 in the 5′ portion of ITS1); and ϵ, 5′-CTAAGAGTCGTACGAGGTCG-3′ (complementary to sequences 6613-6632 spanning the boundary between ITS1 and 5.8S rRNA). The probes (30 pmol) were labeled with [γ-^{32}P]ATP using T4 polynucleotide kinase (New England Biolabs, Beverly MA). Membranes were hybridized overnight at 37°C in ULTRAhyb oligonucleotide hybridization buffer and washed the following morning 3 times with 6 × SSC at 37°C. Washed membranes were subjected to phosphorimage analysis (Phosphorimager SF; Molecular Dynamics, Sunnyvale, CA).

TF-1 cells transduced with lentiviral vectors expressing either a scrambled siRNA or RPS19 siRNA B were used for pulse-chase analysis. Cells were grown in RPMI media containing GM-CSF (5 ng/mL) in the presence or absence of DOX (5 μg/mL) for 4 days. Approximately 1×10^6 cells were harvested and washed with RPMI media lacking methionine (RPMI-Met). GM-CSF was included in the RPMI-Met media and DOX when appropriate. Cells were suspended in 3 mL RPMI-Met media and incubated for 2 hours at 37°C. Each cell suspension was treated with 150 μL (0.037 MBq/mL [1 μCi/μL]) [*methyl*-^{3}H]-Met and pulse-labeled for 30 minutes. Cells were pelleted by centrifugation, media were removed, and cells resuspended in 3.2 mL RPMI media with methionine. Aliquots (1 mL) were chased for 0, 45, and 90 minutes in Met-containing media, after which cells were harvested and total RNA was isolated using RNaqueous kits. Total RNA was fractionated on 1.5% formaldehyde agarose gels and transferred to zetaprobe membranes. Membranes were baked for 2 hours at 80°C and exposed to BioMax MS film at −80°C using a BioMax LE intensifying screen (Eastman Kodak Co, Rochester NY).

Polysome analysis

TF-1 A cells were grown for 4 days in RPMI media containing GM-CSF with or without DOX. Extracts for polysome analysis were prepared as described by Tang et al.[22] Extracts were layered on 16 mL 15% to 55% sucrose gradients and centrifuged in a SW28.1 rotor (Beckman Instruments, Fullerton CA) for 5 hours at 67 000*g*. Gradients were fractionated and absorbance at 254_{nm} monitored on an ISCO model 185 gradient fractionator and a UA-6 absorbance detector (Lincoln, NE). Chart records were digitized using Adobe Photoshop (San Jose, CA).

Results

RPS19-deficient TF-1 cells exhibit a defect in pre-rRNA processing

To assess the effect of reductions in RPS19 expression on ribosome synthesis in human hematopoietic cells we used a system in which RPS19 expression is controlled by a DOX-induced siRNA against RPS19 mRNA.[19] The cell line used for these studies is the hematopoietic progenitor cell line TF-1, which can be induced to differentiate along the erythroid and myeloid lineages. Cells containing lentiviruses encoding 1 of 2 siRNAs against the RPS19 message or a scrambled siRNA control were either untreated or induced to express siRNAs by the addition of DOX to the culture media. Previous studies using these TF-1 cells have shown that by day 5 after DOX induction the steady-state level of the RPS19 protein is decreased by 40% to 60%.[19] The growth rate of cells expressing the siRNAs targeted to RPS19 begins to decline relative to scrambled controls by day 4, suggesting that the effects of depleting RPS19 may appear at this time point (data not shown). We therefore harvested cells after 4 days of DOX induction and total RNA was isolated, fractionated on formaldehyde-agarose gels, and blotted with a series of oligonucleotide probes complementary to regions within the human rRNA repeat unit. The human rRNA-processing pathway and the probes used for Northern blot analysis are shown in Figure 1. Oligonucleotide β hybridizes to sequences within the coding region for 18S rRNA. Cell lines expressing siRNAs targeted to RPS19 (siRNAs A and B plus DOX) show a reduction in 18S rRNA compared with the same cell lines in the absence of DOX or cell lines containing scrambled siRNAs (Figure 2; β). In addition to a reduction in 18S rRNA, cell lines expressing siRNA to RPS19 have a novel species migrating just above 18S rRNA (labeled 21S).

In yeast cells depleted of RPS19, a 21S pre-rRNA accumulates at high levels relative to wild-type strains.[18] The 21S pre-RNA extends through the 3′ end of mature 18S rRNA into the ITS1. To

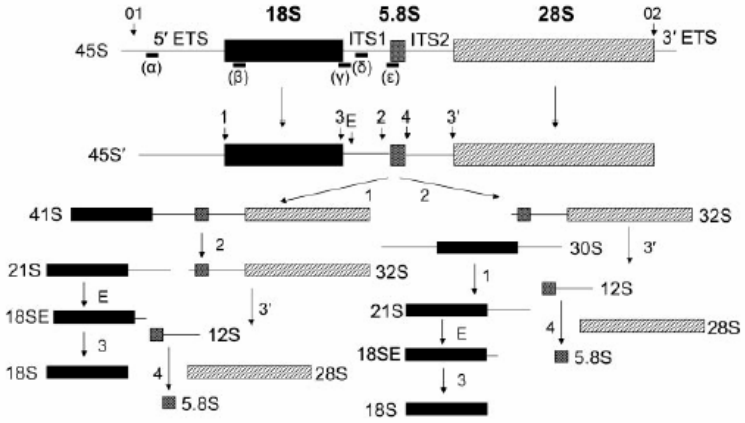

Figure 1. Pre-rRNA processing in human cells. The major rRNA-processing pathways in human cells as initially derived from Hadjiolova et al[23] and modified by Rouquette et al.[24] Mature rRNA species are shown as filled boxes: 18S, ■; 5.8S, □; and 28S, ▨. External and internal transcribed sequences are shown as lines and are labeled above the primary transcript. Cleavage sites are designated with numbered and lettered arrows. Oligonucleotide probes used in Northern blot analysis are shown as lines below the primary transcript and are labeled with Greek letters. Two alternative pathways observed in human cells are shown below the 45S′ pre-rRNA that differ in the order of cleavages 1 and 2.

determine whether the novel 18S-related species observed in cells expressing siRNA to RPS19 extended into ITS1, the membrane was probed with oligonucleotide γ, which spans cleavage site 3 at the 3′ end of 18S rRNA. In Figure 2, γ shows that in control cell lines oligonucleotide γ recognizes a species referred to as 18SE, which extends 56 nucleotides downstream of the 3′ end of 18S rRNA to a newly identified cleavage site E in ITS1.[24] In contrast, cell lines expressing siRNA targeted to RPS19 show a dramatic reduction in18SE and a corresponding increase in 21S rRNA. These data indicate that the 21S rRNA extends beyond the 3′ end of 18S rRNA into ITS1 and that cleavage at site E is affected in cells depleted of RPS19. We have used probes internal to ITS1 (oligonucleotide δ) and at the 3′ end of ITS1 overlapping with the 5′ end of 5.8S rRNA (oligonucleotides ϵ) to determine how far 21S rRNA extends into ITS1. In Figure 2, δ and ϵ indicate that 21S rRNA hybridizes with the internal probe but not with the 3′ probe, indicating that 21S rRNA likely terminates at site 2 within ITS1.

To further examine the rRNA-processing defect in cells expressing siRNA against RPS19 we turned to pulse-chase studies. In these experiments, cells expressing RPS19 siRNA B were compared with cells expressing a scrambled siRNA. Cells were grown in the presence or absence of DOX, and approximately 1×10^6 cells were harvested 4 days after DOX induction. Each cell line was grown for 2 hours in 3 mL RPMI media lacking methionine followed by the addition of 5.55 MBq (150 μCi) of [*methyl*-^{3}H]-methionine and further incubation at 37°C for 30 minutes. During the pulse-labeling period the added methionine rapidly equilibrates with the S-adenosyl-methionine pool, which is subsequently used to methylate rRNA precursors. After the pulse period, the radiolabel was removed from the culture media and 3 mL RPMI media containing unlabeled methionine was added. Aliquots (1 mL) from each cell line were withdrawn, and cells were harvested after 0, 45, or 90 minutes of chase. Figure 3 shows that cells expressing siRNA against RPS19 produced very little mature 18S rRNA over the course of the 90-minute chase. In contrast, each of the other cell lines had detectable levels of 18S rRNA present in the 45-minute chase period. The decrease in 18S rRNA production in cell lines expressing siRNA to RPS19 was accompanied by an increase in the 21S rRNA species. These data are consistent with the Northern blot analysis data, providing further evidence that cells expressing siRNA targeting RPS19 failed to efficiently cleave 21S pre-rRNAs at the E site within ITS1 forming the mature 3′ end of 18S rRNA.

Cleavage site E in human ITS1 appears to correspond to cleavage site A_2 in yeast ITS1, which is the major site affected in yeast cells depleted of RPS19.[18] In yeast, when cleavage at site A_2 is inhibited, processing still occurs at site A_3 in ITS1.[25] The 27S A_3 pre-RNA resulting from A_3 cleavage can proceed down the large subunit pathway, giving rise to mature 60S ribosomal subunits. On

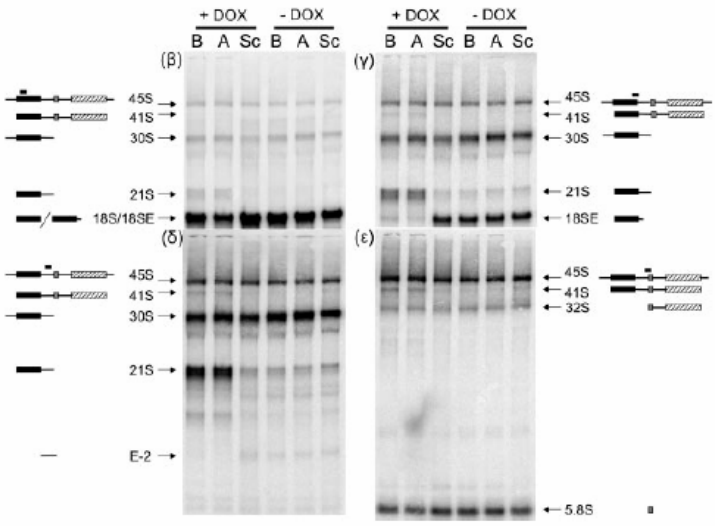

Figure 2. Northern blot analysis demonstrates abnormal pre-rRNA processing in TF-1 cells depleted of RPS19. Total RNA was isolated from TF-1 cells, fractionated on 1.5% formaldehyde-agarose gels, transferred to zetaprobe, and hybridized with oligonucleotides complementary to different regions of the rRNA primary transcript. The siRNAs present in each cell line are listed above each lane. Cell lines in lanes labeled A and B express 2 different siRNAs targeting RPS19. Sc indicates scrambled siRNA. Cell lines were grown for 4 days in the presence (+DOX) or absence (−DOX) of 0.5 μg/mL DOX. Panels are designated according to the oligonucleotide used for hybridization. Pre-rRNAs hybridizing with the different oligonucleotide probes are designated with arrows to the right or left of the panels. Illustrations of rRNA species hybridizing with different probes are included to the sides of each image. Filled boxes represent mature rRNAs: 18S, ■; 5.8S, □; 28S, ▨.

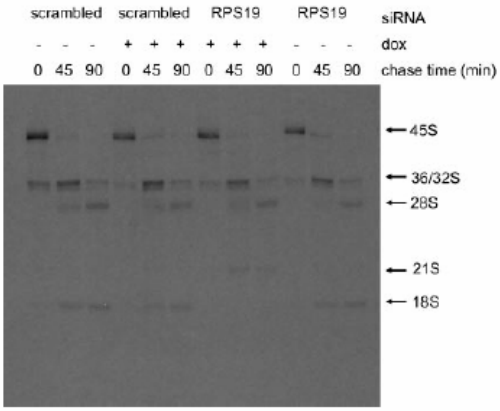

Figure 3. Pulse-chase analysis demonstrates abnormal pre-rRNA processing in TF-1 cells depleted of RPS19. Pulse-chase was carried out as described in "Materials and methods." TF-1 cells infected with lentiviruses containing either siRNA B targeted to RPS19 (RPS19) or a scrambled siRNA (scrambled) were grown for 4 days in the presence (+) or absence (−) of DOX. Chase periods are shown above each lane.

the other hand, 21S pre-RNA that extends from the mature 5′ end of 18S RNA through the A_2 site to the A_3 site is retained in the nucleus and is not efficiently processed to mature 18S rRNA.[18] Consequently, a failure to efficiently cleave at the A_2 site within ITS1 preferentially affects the production of 18S RNA and 40S ribosomal subunits. If cleavage sites E and 2 within ITS1 of human cells were comparable to sites A_2 and A_3 in yeast, respectively, inhibition of cleavage at site E would not be expected to have a dramatic affect on the production of 60S ribosomal subunits.

RPS19 is required for the maturation of 40S ribosomal subunits

To address whether TF-1 cells expressing siRNA against RPS19 have a selective deficiency of 40S ribosomal subunits, cell extracts were prepared and polysome profiles examined after sucrose gradient centrifugation. The TF-1 cells used in Figure 4 (RPS19 siRNA A) were grown for 4 days in the presence and absence of DOX. Cells grown in the presence of DOX showed a reduction in free 40S subunits, an increase in free 60S subunits, and a shift toward smaller polysomes compared with cells grown in the absence of DOX. This profile is expected for cells with a deficiency of 40S ribosomal subunits.

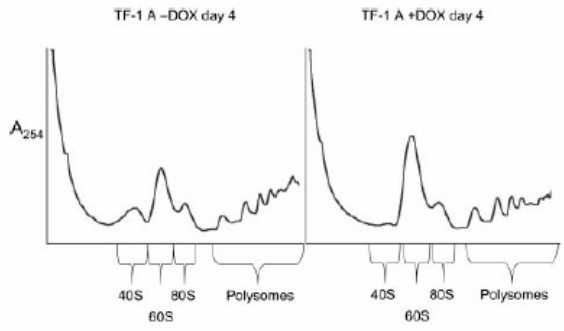

Figure 4. Altered polysome profiles in TF-1 cells depleted of RPS19. Cells extracts were prepared for polysome analysis as described in "Materials and methods." TF-1 cells infected with a lentivirus containing siRNA A targeted to RPS19 were grown for 4 days in the presence (+DOX) or absence (−DOX) of 0.5 μg/mL DOX. Extracts were layered on 15% to 55% sucrose gradients, and centrifugation was carried out for 5 hours at 67 000*g*. Gradients were fractionated using an ISCO-type 185 gradient fractionator, and absorbance at 254_{nm} was monitored with a UA-6 absorbance detector.

BM cells from DBA patients with mutations in *RPS19* exhibit abnormal processing of pre-rRNA

The data derived from TF-1 cells indicate that cells expressing suboptimal levels of RPS19 have defects in the maturation of 40S ribosomal subunits. Failure to efficiently mature 40S ribosomal subunits could therefore play an important role in the pathophysiology of DBA. Because of the high degree of sensitivity of the rRNA-processing assay, we used Northern blot analysis to examine the maturation of 40S subunits in cells derived from patients with DBA and healthy controls. Some of the cells from patients with DBA used in these studies contained mutations in *RPS19*; however, most did not (Tables 1-2). Both $CD34^-$ and $CD34^+$ mononuclear BM cells were studied. We began our analysis with the more abundant $CD34^-$ cell populations. Total RNA isolated from $CD34^-$ cells was isolated, fractionated on 1.5% formaldehyde agarose gels, transferred to zeta-probe membrane, and blotted with oligonucleotide probes to different regions of the rRNA primary transcript. In Figure 5, the γ panel shows an increase in the ratio of 21S to 18SE pre-rRNA in patients with DBA who have mutations in *RPS19* relative to healthy controls. Specific pre-RNA assignments in these primary cell populations were confirmed in blots with other oligonucleotide probes (δ and α panels). The δ panel, where hybridization was carried out with oligonucleotide δ internal to ITS1, shows that 21S pre-rRNA is detected, whereas the α panel, using an oligonucleotide complementary to sequences within ETS1, as expected, shows no evidence of hybridization with 21S pre-rRNA. The ratio of 21S to 18SE pre-rRNA in $RPS19^-$ patient samples was 3- to 4-fold higher than in healthy individuals and patients with DBA lacking *RPS19* mutations (Table 1). These data indicate that like TF-1 cells, $CD34^-$ cells from patients with DBA who have mutations in *RPS19* fail to efficiently cleave rRNA precursors at the E site within ITS1.

Table 1. Abnormal pre-rRNA processing in $CD34^-$ cells from patients with DBA who have mutations in *RPS19*

Clinical status*	*RPS19* status†	No. sample runs‡	21S/18SE ratio§
Control-1	—	2	1.3
Control-2	—	5	1
DBA-1	$RPS19^+$	2	1.2
DBA-2	$RPS19^+$	2	1.2
DBA-3	$RPS19^+$	2	1.2
DBA-4	$RPS19^+$	2	1.2
DBA-5	$RPS19^+$	2	0.8
DBA-6	$RPS19^+$	2	0.9
DBA-7	$RPS19^-$/breakpoint intron 3	2	3.1
DBA-8	$RPS19^-$/complete deletion	4	3.3
DBA-9	$RPS19^-$/frameshift	2	3.8

Comparison of the DBA $RPS19^+$ patient group data sets (rows 3-7) with the control group (rows 1-2) data sets: $P = .5$; DBA $RPS19^-$ patient group data sets (rows 8-11) with the control group: $P < .001$.

— indicates not sequenced.

*Patients diagnosed with DBA are listed as DBA-1 to DBA-9.

†The *RPS19* gene was sequenced in each DBA patient. $RPS19^+$ indicates no mutations were found. $RPS19^-$ indicates mutations were found and the nature of the mutation.

‡The number of times each sample was run on a different agarose gel.

§Average ratio of 21S to 18SE pre-rRNA after phosphorimage analysis. The 21S/18SE ratio for each sample was normalized against the control-2 ratio in the same gel.

Table 2. Pre-rRNA–processing defect in CD34$^+$ cells from patients with DBA who have mutated *RPS19*

Clinical status*	*RPS19* status†	No. sample runs‡	21S/18SE ratio§
Control-1	—	3	1.4
Control-2	—	3	1
Control-3	—	2	1.2
Control-4	—	3	1.2
DBA-5	*RPS19*$^+$	3	1
DBA-6	*RPS19*$^+$	3	0.9
DBA-8	*RPS19*$^-$/complete deletion	3	1.7‖

— indicates not sequenced.

*Patients diagnosed with DBA are listed as DBA-5, DBA-6, and DBA-8.

†The *RPS19* gene was sequenced in each patient with DBA. *RPS19*$^+$ indicates no mutations were found. *RPS19*$^-$ indicates mutations were found.

‡Number of times each sample was run on a different agarose gel.

§Average ratio of 21S to 18SE pre-rRNA after phosphorimage analysis. The 21S/18SE ratio for each sample was normalized against the control-2 ratio in the same gel.

‖$P < .003$. The *P* value reported is for a comparison of the *RPS19*$^-$ data set with the combined control data sets using the Student *t* test.

It is possible that CD34$^-$ from patients with DBA who have normal *RPS19* could have a defect in steps along the rRNA-processing pathway that is different from patients with *RPS19* mutations. Several studies in yeast have shown that mutations in genes encoding different ribosomal proteins can have distinct effects on rRNA processing.[18,26] Examination of the patterns in Figure 5 (γ and δ panels) show a modest increase in ratio of 30S to 18SE, 1.5- and 1.2-fold, in patients DBA-3 and DBA-4, respectively, relative to control samples. Further studies will be necessary to determine if these increases are significant and contribute to the pathophysiology in these patients. Other DBA patient samples with normal *RPS19* showed no obvious differences among each other and with control rRNA-processing patterns.

The primary hematopoietic defect in patients with DBA is thought to reside in the differentiation and amplification of early progenitor cells in the erythroid lineage. We therefore also examined rRNA processing in CD34$^+$ cells from patients with DBA and healthy controls. Figure 6 shows a blot of CD34$^+$ cells hybridized with oligonucleotide γ, the probe which revealed the rRNA-processing defect linked to a reduction in functional RPS19 in TF-1 cells and CD34$^-$ cells. Surprisingly, the CD34$^+$ cells from the patient sample with mutated *RPS19* (DBA-8) showed only a modest but statistically significant increase in the 21S-to-18SE ratio relative to other samples (Table 2). Thus, the rRNA-processing defect observed in CD34$^-$ cells from a patient with DBA who has an *RPS19* mutation appears to be reduced in magnitude in CD34$^+$ cells from the same patient.

Discussion

Previous studies have shown that the yeast RPS19 protein is required for a specific step in the maturation of 40S ribosomal subunits.[18] In yeast cells depleted of RPS19, pre-40S particles accumulate in the nucleus with a corresponding decrease in the amount of mature 40S subunits in the cytoplasm. The pre-40S subunits that accumulate in RPS19-depleted cells contain a 21S precursor to mature 18S rRNA. This precursor begins at the mature 5′ end of 18S rRNA and extends past the mature 3′ end of 18S rRNA to the A_3 cleavage site within ITS1 of the rRNA transcription unit. Thus, yeast cells depleted of RPS19 fail to efficiently cleave pre-RNAs at the A_2 cleavage site within ITS1, resulting in immature subunits that have failed to mature the 3′ end of 18S rRNA.

Our goal here was to monitor rRNA processing and 40S subunit maturation in human cells depleted of RPS19. Cells used for these studies were human TF-1 cells, a hematopoietic progenitor cell line expressing siRNA against the RPS19 mRNA, and cells from patients with DBA heterozygous for mutations in the *RPS19* gene. Results from TF-1 cells indicate that like yeast, human cells depleted of RPS19 accumulate a 21S pre-rRNA extended through the mature 3′ end of 18S rRNA into ITS1. We have not specifically defined the 3′ end of the 21S pre-rRNA, but show that it extends through the recently identified E site within ITS1 of the human transcription unit.[24] Since this precursor does not extend to the extreme 3′ end of ITS1 it most likely terminates at cleavage site 2 within human ITS1. In this respect, cleavage sites E and 2 within the human transcription unit would be comparable to sites A_2 and A_3 of yeast, respectively. Pulse-chase analysis showed a precursor product relationship between the 21S pre-rRNA and mature 18S rRNA, and polysome profiles revealed that TF-1 cells depleted of RPS19 had a deficiency of 40S ribosomal subunits. Thus, like its yeast ortholog, the human RPS19 protein is required for the maturation of 40S subunits and specifically affects a cleavage step within ITS1 needed for the formation of the mature 3′ end of 18S rRNA.

Maturation of the 3′ end of 18S rRNA in humans cells occurs through a stepwise pathway involving cleavage first at site 2 in ITS1, followed by cleavage at site E, and finally formation of the mature 3′ end of 18S rRNA by cleavage at site 3.[24] Northern blot

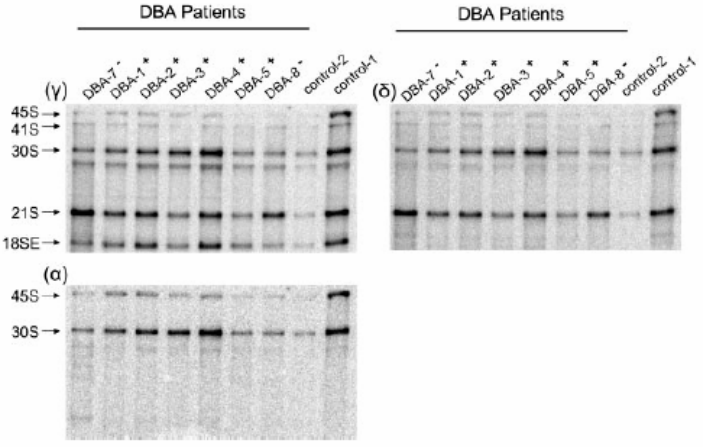

Figure 5. Northern blot analysis of CD34$^-$ BM cells reveals abnormal pre-rRNA processing in patients with DBA who have mutations in *RPS19*. Total RNA was isolated from CD34$^-$ cells and prepared for Northern blot analysis as described in Figure 2. Panels are designated according to oligonucleotides used for hybridization. Patients with DBA who have mutations in *RPS19* are designated DBA-7$^-$ and DBA-8$^-$, while patients with normal *RPS19* are designated DBA-1$^+$ to DBA-5$^+$. Samples from DBA patients labeled DBA-7$^-$ and DBA-8$^-$ have a chromosome breakpoint mutation in *RPS19* and a complete deletion of *RPS19*, respectively. Ratios listed in Table 1 are derived from phosphorimage analysis of signals for the RNA species listed. Not all samples listed in Table 1 are shown in here.

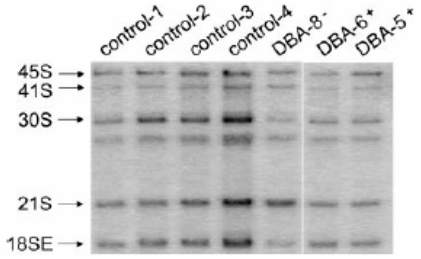

Figure 6. Northern blot analysis displays defective pre-rRNA processing in CD34+ cells from patients with DBA who have mutations in *RPS19*. The figure shows a representative Northern blot using total RNA isolated from CD34+ cells and prepared for Northern blot analysis as described in Figure 2. Pre-rRNAs were hybridized with oligonucleotide γ (Figure 1) to examine the ratio of 21S to 18SE pre-rRNA.

analysis of TF-1 cells depleted of RPS19 show a dramatic decrease in 18SE pre-rRNA that parallels the increase in 21S pre-rRNA. Thus, the human RPS19 protein is required for efficient E site cleavage. We therefore used the ratio of 21S to 18SE as a signature of RPS19 function in cells from patients with DBA and healthy controls.

Analysis of CD34− cells from patients with DBA who have mutations in *RPS19* showed a 3- to 4-fold increase in the ratio of 21S to 18SE pre-RNAs relative to healthy controls and patients with DBA lacking *RPS19* mutations. This increase is less pronounced than the 20- to 40-fold difference observed in TF-1 cells. However, BM-derived CD34− cells represent a complex mixture of different cell types, with approximately 1 in 4 being of the erythroid lineage, mainly in the form of erythroblasts.[27] Moreover, previous studies have shown that the BM of patients with DBA is relatively devoid of erythroid precursors.[28] As such, the rRNA-processing defect measured in the CD34− cells from patients with DBA who have mutations in *RPS19* may be derived from only a small number of cells within the total population.

The finding of a functional defect in 40S subunit maturation linked to suboptimal levels of RPS19 supports the notion that defective ribosome synthesis may be the underlying molecular basis for DBA. However, only 25% of DBA cases have been linked to mutations in *RPS19*. We were therefore interested in determining whether we could measure changes in rRNA processing in CD34− cells from patients with DBA who have normal *RPS19*. While there is a modest increase in the ratios of 30S to 21S pre-rRNA in DBA-3 and DBA-4 CD34− cells relative to controls, suggesting a processing defect elsewhere in the pathway, the significance of this small change is unclear at the present time. The ability to identify specific cell populations manifesting the rRNA-processing defect linked to mutations in *RPS19* may allow us to enrich for these populations in other DBA patient samples, thereby increasing the sensitivity of the rRNA-processing assay which, in turn, may unmask other rRNA-processing defects.

We also examined CD34+ cells for an rRNA-processing defect similar to that observed in CD34− cells. The 21S-to-18SE ratio in CD34+ cells from patient DBA-8 was less than that observed for CD34− cells from the same patient. The decreased magnitude of the rRNA-processing defect in CD34+ relative to CD34− cells from this patient with a complete deletion of *RPS19* could be a reflection of relative percentage of cells expressing the rRNA-processing defect in CD34− and CD34+ cell populations derived from this individual. Alternatively, these data may suggest that the defect in ribosome synthesis manifests itself to a greater extent at later steps in erythroid differentiation after the CD34 antigen is lost. Da Costa et al[29] have shown that RPS19 expression decreases during terminal erythroid differentiation. Expression of RPS19 has also been monitored in normal human hematopoietic BM cells by Northern blot and quantitative reverse transcription–polymerase chain reaction (Q-RT-PCR). RPS19 mRNA levels are relatively high in populations enriched for multipotent progenitors and gradually decrease in more differentiated cell populations.[20,21] Interestingly, the population containing erythroblasts, a cell that has unusually high levels of free ribosomes causing the basophilic cytoplasm, express relatively low levels of RPS19 mRNA.[30] It is therefore possible that RPS19 haploinsufficiency may not become limiting for 40S subunit maturation until the latter stages of erythroid differentiation, when the level of RPS19 is naturally reduced.

In conclusion, we have shown that a human progenitor cell line expressing siRNAs to RPS19 exhibits a specific defect in rRNA processing and the maturation of 40S ribosomal subunits. The rRNA-processing defect can be measured in patients with DBA patients who have mutant alleles of *RPS19*. The defect appears in CD34− cells and, to a somewhat lesser extent, in CD34+ cells derived from the BM of the patients with DBA. Identification of the specific cell types manifesting this defect in 40S subunit maturation should contribute to our understanding of the molecular mechanisms underlying the pathophysiology of DBA.

Acknowledgments

We wish to thank Dr Isao Hamaguchi, Dr Thomas Kiefer, and Karin Olsson for scientific discussions and help with collecting patient bone marrow cells. We also thank Drs Niklas Dahl and Johan Richter for help in recruiting patients for this study.

Supported by National Institutes of Heath grant RO1 HL079583 (S.R.E.), the Kentucky Lung Cancer Research Program (S.R.E.), the Ronald McDonald Foundation (J.F.), the Royal Physiographic Society in Lund (J.F.), the Swedish Cancer Society (S.K.), the European Commission (CONCERT) (S.K.), the Swedish Medical Council (S.K.), Crafoordska Stiftelsen (S.K.), the Swedish Children Cancer Foundation (S.K.), a clinical research award from Lund University Hospital (S.K.), and grants from the Diamond Blackfan Anemia Foundation (S.R.E. and S.K.). The Joint Program on Stem Cell Research at Lund University Hospital is supported by the Juvenile Diabetes Research Foundation and the Swedish Medical Research Council. The Lund Stem Cell Center is supported by a Center of Excellence grant in Life Sciences from the Swedish Foundation for Strategic Research.

Authorship

Author contributions: J.F. and A.A. performed research and analyzed data; J.C.B. and K.M. contributed reagents; J.M.C. contributed to early phases of the study; and S.K. and S.R.E. have responsibility for the entire manuscript.

Conflict-of-interest statement: The authors declare no competing financial interests.

J.F. and A.A. contributed equally to the present work.

Correspondence: Steven R. Ellis, Department of Biochemistry and Molecular Biology, University of Louisville School of Medicine, Louisville, KY 40292; e-mail: srellis@louisville.edu; or Stefan Karlsson, Department of Molecular Medicine and Gene Therapy, Lund Stem Cell Center, Lund University Hospital, BMC A12, 221 84, Lund, Sweden; e-mail: stefan.karlsson@molmed.lu.se.

References

1. Bagby GC, Lipton JM, Sloand EM, Schiffer CA. Marrow failure. Hematology. 2004;2004:318-336.
2. Draptchinskaia N, Gustavsson P, Andersson B, et al. The gene encoding ribosomal protein S19 is mutated in Diamond-Blackfan anaemia. Nat Genet. 1999;21:169-175.
3. Gazda HT, Zhong R, Long L, et al. RNA and protein evidence for haplo-insufficiency in Diamond-Blackfan anaemia patients with RPS19 mutations. Br J Haematol. 2004;127:105-113.
4. Willig TN, Draptchinskaia N, Dianzani I, et al. Mutations in ribosomal protein S19 gene and Diamond Blackfan anemia: wide variations in phenotypic expression. Blood. 1999;94:4294-4306.
5. Liu JM, Ellis SR. Ribosomes and marrow failure: coincidental association or molecular paradigm? Blood. 2006;107:4583-4588.
6. Heiss NS, Knight SW, Vulliamy TJ, et al. X-linked dyskeratosis congenita is caused by mutations in a highly conserved gene with putative nucleolar functions. Nat Genet. 1998;19:32-38.
7. Ridanpaa M, van Eenennaam H, Pelin K, et al. Mutations in the RNA component of RNase MRP cause a pleiotropic human disease, cartilage-hair hypoplasia. Cell. 2001;104:195-203.
8. Boocock GRB, Morrison JA, Popovic M, et al. Mutations in SBDS are associated with Shwachman-Diamond syndrome. Nat Genet. 2003;33:97-101.
9. Peng WT, Robinson MD, Mnaimneh S, et al. A panoramic view of yeast noncoding RNA processing. Cell. 2003;113:919-933.
10. Savchenko A, Krogan N, Cort JR, et al. The Shwachman-Bodian-Diamond syndrome protein family is involved in RNA metabolism. J Biol Chem. 2005;280:19213-19220.
11. Shammas C, Menne TF, Hilcenko C, et al. Structural and mutational analysis of the SBDS protein family: insight into the leukemia-associated Shwachman-Diamond syndrome. J Biol Chem. 2005;280:19221-19229.
12. Mitchell JR, Wood E, Collins K. A telomerase component is defective in the human disease dyskeratosis congenita. Nature. 1999;402:551-555.
13. Vulliamy TJ, Knight SW, Mason PJ, Dokal I. Very short telomeres in the peripheral blood of patients with X-linked and autosomal dyskeratosis congenita. Blood Cells Mol Dis. 2001;27:353-357.
14. Yamaguchi H, Calado RT, Ly H, et al. Mutations in TERT, the gene for telomerase reverse transcriptase, in aplastic anemia. N Engl J Med. 2005;352:1413-1424.
15. Thiel CT, Horn D, Zabel B, et al. Severely incapacitating mutations in patients with extreme short stature identify RNA-processing endoribonuclease RMRP as an essential cell growth regulator. Am J Hum Genet. 2005;77:795-806.
16. Revollo I, Nishiura H, Shibuya Y, et al. Agonist and antagonist dual effect of the cross-linked S19 ribosomal protein dimer in the C5a receptor-mediated respiratory burst reaction of phagocytic leukocytes. Inflamm Res. 2005;54:82-90.
17. Koga YM, Ohga SM, Nomura AM, Takada HM, Hara TM. Reduced gene expression of clustered ribosomal proteins in Diamond-Blackfan anemia patients without RPS19 gene mutations. J Pediatr Hematol Oncol. 2006;28:355-361.
18. Leger-Silvestre I, Caffrey JM, Dawaliby R, et al. Specific role for yeast homologs of the Diamond Blackfan anemia-associated Rps19 protein in ribosome synthesis. J Biol Chem. 2005;280:38177-38185.
19. Miyake K, Flygare J, Kiefer T, et al. Development of cellular models for ribosomal protein S19 (RPS19)-deficient diamond-blackfan anemia using inducible expression of siRNA against RPS19. Mol Ther. 2005;11:627-637.
20. Hamaguchi I, Flygare J, Nishiura H, et al. Proliferation deficiency of multipotent hematopoietic progenitors in ribosomal protein S19 (RPS19)-deficient diamond-Blackfan anemia improves following RPS19 gene transfer. Mol Ther. 2003;7:613-622.
21. Hamaguchi I, Ooka A, Brun A, et al. Gene transfer improves erythroid development in ribosomal protein S19-deficient Diamond-Blackfan anemia. Blood. 2002;100:2724-2731.
22. Tang H, Hornstein E, Stolovich M, et al. Amino acid-induced translation of TOP mRNAs is fully dependent on phosphatidylinositol 3-kinase-mediated signaling, is partially inhibited by rapamycin, and is independent of S6K1 and rpS6 phosphorylation. Mol Cell Biol. 2001;21:8671-8683.
23. Hadjiolova KV, Nicoloso M, Mazan S, Hadjiolov AA, Bachellerie JP. Alternative pre-rRNA processing pathways in human cells and their alteration by cycloheximide inhibition of protein synthesis. Eur J Biochem. 1993;212:211-215.
24. Rouquette J, Choesmel V, Gleizes PE. Nuclear export and cytoplasmic processing of precursors to the 40S ribosomal subunits in mammalian cells. EMBO J. 2005;24:2862-2872.
25. Venema J, Tollervey D. Ribosome synthesis in Saccharomyces cerevisiae. Annu Rev Genet. 1999;33:261-311.
26. Ferreira-Cerca S, Poll G, Gleizes PE, Tschochner H, Milkereit P. Roles of eukaryotic ribosomal proteins in maturation and transport of pre-18S rRNA and ribosome function. Mol Cell. 2005;20:263-275.
27. Zamir E, Geiger B, Cohen N, Kam Z, Katz BZ. Resolving and classifying haematopoietic bone-marrow cell populations by multi-dimensional analysis of flow-cytometry data. Br J Haematol. 2005;129:420-431.
28. Nathan DG, Clarke BJ, Hillman DG, Alter BP, Housman DE. Erythroid precursors in congenital hypoplastic (Diamond-Blackfan) anemia. J Clin Invest. 1978;61:489-498.
29. Da Costa L, Narla G, Willig TN, et al. Ribosomal protein S19 expression during erythroid differentiation. Blood. 2003;101:318-324.
30. Dessypris NE. Erythropoiesis. In: Pine JW, ed. Wintrobe's Clinical Hematology. Baltimore, MD: Williams and Wilkins; 1999:169-192.

Chapter 5

Conclusions and future perspectives

The first DBA gene was discovered in 1999, but despite the efforts to unravel its pathogenic role, the molecular mechanisms underlying this disease are still mostly unknown.

DBA is a rare anemia characterized by heterogeneous clinical features and an unpredictable outcome. Available therapies cannot cure the causes and they target only the symptoms, but they have adverse side effects that can limit patients' quality of life.

What is intriguing about this disease is the mysterious link between the ribosome and the red cell aplasia. The mutation of a protein of the ribosomal machinery, that is essential for any cellular process, would be expected to cause a systemic defect. Instead, many patients show no other symptoms but anemia.

DBA is the first known disease due to mutations in a ribosomal protein. Other bone marrow failure syndromes are related to ribosome dysfunction; for instance, Shwachman Diamond syndrome gene, SBDS, is believed to be a crucial factor for the joining of 60S and 40S subunits and for translation initiation. Also dyskeratosis congenita, another disease characterized like DBA by bone marrow failure, malformations and increased risk of cancer, can be caused by mutations in a gene necessary for the maturation of rRNA. Moreover, Ebert *et al.* very recently demonstrated that the $5q^-$ syndrome is due to deficiency of RPS14 and that RPS14 is required for 18S pre-rRNA processing and 40S ribosomal subunit formation (Ebert *et al.*, 2008).

The causal link between defective ribosomes and impaired hematopoiesis appears evident, but so far unexplained. To this regard, two major hypotheses have been proposed and they imply either tissue-specific insufficient translation or the existence of an essential function of RPS19 in erythropoiesis. The first one is classically based on the observation that in the *Minute* mutants of *Drosophila melanogaster* the ablation of a RP gene results in a

phenotype characterized by small body size, thin bristles and delayed larval development. According to this theory, haploinsufficiency of RPS19 would diminish the number of total ribosomes and the translational capacity of the cell, and this effect would be more severe in high proliferating tissues such as the bone marrow. Actually, hematopoiesis is a process with enormous demands for protein synthesis, expecially during the differentiation of the erythroid precursors, that is the stage affected in DBA. Ellis and Massey suggested that ribosomal proteins can be expressed in variable amounts in different tissues and that the haploinsufficiency of RPS19 could be limiting for ribosome assembly in the bone marrow and not in other tissues (Ellis and Massey, 2005). The discovery that translational efficiency is affected in DBA patients supports the pathogenic hypothesis of a defective protein synthesis (Cmejlova *et al.*, 2006).

We demonstrated that RPS19 deficient cells have a reduced amount of 40S subunits because of a pre-rRNA processing defect. In fact, bone marrow cells from DBA patients with mutated RPS19 show impaired maturation of the 18S rRNA; this is more evident in $CD34^-$ compared to $CD34^+$ cells suggesting that differentiated cells are the most affected. A very recent report displays that another DBA gene, *RPS24*, is required for a different step in the processing of the pre-rRNA precursor (Choesmel *et al.*, 2008).

The second hypothesis proposed to explain DBA invokes the existence of an extraribosomal function of RPS19 important for erythropoiesis. We investigated this possibility by searching for protein interactors of RPS19, at first with a yeast two-hybrid assay, and then with a proteomic approach. We showed that RPS19 binds PIM-1, a serine threonine kinase involved in hematopoietic growth factor signaling. PIM-1 localizes on ribosomes and phosphorylates RPS19 *in vitro*. This behaviour reminds the model illustrated for RPL13a, that when is phosphorilated inhibits the translation of ceruloplasmin mRNA

(Mazumder *et al.*, 2003). A role of RPS19 in general or specific translation control can therefore be speculated. We identified a number of other RPS19 interactors, mostly nucleolar proteins involved in ribosome biogenesis, but also splicing and transcription factors and proteins important for translation regulation. Hence the erythroid defect in DBA probably results from the coparticipation of more mechanisms.

In order to further elucidate the cellular events caused by RPS19 downregulation, we are now studying if RPS19 deficiency can modulate the expression of other proteins and transcripts. Microarray analysis and differential in-gel electrophoresis (DIGE) on TF-1 cells expressing siRNA against RPS19 are in progress.

BIBLIOGRAPHY

Angelastro JM, Töröcsik B, Greene LA. Nerve growth factor selectively regulates expression of transcripts encoding ribosomal proteins. *BMC Neurosci* 3 (2002).

Bachmann M, Moroy T. The serine/threonine kinase Pim-1. *Int J Biochem Cell Biol* 37, 726-730 (2005).

Bagnara GP, Zauli G, Vitale L, Rosito P, Vecchi V, Paolucci G, Avanzi GC, Ramenghi U, Timeus F, Gabutti V. In vitro growth and regulation of bone marrow enriched $CD34^+$ hematopoietic progenitors in Diamond-Blackfan anemia. *Blood* 78, 2203-2210 (1991).

Bommer UA, Stahl J, Henske A, Lutsch G, Bielka H. Identification of proteins of the 40S ribosomal subunit involved in interaction with initiation factor eIF-2 in the quaternary initiation complex by means of monospecific antibodies. *FEBS Lett* 233, 114-118 (1988).

Bortoluzzi S, d'Alessi F. Romualdi C, Danieli GA. Differential expression of genes coding for ribosomal proteins in different human tissues. *Bioinformatics* 17, 1152-1157 (2001).

Campagnoli MF, Garelli E, Quarello P, Carando A, Varotto S, Nobili B, Longoni D, Pecile V, Zecca M, Dufour C, Ramenghi U, Dianzani I. Molecular basis of Diamond-Blackfan anemia: new findings from the Italian registry and a review of the literature. *Haematologica* 89, 480-489 (2004).

Cathie IA. Erythrogenesis imperfecta. *Arch Dis Child* 25, 313-324 (1950).

Choesmel V, Fribourg S, Aguissa-Touré AH, Pinaud N, Legrand P, Gazda HT, Gleizes PE. Mutation of ribosomal protein RPS24 in Diamond-Blackfan anemia results in a ribosome biogenesis disorder. *Hum Mol Genet* 2008 [Epub ahead of print].

Cmejla R, Blafkova J, Stopka T, Zavadil J, Pospisilova D, Mihal V, Petrtylova K, Jelinek J. Ribosomal protein S19 gene mutations in patients with Diamond-Blackfan anemia and identification of ribosomal protein S19 pseudogenes. *Blood Cells Mol Dis* 26, 124-132 (2000).

Cmejla R, Cmejlova J, Handrkova H, Petrak J, Pospisilova D. Ribosomal protein S17 gene (RPS17) is mutated in Diamond-Blackfan anemia. *Hum Mutat* 28, 1178-1182 (2007).

Cmejlova J, Dolezalova L, Pospisilova D, Petrtylova K, Petrak J, Cmejla R. Translational efficiency in patients with Diamond-Blackfan anemia. *Haematologica* 91, 1456-1464 (2006).

Da Costa, Narla G, Willig TN, Peters LL, Parra M, Fixler J, Tchernia G, Mohandas N. Ribosomal protein S19 expression during erythroid differentiation. *Blood* 101, 318-324 (2003).

Dai MS, Lu H. Inhibition of MDM2-mediated p53 ubiquitination and degradation by ribosomal protein L5. *J Biol Chem* 279, 44475-44482 (2004).

Diamond LK, Blackfan KD. Hypoplastic anemia. *Am J Dis Child* 56, 464-467 (1938).

Dianzani I, Garelli E, Dompè C, Crescenzio N, Locatelli F, Schillirò G, Castaman G, Bagnara GP, Olivieri NF, Gabutti V, Ramenghi U. Mutations in the erythropoietin receptor gene are not a common cause of Diamond-Blackfan anemia. *Blood* 87, 2568-2572 (1996).

Dianzani I, Garelli E, Crescenzio N, Timeus F, Mori PG, Varotto S, Nobili B, Brandalise S, Olivieri NF, Gabutti V, Ramenghi U. Diamond-Blackfan anemia: expansion of erythroid progenitors in vitro by IL-9, but exclusion of a significant pathogenetic role for the IL-9 gene and the hematopoietic gene cluster on chromosome 5q. *Exp Hematol* 25, 1270-1277 (1997).

Dianzani I, Garelli E, Ramenghi U. Diamond-Blackfan anemia: an overview. *Paediatr Drugs* 2, 345-355 (2000).

Domen J, van der Lugt NM, Laird PW, Saris CJ, Clarke AR, Hooper ML, Berns A. Impaired interleukin-3 response in Pim-1-deficient bone marrow-derived mast cells. *Blood* 82, 1445-1452 (1993).

Draptchinskaia N, Gustavsson P, Andersson B, Pettersson M, Willig TN, Dianzani I, Ball S, Tchernia G, Klar J, Matsson H, Tentler D, Mohandas N, Carlsson B, Dahl N. The gene encoding ribosomal protein S19 is mutated in Diamond-Blackfan anemia. *Nat Genet* 21, 169-175 (1999).

Ebert BL, Pretz J, Bosco J, Chang CY, Tamayo P, Galili N, Raza A, Root DE, Attar E, Ellis SR, Golub TR. Identification of RPS14 as a 5q- syndrome gene by RNA interference screen. *Nature* 451, 335-339 (2008).

Ellis SR, Massey AT. Diamond Blackfan anemia: a paradigm for a ribosome-based disease. *Med Hypotheses* 66, 643-648 (2006).

Farrar J, Nater M, Caywood E, McDevitt M, Kowalski J, Takemoto C, Talbot C, Meltzer P, Esposito D, Beggs A, Schneider H, Grabowska A, Ball S, Niewiadomska E, Sieff C, Vlachos A, Atsidaftos E, Ellis S, Lipton J, Gazda H, Arceci RJ. A Large Ribosomal Subunit Protein Abnormality in Diamond-Blackfan Anemia (DBA). The American Society of Hematology, 49th Annual Meeting, Atlanta, Georgia, December 8-11, 2007.

Flygare J, Kiefer T, Miyake K, Utsugisawa T, Hamaguchi I, Da Costa L, Richter J, Davey EJ, Matsson H, Dahl N, Wiznerowicz M, Trono D, Karlsson S. Deficiency of ribosomal protein S19 in CD34+ cells generated by siRNA blocks erythroid development and mimics defects seen in Diamond-Blackfan anemia. *Blood* 105, 4627-4634 (2005).

Flygare J, Karlsson S. Diamond-Blackfan anemia: erythropoiesis lost in translation. *Blood* 109, 3152-3160 (2007).

Ganapathi KA, Austin KM, Lee CS, Dias A, Malsch MM, Reed R, Shimamura A. The human Shwachman-Diamond syndrome protein, SBDS, associates with ribosomal RNA. *Blood* 110, 1458-1465 (2007).

Gazda H, Lipton JM, Willig TN, Ball S, Niemeyer CM, Tchernia G, Mohandas N, Daly MJ, Ploszynska A, Orfali KA, Vlachos A, Glader BE, Rokicka-Milewska R, Ohara A, Baker D, Pospisilova D, Webber A, Viskochil DH, Nathan DG, Beggs AH, Sieff CA. Evidence for linkage of familial Diamond-Blackfan anemia to chromosome 8p23.3-p22 and for non-19q non-8p disease. *Blood* 97, 2145-2150 (2001).

Gazda HT, Zhong R, Long L, Niewiadomska E, Lipton JM, Ploszynska A, Zaucha JM, Vlachos A, Atsidaftos E, Viskochil DH, Niemeyer CM, Meerpohl JJ, Rokicka-Milewska R, Pospisilova D, Wiktor-Jedrzejczak W, Nathan DG, Beggs AH, Sieff CA. RNA and protein evidence for haplo-insufficiency in Diamond-Blackfan anaemia patients with *RPS19* mutations. *Br J Haematol* 127, 105-113 (2004).

Gazda HT, Grabowska A, Merida-Long LB, Latawiec E, Schneider HE, Lipton JM, Vlachos A, Atsidaftos E, Ball SE, Orfali KA, Niewiadomska E, Da Costa L, Tchernia G, Niemeyer C, Meerpohl JJ, Stahl J, Schratt G, Glader B, Backer K, Wong C, Nathan DG, Beggs AH, Sieff CA. Ribosomal protein S24 is mutated in Diamond-Blackfan anemia. *Am J Hum Genet* 79, 1110-1118 (2006).

Gazda HT, Sheen MR, Darras N, Shneider H, Sieff CA, Ball SE, Niewiadomska E, Newburger PE, Atsidaftos E, Vlachos A, Lipton JM, Beggs AH. Mutations of the Genes for Ribosomal Proteins L5 and L11 Are a Common Cause of Diamond-Blackfan Anemia. The American Society of Hematology, 49th Annual Meeting, Atlanta, Georgia, December 8-11, 2007.

Glader BE, Backer K. Elevated red cell adenosine deaminase activity: a marker of disordered erythropoiesis in Diamond-Blackfan anaemia and other haematologic diseases. *Br J Haematol* 68, 165-168 (1988).

Gregory LA, Aguissa-Touré AH, Pinaud N, Legrand P, Gleizes PE, Fribourg S. Molecular basis of Diamond-Blackfan anemia: structure and function analysis of RPS19. *Nucleic Acids Res* 35, 5913-5921 (2007).

Gustavsson P, Skeppner G, Johansson B, Berg T, Gordon L, Kreuger A, Dahl N. Diamond-Blackfan anaemia in a girl with a de novo balanced reciprocal X;19 translocation. *J Med Genet* 34, 779-782 (1997).

Hamaguchi I, Ooka A, Brun A, Richter J, Dahl N, Karlsson S. Gene transfer improves erythroid development in ribosomal protein S19-deficient Diamond-Blackfan anemia. *Blood* 100, 2724-2731 (2002).

Hamaguchi I, Flygare J, Nishiura H, Brun ACM, Ooka A, Kiefer T, Ma Z, Dahl N, Richter J, Karlsson S. Proliferation deficiency of multipotent hematopoietic progenitors in ribosomal protein S19 (RPS19)- deficient Diamond-Blackfan anemia improves following *RPS19* gene transfer. *Mol Ther* 7, 613-622 (2003).

Josephs HW. Anemia of infancy and early childhood. *Medicine* 15, 307-451 (1936).

Kirwan M, Dokal I. Dyskeratosis congenita: a genetic disorder of many faces. *Clin Genet* 73, 103-112 (2008).

Kongsuwan K, Yu Q, Vincent A, Frisardi MC, Rosbash M, Lengyel JA, Merriam J. A Drosophila Minute gene encodes a ribosomal protein. *Nature* 317, 555-558 (1985).

Laird PW, van der Lugt NM, Clarke A, Domen J, Linders K, Berns A. In vivo analysis of Pim-1 deficiency. *Nucl Acid Res* 21, 4750-4755 (1993).

Léger-Silvestre I, Caffrey JM, Dawaliby R, Alvarez-Arias DA, Gas N, Bertolone SJ, Gleizes PE, Ellis SR. Specific role for yeast homologs of the Diamond Blackfan anemia-associated RPS19 protein in ribosome synthesis. *J Biol Chem* 280, 38177-38185 (2005).

Li X, Zhong S, Wong WH. Reliable prediction of transcription factor binding sites by phylogenetic verification. *Proc Natl Acad Sci USA* 102, 16945-16950 (2005).

Lipton JM. Diamond Blackfan anemia: new paradigms for a “not so pure” inherited red cell aplasia. *Semin Hematol* 43, 167-177 (2006).

Liu JM, Ellis SR. Ribosomes and marrow failure: coincidental association or molecular paradigm? *Blood* 107, 4583-4588 (2006).

Lodish HF. Model for the regulation of mRNA translation applied to haemoglobin synthesis. *Nature* 251, 385-388 (1974).

Lohrum MA, Ludwig RL, Kubbutat MH, Hanlon M, Vousden KH. Regulation of HDM2 activity by the ribosomal protein L11. *Cancer Cell* 3, 577-587 (2003).

Lutsch G, Stahl J, Kärgel HJ, Noll F, Bielka H. Immunoelectron microscopic studies on the location of ribosomal proteins on the surface of the 40S ribosomal subunit from rat liver. *Eur J Cell Biol* 51, 140-150 (1990).

Matsson H, Davey EJ, Draptchinskaia N, Hamaguchi I, Ooka A, Levéen P, Forsberg E, Karlsson S, Dahl N. Targeted disruption of the ribosomal protein S19 gene is lethal prior to implantation. *Mol Cell Biol* 24, 4032-4037 (2004).

Mazumder B, Sampath P, Seshadri V, Maitra RK, DiCorleto PE, Fox PL. Regulated release of L13a from 60S subunit as a mechanism of transcript-specific translational control. *Cell* 115, 187-198 (2003).

Menne TF, Goyenechea B, Sánchez-Puig N, Wong CC, Tonkin LM, Ancliff PJ, Brost RL, Costanzo M, Boone C, Warren AJ. The Shwachman-Bodian-Diamond syndrome protein mediates translational activation of ribosomes in yeast. *Nat genet* 39, 486-495 (2007).

Miyake K, Utsugisawa T, Flygare J, Kiefer T, Hamaguchi I, Richter J, Karlsson S. RPS19 deficiency leads to reduced proliferation and increased apoptosis but does not affect terminal differentiation in a cell line model of Diamond-Blackfan anemia. *Stem Cells* 26, 323-329 (2008).

Nathan DG, Bryan JC, Hillman DG, Alter BP, Housman DE. Erythroid precursors in congenital hypoplastic (Diamond-Blackfan) anemia. *J Clin Invest* 61, 489-498 (1978).

Ohene-Abuakwa Y, Orfali KA, Marius C, Ball SE. Two-phase culture in Diamond Blackfan anemia: localization of erythroid defect. *Blood* 105, 838-846 (2005).

Perdahl EB, Naprstek BL, Wallace WC, Lipton JM. Erythroid failure in Diamond-Blackfan anemia is characterized by apoptosis. *Blood* 83, 645-650 (1994).

Perry RP. The architecture of mammalian ribosomal protein promoters. *BMC Evol Biol* 5, 15 (2005).

Pircher TJ, Zhao S, Geiger JN, Wojchowski DM. Pim kinase protects hematopoietic FDC cells from genotoxin-induced death. *Oncogene* 19, 3684-3692 (2000).

Ridanpaa M, van Eenennaam H, Pelin K, Chadwick R, Johnson C, Yuan B, vanVenrooij W, Pruijn G, Salmela R, Rockas S, Makitie O, Kaitila I, de la Chapelle A, Mutations in the RNA component of RNase MRP cause a pleiotropic human disease, cartilage-hair hypoplasia. *Cell* 104, 195-203 (2001).

Rouquette J, Choesmel V, Gleizes PE. Nuclear export and cytoplasmic processing of precursors to the 40S ribosomal subunits in mammalian cells. *EMBO J* 24, 2862-2872 (2005).

Roy V, Pérez WS, Eapen M, Marsh JCW, Pasquini M, Pasquini R, Mustafa MM, Bredeson CN. Bone marrow transplantation for Diamond-Blackfan anemia. *Biol Blood Marrow Transplant* 11, 600-608 (2005).

Soulet F, Al Saati T, Roga S, Amalric F, Bouche G. Fibroblast growth factor-2 interacts with free ribosomal protein S19. *Biochem Biophys Res Commun* 289, 591-596 (2001).

Shrestha A, Horino K, Nishiura H, Yamamoto T. Acquired immune response as a consequence of the macrophage-dependent apoptotic cell clearance and role of the monocyte chemotactic S19 ribosomal protein dimer in this connection. *Lab Invest* 94, 1629-1642 (1999).

Takagi M, Absalon MJ, McLure KG, Kastan MB. Regulation of p53 translation and induction after DNA damage by ribosomal protein L26 and nucleolin. *Cell* 123, 49-63 (2005).

Tschochner H, Hurt E. Pre-ribosomes on the road from the nucleolus to the cytoplasm. *Trends Cell Biol* 13, 255-263 (2003).

van der Houven van Oordt CW, Schouten TG, van Krieken JH, van Dierendonck JH, van der Eb AJ, Breuer ML. X-ray-induced lymphomagenesis in E mu-pim-1 transgenic mice: an investigation of the co-operating molecular events. *Carcinogenesis* 19, 847-853 (1998).

Volarevic S, Thomas G. Role of S6 phosphorylation and S6 kinase in cell growth. *Prog Nucl Acid Res Mol Biol* 65, 101-127 (2001).

Warner JR. The economics of ribosome biosynthesis in yeast. *Trends Biochem Sci* 24, 437-440 (1999).

Willig TN, Draptchinskaia N, Dianzani I, Ball S, Niemeyer C, Ramenghi U, Orfali K, Gustavsson P, Garelli E, Brusco A, Tiemann C, Pérignon JL, Bouchier C, Cicchiello L, Dahl N, Mohandas N, Tchernia G. Mutations in ribosomal protein S19 gene and Diamond Blackfan anemia: wide variations in phenotypic expression. *Blood* 94, 4294-4306 (1999).

Wool IG. Extraribosomal functions of ribosomal proteins. *Trends Biochem Sci* 21, 164-165 (1996).

Yoon A, Peng G, Brandenburger Y, Zollo O, Xu W, Rego E, Ruggero D. Impaired control of IRES-mediated translation in X-linked dyskeratosis congenita. *Science* 312, 902-906 (2006).